

Interest rate models for direct participation products under IFRS 17

Zinatu Ibrahim

A Thesis

in

The Department

of

Mathematics and Statistics

Presented in Partial Fulfillment of the Requirements
for the Degree of Master of Science (Mathematics) at

Concordia University

Montreal, Quebec, Canada

October 2020

©Zinatu Ibrahim, 2020

CONCORDIA UNIVERSITY

School of Graduate Studies

This is to certify that the thesis prepared

By: Zinatu Ibrahim

Entitled: Interest rate models for direct participation products under IFRS 17
and submitted in partial fulfillment of the requirements for the degree of

Master of Science (Mathematics)

complies with the regulations of the University and meets the accepted standards with respect to originality and quality.

Signed by the final Examining Committee:

_____ Thesis Supervisor

Prof. F. Godin

_____ Examiner

Prof. C. Hyndman

_____ Examiner

Prof. P. Gaillardetz

Approved by _____

Prof. Galia Dafni

Graduate Program Director

_____ Prof. Pascale Sicotte

Dean of Faculty

_____ Date

ABSTRACT

Interest rate models for direct participation products under IFRS 17

Zinatu Ibrahim

The incoming IFRS 17 standard will require insurers to adopt market-consistent methods in valuing their insurance contract liabilities. Insurance contracts such as segregated funds categorized as direct participation contracts are highly dependent on the choice of interest rate model. This thesis describes the general steps in the calibrating the G2++ and G3++ short rate models to swaptions. The calibration process is an optimization problem where parameters that minimize the difference between market and model implied prices are determined. We highlight some issues that arise during the calibration such as the choice of a calibration method and an optimization algorithm as well the imposed constraints used in solving this inherent non-convex global optimization problem. An evaluation of the calibrated models' consistency to replicate market volatility surface is made via Monte-Carlo simulations. Then a simulation scheme devoid of discretization errors is provided for the stochastic discount factor, the short rate and bond prices which are useful in market-consistent valuations. We provide an illustration of a market-consistent valuation of a segregated fund fully invested bonds and compare the models' results. Finally, we assess the robustness of the models' calibration to different market data and parameter specification. This is to ensure that the calibrated models provide stable financial results for annual regulatory reporting.

Acknowledgments

I would like to thank my supervisor Dr. Frédéric Godin for guiding me to such an interesting and relevant thesis topic. I am grateful for his patience, guidance and support throughout my graduate studies. I only hope to have assimilated a tiny portion of his vast knowledge in very diverse fields. A sincere gratitude also goes out to my thesis examining committee: Dr. Patrice Gaillardetz and Dr. Cody Hyndman for their presence on my thesis defense and their helpful suggestions.

I would also like to thank my incredible support system of family and friends for their support during these time. A special thanks to my mother for her encouragement, prayers and support. It is only by Allah's grace that we have made it thus far.

This thesis was supported by the Department of Mathematics and Faculty of Arts and Science Graduate Fellowship from Concordia University. Support from the Institut des sciences mathématiques (ISM) and the Centre de Recherches Mathématiques (CRM) is also acknowledged.

Dedication

To the memory of my beloved Baba, Ibrahim Lomotey.

Contents

List of Figures	ix
List of Tables	xi
1 Interest Rates And Interest Rate Derivatives	8
1.1 Definition and Notations	8
1.1.1 No-Arbitrage Assumption And The Forward Measure	12
1.2 Interest Rate Swaps and Swaptions	13
1.2.1 Interest Rate Swaps	13
1.2.2 Swaptions	15
2 The Interest Rate Model	19
2.1 Short-Rate Models	19
2.1.1 Endogenous Models	20
2.1.2 Exogenous One-Factor Models	21
2.1.3 Exogenous Multi-Factor Models	22
2.2 The Gn++ Short-Rate Model	23
2.2.1 The Risk-Neutral Short-Rate Dynamics	23
2.2.2 Analytical Zero Coupon Bond Price	25
2.2.3 The Short-Rate Dynamics Under The Forward Measure	28
2.2.4 Swaption Price Under The Gn++ Model	29
3 Gn++ Model Calibration to Market Data	32
3.1 The Calibration Problems	33

3.2	Optimization Algorithm	36
3.2.1	Differential Evolution Algorithm	39
3.3	Calibration Results	42
4	Model Validation of the Gn++ model	47
4.1	Simulation of Swaption Prices	47
4.2	Simulation of The Discount Factor	58
4.3	Application To A Segregated Fund Policy	62
4.3.1	GMMB Contract Cashflows	63
5	Robustness Study	68
5.1	Calibration To Three Days With A Two Day Lag	69
	Bibliography	82
A		85
A.1	Validation Results On Monday June 24	85
A.2	Validation Results On Wednesday June 26	89

List of Figures

3.1	Market yield curve on June 28, 2019	42
3.2	Market interpolated yield curve	43
3.3	Market volatility surface on June/28/2019	44
3.4	General phenomenon of market swaption prices and implied volatility . .	45
4.1	G2++ calibration to market prices on June 28: volatility surface	50
4.2	G2++ calibration to market prices on June 28: calibration errors	50
4.3	G2++ calibration to market implied volatilities on June 28: volatility surface	52
4.4	G2++ calibration to market implied Volatilities on June 28: calibration errors	53
4.5	G3++ calibration to market prices on June 28: volatility surface	54
4.6	G3++ calibration to market prices on June 28: calibration errors	54
4.7	G3++ calibration to market implied volatilities on June 28: volatility surface	56
4.8	G3++ calibration to market implied Volatilities on June 28: calibration errors	56
4.9	Evolution of the short rate over time	61
4.10	Proportion of $r(t) < -0.0075$	62
4.11	Distribution of discount factor	62
5.1	Market yield curves	69
5.2	Market volatility surface on all three days	70
5.3	Distribution of five year short rate	72

5.4	Distribution of thirty year short rate	73
5.5	Deviations of $r(t)$ across the three days	74
5.6	$f(t)$ across the three days	75
5.7	Deviations of F_t across the three days	77
A.1	Market interpolated spot curve on Monday June 24	85
A.2	G2++ implied volatility surface on June 24	86
A.3	G2++ calibration errors on June 24	87
A.4	G3++ implied volatilities on June 24	87
A.5	G3++ calibration errors on June 24	88
A.6	Market interpolated curve on Monday June 26	89
A.7	G2++ volatility surface on June 26	90
A.8	G2++ calibration errors on June 26	90
A.9	G3+ volatility surface on June 26	91
A.10	G3++ calibration errors on June 26	91

List of Tables

3.1	Market volatilities on June 28	44
3.2	G2++ Model Parameters	45
3.3	G3++ Model Parameters	45
4.1	G2++ calibration to market prices on June 28: implied volatilities	51
4.2	G2++ calibration to market prices on June 28: calibration errors	51
4.3	G2++ calibration to market implied volatilities on June 28: implied volatilities	53
4.4	G2++ calibration to market implied Volatilities on June 26: calibration errors	54
4.5	G3++ calibration to market prices on June 28: implied volatilities	55
4.6	G3++ calibration to market prices on June 28: calibration errors	55
4.7	Mean of absolute relative calibration errors	57
4.8	G3++ calibration to market implied volatilities on June 28: implied volatilities	57
4.9	G3++ calibration to market implied volatilities on June 28: calibration errors	57
4.10	Market-consistent GMMB Valuations on June 28, 2019	66
5.1	G2++ Model Parameters	70
5.2	G3++ Model Parameters	71
5.3	Deviations of r	75
5.4	G2++	75
5.5	G3++	75

5.6	GMMB Valuations: G2++ model	76
5.7	GMMB Valuations: G3++ model	76
5.8	Deviations of F	78
5.9	G2++	78
5.10	G3++	78
A.1	Market volatilities on June 24	85
A.2	G2++ implied volatilities on June 24	86
A.3	G2++ calibration errors on June 24	86
A.4	G3++ implied volatilities on June 24	88
A.5	G3++ calibration errors on June 24	88
A.6	Market volatilities on June 26	89
A.7	G2++ implied volatilities on June 26	90
A.8	G2++ calibration errors on June 26	91
A.9	G3+ implied volatilities on June 26	92
A.10	G3++ calibration errors on June 26	92

General Introduction

Background

Effective January 1, 2023, entities issuing insurance contracts in many jurisdictions will be subject to the IFRS 17 standard in their regulatory reporting. Under the incoming IFRS 17 framework, insurers are required to adopt market-consistent methods in valuing their insurance contract liabilities. A valuation is said to be market-consistent if its assigned value agrees with prevailing market prices or if it is estimated, the model that estimates the price replicates the observable market prices it is calibrated to within an acceptable tolerance. The objective behind the requirement for market-consistent valuation per the standard is to reduce subjectivity and reflect evident information available to users of financial statements. It also provides the use of a common and publicly available benchmark that users of financial information can easily understand.

IFRS 17 distinguishes between two types of insurance contracts; those with direct participation features and those without direct participation features (see paragraphs *BC227* of the basis of conclusions IASB [2017])¹. Due to the nature of insurance contracts with direct participation features, they are considered by the standard to generate cash flows *that vary based on the underlying item* where the underlying item could be an equity index, a bond etc. Segregated funds (with guarantees; called variable annuities in the US and unit-linked insurance in the United Kingdom) are examples of contracts categorised as *insurance contracts with direct participation features* [Canadian Institute of Actuaries, 2018]. These fund-linked products offer direct participation in financial market growth

¹Reference from the basis of conclusions of the IFRS 17 standard will be italicized with the prefix BC. References from the standard will not include the prefix

while protecting the initial premium. The guarantee acts a financial option and the contract may be surrendered at anytime before the maturity of the contract.

According to paragraph *BC152*, insurance contracts with embedded options and guarantees such as segregated funds are to be measured (valued) in a way that reflects their inherent financial risk either through estimates of future cash flows or through their discount rates. However since these embedded options and guarantees are not openly traded on the market, it is difficult to assign them a market value.

With regards to the methodology in their valuation, the standard does not explicitly require a specific technique although it allows the use of a replicating portfolio whose cash flows exactly match in all *scenarios, timing and uncertainty* to the contract at hand. Paragraph *B48* however explains that stochastic modeling may be *robust* and that given the specific situation, “judgement” is required to determine the best technique that meets the market-consistency criterion. From a mathematical finance perspective, this may be translated to “where closed-forms exist for the option prices, they may be used, otherwise Monte Carlo simulation might prove useful”.

In terms of the market variables used in the valuation, entities are by paragraph *B44* expected to maximise the use of all observable market variables such as interest rates as direct model inputs on the valuation date without adjustments if possible. If certain variables are unobservable (e.g. market prices of long dated options, long maturity yields etc.), they should be derived as consistently as possible with those that can be directly observed without any contradictions. Estimates of the discount rates used in discounting the cash flow scenarios are to reflect the variability of the cash flows. While the standard does not specify an exact estimating technique for discount rates applied to cash flows that vary with the underlying item, it recommends the use of stochastic/risk-neutral modeling techniques that maximize market input to ensure that the estimated discount rates are current and market-consistent. For non-market variables, the entity is encouraged to use its own perspective suitable for their risk profile, see paragraphs *B50-B53*.

Motivation

The principle-based approach of the standard presents a great challenge to insurers since it does not exactly specify a practice. Yet, insurers must make justifiable choices in the entire development of their valuation scheme, which are compliant with the standard. For insurers already familiar with market-consistency techniques, this task may not be daunting. For others unfamiliar with this area, particularly those outside of Europe and North America, this challenge gives rise to several questions [Moody's Analytics, 2020].

1. Do closed forms exist for the embedded options and guarantees?
2. Which stochastic modeling techniques should be used (e.g. interest rate models)?
3. Which market instruments/data will the models be calibrated to ?
4. How consistent are the models in replicating observable market inputs?
5. Are the models robust?

In this thesis, we attempt to address these questions in addition to other issues subsequently raised. Our primary focus shall be on the calibration of interest rate models as they represent the key drivers of stochastic discounting. In addition, valuation of embedded guarantee products highly depends on the choice of interest model and their underlying assumptions since it is used to simulate the future evolution of the underlying fund, the policy account values as well the stochastic discount factors applied to the generated cash flow scenario. The instantaneous interest rate also represents the drift of most underlying assets (for example equity and real estate) under the risk-neutral measure \mathbb{Q} . This necessitates the use of robust interest rate models that accommodate the current ultra-low interest rates we are experiencing [Pedersen et al., 2016].

In this thesis, we provide the general steps of calibrating the two and three-factor-additive Gaussian interest rate model (known in literature as G2++ [Brigo and Mercurio, 2007] and G3++ short-rate models respectively) to swaptions by first presenting the theoretical framework and assumptions of a general n -factor-additive model following Di Francesco [2012]. The Gn++ interest rate model is a general framework for a deterministically

shifted sum of n Gaussian processes which provides an exact fit to the market term structure. We also highlight certain issues that arise during the calibration process such as the calibration method; whether to minimize the relative difference of the model and market (Black) prices or to minimize the relative difference between the model and market implied volatility. In addition, we explain some constraints imposed on this inherent global optimization problem to facilitate the optimization algorithm.

To validate the quality of the calibration, we provide a simulation scheme for swaption prices used in computing the model implied volatilities. This allows us to assess the calibrated model's fit in replicating the market volatility surface. In addition, we attempt to provide an exact simulation scheme of the short-rate under the forward and risk-neutral measures which is important in derivative pricing and risk-neutral valuation. We also provide details on simulating the stochastic discount factor under the Gn++ model based on an exact simulation devoid of discretization errors. After verifying the consistency of the calibrated model with market input, we provide an illustration of a market-consistent valuation of a segregated fund where the premium is fully invested in fixed income (bonds). This is to circumvent the need for equity modeling which is outside the scope of this work.

We also examine the issue of robustness of the interest rate model with respect to the valuation date. Interest rate models are highly sensitive to the data used to calibrate them. However these observable market inputs (e.g. implied volatilities, yield curves etc.) are designed to change following each trade to reflect their realized prices. Hence it is not surprising for calibrated model parameters to greatly differ by day. For the derivatives trader, this might not have an great implications as she calibrates the models everyday [Park, 2004]. For the valuation actuary however, this might be of practical consequence since the calibration is done on a single day of the year to satisfy regulatory requirements. Hence it is important for the financial models to not only satisfy the market-consistency criterion but also to be robust enough to provide stable financial statements. We investigate the impact of reparameterization of the interest rate model to three sets of market data with a two-day lag, where there does not seem to be a huge shift

in the market conditions e.g. yield curve and implied volatility surface. We analyse the distribution/evolution of future interest rates across the three calibration dates by first visualizing their distributions. Next we investigate the deviation of the short rate implied by the three sets of calibrations by computing their pairwise root mean square deviation across simulated short rate paths. We also analyze the stability of the segregated fund valuation results with respect to these three calibration dates.

Organization of Study

This study is organized as follows; in Chapter 1 we introduce an overview of interest rates concepts, zero-coupon bonds, interest rates derivatives specifically swaptions which are appropriate for the considered multi-factor interest rate model calibration. We also present important concepts, definitions and notations used through out this thesis. Then in Chapter 2 we present the Gn++ interest rate model following Di Francesco [2012]. Under this model, the short-rate, is a sum of n correlated Gaussian processes and a deterministic function used to provide an exact fit to the market discount curve. We introduce the dynamics of the short-rate under the risk-neutral measure and analytical formulas of the zero-coupon bond prices. We then switch to the forward-measure dynamics of the short-rate model in order to present a semi-analytic expression of the swaption price proposed by Brigo and Mercurio [2007]. Due to the numerical inefficiency of the semi-analytic formula during the calibration process, we use an approximated closed-form formula of the swaption price under the framework of Gaussian interest rate models proposed by Schrager and Pelsser [2006]. Closed-formed zero-coupon bond and swaption prices facilitates a computationally efficient calibration process to market implied swaption volatilities as opposed to using Monte-Carlo simulations or numerical techniques in calibration algorithm; albeit it comes at a cost of some approximation errors.

In Chapter 3 we discuss the general steps of calibrating the Gn++ model to market implied swaption volatilities. We also describe the nature of the relevant market input (which includes the market yield curve and the market implied volatility surface) and

consistently derive unobservable market yields by cubic spline interpolation. The calibration of the interest rate model to swaption volatilities is an optimization problem where the optimization algorithm finds parameters that minimizes the difference of observable and model implied prices. Therefore the choice of an optimization algorithm is a delicate step in the interest rate calibration because the the generated parameters are the building blocks of the model simulated cash flow scenarios used in derivative pricing and insurance contract valuation. We discuss the drawbacks of deterministic algorithms in calibrating the interest rate model and the suitability of stochastic optimization algorithms to this inherent global optimization problem; with a specific focus on the differential evolution algorithm implemented in the R package `DEoptim` by Mullen et al. [2009]. We conclude the chapter by presenting the calibration results using the techniques described.

Chapter 4 illustrates the procedures of validating the market-consistency of the calibrated interest rate model via Monte-Carlo simulation of the observable market prices as described in Pedersen et al. [2016]. We simulate the Monte-Carlo swaption prices then we use the market Black formula to find the model implied volatilities. The model implied volatility surface is then compared to the market volatility surface to assess the goodness of fit. We also provide an exact simulation scheme of the short-rate, stochastic discount factor and zero-coupon bond prices under both risk-neutral and forward-measures devoid of discretization errors by virtue of the distributional properties of the short rate. These simulated quantities are useful in generating scenarios for the underlying fund of embedded guarantee products. Then we provide an illustration of a market-consistent valuation of segregated fund invested in rolling-horizon bonds. We assume a dynamic policyholder behaviour and a deterministic mortality assumption to make our valuations more realistic.

In chapter 5, we examine the robustness of the Gn++ model and the stability of valuation results with respect to the market inputs on three different days with a two-day lag. We present the calibrated parameters of both models on the three different days and analyze the distribution of the short rate implied by different set of calibrations. We compute the root mean square deviation (RMSD) of the short rate implied by the calibration sets

for the two models separately and analyze their magnitude. Using a similar technique as before, we compute the RMSD of the underlying fund as implied by the multiple calibration set. This step ensures that the Gn++ model produces stable valuation results for financial reporting when calibrated to the different market data where there has not been a significant shift in the market.

Chapter 1

Interest Rates And Interest Rate Derivatives

1.1 Definition and Notations

Before introducing the interest rate models and its calibration to the market data, we first present the concepts underlying the interest rate theory widely documented in literature (particularly in Brigo and Mercurio [2007]). We also provide definitions and relationships of different interest rates, some important derivatives pertinent to this work together and key notations used throughout this work.

The Bank Account/Money market account

The bank account is a riskless investment for which profit is accrued continuously at the prevailing market risk-free rate Brigo and Mercurio [2007]. We denote $B(t)$ as the bank account value at any time $t \geq 0$ and assume that $B(0) = 1$. It is also assumed that the bank account evolves according to the differential equation;

$$dB(t) = r(t)B(t)dt, \quad B(0) = 1 \tag{1.1}$$

where $r(t)$ is the rate at which the bank account accrues and is referred to as the *short rate* or the *instantaneous short rate*. It can be defined as the interest rate at time t that

applies to an investment of an infinitesimally short period of time. (1.1) may be also expressed as

$$B(t) = \exp \left(\int_0^t r(s) ds \right). \quad (1.2)$$

Stochastic Discount Factor

The stochastic discount factor $D(t, T)$ between times t and T is the amount at time t that is equivalent to a unit of currency payable at time T . It is given by

$$D(t, T) = \frac{B(t)}{B(T)} = \exp \left(- \int_t^T r(s) ds \right). \quad (1.3)$$

Zero-Coupon Bond

A T -maturity zero-coupon bond is a contract that guarantees its holder the payment of one unit of currency at time T with no intermediate payments. The value of the zero-coupon bond at any time $t < T$ is denoted as $P(t, T)$ and it depends on interest rate fluctuations. Since the bond matures at T , $P(T, T) = 1$.

If the short rate process r is assumed to be deterministic, then the discount factor is also deterministic with

$$D(t, T) = P(t, T)$$

for each pair (t, T) . However if r is stochastic, which is the underlying theme of this work and consistent with happens in reality, the discount factor is also random and is related to the bond price under certain conditions described shortly.

Continuously-compounded spot interest rate

The spot interest rate is the market interest rate today that would be appropriate to determine the present value today of a single payment at time T . The continuously-compounded spot interest rate $R(t, T)$ at time t is referred to as the yield on the zero coupon bond is the constant rate at which an investment of $P(t, T)$ at time t accrues

continuously to yield a unit of currency at maturity T . Thus

$$P(t, T)e^{R(t, T)(T-t)} = 1$$

which gives

$$R(t, T) = \frac{-\ln P(t, T)}{T - t}. \quad (1.4)$$

Simply-compounded spot interest rate

The simply-compounded interest rate $L(t, T)$ at time t is the constant rate at which an investment of $P(t, T)$ accrues to one unit of currency at maturity T when accruing occurs proportionally to the investment time. Thus

$$(1 + L(t, T)(T - t))P(t, T) = 1$$

which gives

$$L(t, T) = \frac{1 - P(t, T)}{(T - t)P(t, T)}. \quad (1.5)$$

The term structure of interest rates

The term structure of interest rates also referred to as the *yield curve*, *zero-coupon curve* or *spot curve* is the function mapping maturities into spot rates at a given time t . It is given by

$$T \mapsto R(t, T), \quad T > t. \quad (1.6)$$

The spot rates on the yield curve may also be quoted in terms of other compounding conventions. The term structure of interest rates provides an indication of the market's expectation about future interest rates.

Forward rates

Forward rates are interest rates that can be locked in today for an investment in a future time period. They are interest rates known at a time t , used to discount cash flows between future time periods $[T, S]$. They are characterized by three time instants, the time t at which the rate is considered, the future time T and the maturity S with $t \leq T \leq S$.

Simply-compounded forward interest rate

The simply compounded forward rate $F(t; T, S)$ at time t for a future time T and maturity $S > T$ satisfies

$$P(t, S) = P(t, T)[1 + (S - T)F(t; T, S)].$$

Hence

$$F(t; T, S) = \frac{1}{S - T} \left(\frac{P(t, T)}{P(t, S)} - 1 \right). \quad (1.7)$$

The forward rate $F(t; T, S)$ is an estimate of the future simply compounded spot rate $L(T, S)$ which is random at time t based on market conditions. Similarly, the continuously compounded forward rate is an estimate of the future continuously compounded spot rate.

Instantaneous forward interest rate

The instantaneous forward rate $f(t, T)$ at time t for maturity $T > t$ is defined as the interest rate known at time t for an investment at a future time T for an infinitesimally short period of time. It is given by

$$f(t, T) = \lim_{S \rightarrow T^+} F(t; T, S) = \frac{-\partial \ln P(t, T)}{\partial T} \quad (1.8)$$

which gives

$$P(t, T) = \exp \left(- \int_t^T f(t, u) du \right). \quad (1.9)$$

1.1.1 No-Arbitrage Assumption And The Forward Measure

The assumptions and proofs in this subsection are not rigorous and the interested reader is directed to for example Björk [2009] and Steele [2012] for a comprehensive treatment and discussion about arbitrage theory. We assume the existence of a strictly positive and adapted process on a filtered probability space $(\Omega, \mathbb{Q}, (\mathcal{F}_t)_{0 \leq t \leq T^*})$ where T^* is the fixed time horizon for all market activities to end. \mathcal{F}_t is the sigma-algebra which represents the market information available at time t . We also assume the absence of arbitrage opportunities which implies the existence of the risk-neutral measure \mathbb{Q} such that all future discounted price processes are martingales. By this, we assume that by investing zero today, it is impossible to obtain a positive gain on your portfolio with a positive probability, without taking any loss with certainty. This also implies that portfolios having the same payoff must have the same price today. Under \mathbb{Q} , the numeraire¹ is the bank account B . For a series of zero-coupon bonds maturing at time T with price $P(t, T)$, the process $\left\{ \frac{P(t, T)}{B(t)} \right\}_{t \in [0, T]}$ is a martingale under \mathbb{Q} . Thus,

$$\begin{aligned} \frac{P(t, T)}{B(t)} &= \mathbb{E}^{\mathbb{Q}} \left[\frac{P(T, T)}{B(T)} \middle| \mathcal{F}_t \right] = \mathbb{E}^{\mathbb{Q}} \left[\frac{1}{B(T)} \middle| \mathcal{F}_t \right], \\ P(t, T) &= \mathbb{E}^{\mathbb{Q}} \left[\frac{B(t)}{B(T)} \middle| \mathcal{F}_t \right] = \mathbb{E}^{\mathbb{Q}} \left[D(t, T) \middle| \mathcal{F}_t \right]. \end{aligned} \quad (1.10)$$

The last equation is the price of the zero-coupon bond and it represents the relationship between the stochastic discount factor and the zero-coupon bond price with a unit maturity value.

¹A numeraire is a positive non-dividend paying asset used as reference to normalize other asset prices.

The Forward Measure

Sometimes \mathbb{Q} is the not most convenient measure in pricing derivatives because the stochastic discount factor $D(t, T) = \exp\left(-\int_t^T r(s)ds\right)$ complicates the expected value calculation since its joint distribution and the underlying claim to be priced has to be dealt with. We consider a martingale measure \mathbb{Q}^T equivalent to \mathbb{Q} , where \mathbb{Q}^T represents the risk-adjusted forward measure or simply the forward measure. The associated numeraire of \mathbb{Q}^T is a zero-coupon bond with maturity T . Given an asset with price process $\{S_t\}_{t \in [0, T]}$ and a terminal payoff on the asset $H(S_T)$, we know that its price at time $t \in [0, T]$ is

$$\pi_t = \mathbb{E}^{\mathbb{Q}} \left[D(t, T) H(S_T) \middle| \mathcal{F}_t \right].$$

This is mathematically equivalent to

$$\pi_t = P(t, T) \mathbb{E}^T [H(S_T) | \mathcal{F}_t] \tag{1.11}$$

where \mathbb{E}^T implies expectation under \mathbb{Q}^T . In the first equation the dynamics of S_T are postulated under \mathbb{Q} while in the second, it is postulated under \mathbb{Q}^T .

1.2 Interest Rate Swaps and Swaptions

1.2.1 Interest Rate Swaps

An interest rate swap (IRS) is a contract between two counterparties at time $t \leq T_\alpha$ to exchange interest rates at a set of pre-specified dates called settlement dates. The counterparties agree to exchange a fixed interest rate and a floating (variable) one. The exchanges are usually referred to as the legs of the swap. If we denote $\mathcal{T} = \{T_{\alpha+1}, \dots, T_\beta\}$ as the set of settlement dates, at every time $T_i, i = \alpha + 1, \dots, \beta$, the fixed leg of the contract pays

$$N\tau_i K$$

where K is the fixed interest rate (also called the *strike*), N the notional amount and $\tau_i = T_i - T_{i-1}$ while the floating leg pays the variable rate

$$N\tau_i L(T_{i-1}, T_i).$$

Although the dates of the fixed rate and floating rate payments might differ, for what concerns this work, we will only consider the case where the payments are made on the same dates throughout the duration of the contract. The duration $T_\beta - T_\alpha$ is called the swap tenor.

Where the counterparty pays the fixed rate and receives the floating rate, the IRS contract is a *Payer Swap* while a holder of a *Receiver Swap* pays the floating rate and receives the fixed rate. The floating rate is usually associated to an interbank offered rate such the LIBOR in the United Kingdom or CAD-IBOR in Canada.

The discounted payoff of a *Payer Swap* at time $t \leq T$ is

$$\sum_{i=\alpha+1}^{\beta} D(t, T_i) N\tau_i (L(T_{i-1}, T_i) - K)$$

whereas that of a *Receiver Swap* is

$$\sum_{i=\alpha+1}^{\beta} D(t, T_i) N\tau_i (K - L(T_{i-1}, T_i)).$$

Referring to Brigo and Mercurio [2007], it can be shown that the value of the *Payer Swap* contract at time t is

$$N \sum_{i=\alpha+1}^{\beta} P(t, T_i) \tau_i (F(t; T_{i-1}, T_i) - K). \quad (1.12)$$

Definition 1.2.1 *Forward Swap Rate:* *The forward swap rate at time t is the value of the fixed interest rate (strike) K that makes the IRS swap a fair contract, i.e such that the value of the contract is zero at inception.*

Notice that if we substitute the expression of the simple forward rate in (1.7), we can rewrite the value of the payer swap contract as

$$NP(t, T_\alpha) - NP(t, T_\beta) - N \sum_{i=\alpha+1}^{\beta} \tau_i K P(t, T_i). \quad (1.13)$$

The value of the *Receiver Swap* contract could also be derived by changing the signs in (1.13). By setting (1.13) equal to 0, we can solve for the the forward swap rate at time t , $S_{\alpha\beta}(t)$ as

$$S_{\alpha\beta}(t) = \frac{P(t, T_\alpha) - P(t, T_\beta)}{\sum_{i=\alpha+1}^{\beta} \tau_i P(t, T_i)}. \quad (1.14)$$

We can then express the value of IRS payer swap at t in terms of the forward swap rate as

$$N (S_{\alpha\beta}(t) - K) \sum_{i=\alpha+1}^{\beta} \tau_i P(t, T_i). \quad (1.15)$$

1.2.2 Swaptions

Definition 1.2.2 *A swaption is a combination of two types of contracts; an option and a swap. It is defined as an option on an interest rate swap. A payer (receiver) swaption gives its holder the right (and not the obligation) to enter into a payer (receiver) swap at the maturity of the swaption with a pre-determined strike K .*

There are three main types of swaptions namely; European, Bermudan and American swaptions whose differences mainly lie with their exercise dates as in equity options. In this thesis, we shall only consider European swaptions. The maturity date of an European swaption usually coincides with the first reset date T_α of the underlying IRS. A swaption with maturity T_α and tenor $T_\beta - T_\alpha$ (duration of the underlying swap) is termed a $T_\alpha \times (T_\beta - T_\alpha)$ swaption. Since an option will only be exercised if it generates a

positive a payoff, for a payer swaption payoff at the maturity of the swaption T_α is then

$$N \left(\sum_{i=\alpha+1}^{\beta} P(T_\alpha, T_i) \tau_i (F(T_\alpha; T_{i-1}, T_i) - K) \right)^+. \quad (1.16)$$

We can see that it is not feasible to decompose the payoff additively since summation is inside the convex function $()^+$. Consequently, when valuing the swaption, the joint distribution of the forward rates between the settlement dates of the swap has an impact on the price and so they need to be appropriately dealt with.

As previously described, the value of the IRS can be expressed in the terms of the forward swap rate. By making the relevant substitutions, we can express the payoff of the payer swaption in a similar fashion as

$$\left(N (S_{\alpha\beta}(T_\alpha) - K) \sum_{i=\alpha+1}^{\beta} \tau_i P(T_\alpha, T_i) \right)^+.$$

The value of the swaption with a strike K at time $t \leq T_\alpha$ is

$$\begin{aligned} PS[t, T_\alpha, T_\beta, K, N] &= \mathbb{E}^{\mathbb{Q}} \left[D(t, T_\alpha) \left(N (S_{\alpha\beta}(T_\alpha) - K)^+ \sum_{i=\alpha+1}^{\beta} \tau_i P(T_\alpha, T_i) \right) \middle| \mathcal{F}_t \right] \\ &= P(t, T_\alpha) \mathbb{E}^{T_\alpha} \left[\left(N (S_{\alpha\beta}(T_\alpha) - K)^+ \sum_{i=\alpha+1}^{\beta} \tau_i P(T_\alpha, T_i) \right) \middle| \mathcal{F}_t \right]. \end{aligned} \quad (1.17)$$

The term $\sum_{i=\alpha+1}^{\beta} \tau_i P(T_\alpha, T_i)$ is called the Present Value of a Basis Point (PVBP) or annuity factor and it reflects the changes in the fixed rates as the swap rate changes by a basis point. Thus a payer swaption can be viewed as a call option on the swap rate. Similarly we can find the price of a receiver swaption at time t , $RS[t, T_\alpha, T_\beta, K, N]$, by changing the minus sign in (1.17) to a positive sign and negating the swap rate at maturity. The receiver swaption can also be viewed as a put option on the forward swap rate.

Definition 1.2.3 *A payer (receiver) swaption is said to be At-The-Money (ATM) if the*

strike K is equal to the forward swap rate at time $t = 0$:

$$K = S_{\alpha,\beta}(0) = \frac{P(0, T_\alpha) - P(0, T_\beta)}{\sum_{i=\alpha+1}^{\beta} \tau_i P(0, T_i)}.$$

A payer swaption is *In-The-Money* if $S_{\alpha\beta}(0) > K$, and *Out-Of-The money* if $S_{\alpha\beta}(0) < K$. The opposite holds for a receiver swaption.

Now consider portfolio where you are holder of payer swaption and the counterparty of a receiver swaption with the same strike K , maturity T_α , settlement dates $\mathcal{T} = \{T_{\alpha+1}, \dots, T_\beta\}$ and notional value N . The value of this portfolio at any time $t \leq T_\alpha$ is

$$\pi_t = PS[t, T_\alpha, T_\beta, K, N] - RS[t, T_\alpha, T_\beta, K, N]$$

so that at the maturity T_α , the payoff on the portfolio is

$$\pi_{T_\alpha} = N \sum_{i=\alpha+1}^{\beta} \tau_i P(T_\alpha, T_i) [(S_{\alpha\beta}(T_\alpha) - K)^+ - (K - S_{\alpha\beta}(T_\alpha))^+].$$

If the strike K is less than the swap rate $S_{\alpha\beta}(T_\alpha)$, you will exercise the payer swaption to pay a fixed rate and receive the floating rate; the holder of the receiver swaption will not exercise their swaption. On the hand, if the strike $K > S_{\alpha\beta}(T_\alpha)$, you not will not exercise the payer swaption but the receiver swaption holder will exercise their swaption for you to pay the fixed rate and receive the floating one. In any case, you will pay a fixed rate and receive a floating one so that the payoff of the portfolio is equal to that of a payer swap with the same strike and contract terms. Hence

$$\pi_{T_\alpha} = \text{payoff of a payer swap} .$$

The strike K which makes for a fair payer swap i.e. equals 0 is the ATM strike. By the no-arbitrage assumption, the value of the portfolio should also be 0 for this same strike. Hence for an ATM strike, the price of a payer swaption will equal that of a receiver

swaption.

Remark 1.2.1 *In the financial markets, swaption prices are often based on a Black-like formula formally known as the Black-76 formula.*

The Black-76 model

Definition 1.2.4 Black Price: *The Black price of a swaption at time $t = 0$ is defined as*

$$\text{Black Price} = N\omega [S_{\alpha,\beta}(0)\Phi(\omega d_1) - K\Phi(\omega d_2)] \sum_{i=\alpha+1}^{\beta} \tau_i P(T_\alpha, T_i) \quad (1.18)$$

where

$$d_1 = \frac{\ln\left(\frac{S_{\alpha,\beta}(0)}{K}\right) + \frac{\sigma_{\alpha,\beta}^2 T_\alpha}{2}}{\sigma_{\alpha,\beta}\sqrt{T_\alpha}} \quad \text{and} \quad d_2 = \frac{\ln\left(\frac{S_{\alpha,\beta}(0)}{K}\right) - \frac{\sigma_{\alpha,\beta}^2 T_\alpha}{2}}{\sigma_{\alpha,\beta}\sqrt{T_\alpha}}$$

where Φ is cumulative normal distribution function, $\omega = 1$ for a payer swaption and $\omega = -1$ for a receiver swaption. $\sigma_{\alpha,\beta}$ is the Black volatility of the swaption provided on the market volatility surface.

The Black model makes use of some assumptions in the derivation of the European swaption price. It assumes the swap rate is, under some suitable martingale measure, a driftless geometric Brownian motion which is lognormally distributed. Although this assumption is inconsistent with our chosen interest rate model described subsequently, the Black-76 model is useful as a *standard metric* by market traders in solving for the implied volatility $\sigma_{\alpha,\beta}$ such that when plugged into d_1 in (1.18), the Black price matches the prevailing market swaption price, hence its relevance in our study.

Since the price of an *ATM* receiver swaption equals that of an *ATM* payer swaption, we can drop ω in the Black price formula in (1.18) and with $S_{\alpha,\beta}(0) = K$, $d_1 = \frac{\sigma_{\alpha,\beta}\sqrt{T_\alpha}}{2}$ and $d_2 = -d_1$, the Black price for *ATM* swaptions is given as

$$\text{Black Price}^{ATM} = NS_{\alpha,\beta}(0) [2\Phi(d_1) - 1] \sum_{i=\alpha+1}^{\beta} \tau_i P(T_\alpha, T_i).$$

Chapter 2

The Interest Rate Model

There is a wide variety of interest rate models in literature; from simple one-factor models to more complex multi-factor models. The choice of an interest rate model particularly depends on the application, the theoretical assumptions of the model such as mean-reversion, the model's analytical tractability (allowing for closed-form solutions of zero-coupon bond prices, bond-option prices etc), ease of implementation etc. Term structure models like the Nelson-Siegel model provide polynomial representations of the yield curve that are used for interpolating and forecasting the yield curve based on observed rates. Although they are easy to implement and interpret, they prescribe the shape of the yield curve and are not arbitrage-free. Due to this, they can not be used to price most interest-rate derivatives and consequently value direct participation insurance contracts. The Nelson-Siegel model is still heavily relied on by most central banks and wealth managers for daily yield curve construction and forecasting [Coroneo et al., 2011].

2.1 Short-Rate Models

Short-rate models characterize the evolution of the yield curve by modeling the instantaneous short-rate. From 1.10 and 1.3, we can observe that, when we model the distributional properties of the short-rate r , conditional on \mathcal{F}_t , we are able to compute bond prices at all maturities T and time references t from which we can compute the spot rates, forward rates etc, through the various relationships described in the previous chap-

ter. This implies that choosing the appropriate short-rate model is crucial in describing a realistic evolution of the yield curve. [Brigo and Mercurio, 2007].

2.1.1 Endogenous Models

The Vasicek model is one of the earliest short-rate models that was proposed. In this model, the short rate evolves as an Ornstein-Uhlenbeck (OU) process. The Vasicek model assumes that the short-rate is normally distributed which makes it analytically tractable although this implies the possibility of negative interest rates which is considered a drawback of the model. As an OU process, it is mean-reverting which is a desirable property of interest rates models. Unlike stock prices, interest rates cannot rise indefinitely; otherwise the economy will crash. Hence it is desirable for the model assumption to allow interest rates to move within a bounded range, showing a tendency to revert to a long term mean as described by general economic phenomenon [Hull, 2018]. The Cox–Ingersoll–Ross (CIR), Exponential Vasicek (EV) (extensions of the Vasicek model) and Dothan models were proposed to address the negativity of the short rate. The CIR model assumes that the short rate has a noncentral chi-squared distribution while the EV and Dothan models assume that the short rate is a geometric Brownian motion hence lognormally distributed. Although the distributional assumption of the EV and Dothan models eradicates the possibility of a negative short rate, this can lead to explosion in the bank account value in an arbitrary small time δt as shown in Brigo and Mercurio [2007]. The Vasicek, CIR, EV and Dothan short-rate models are endogenous models such that the market term structure is a model output specified by the calibrated parameters. It has been shown that regardless of how they are calibrated, they cannot exactly match the market yield curve Brigo and Mercurio [2007]. Therefore for the purpose of market-consistent valuations, these models are not appropriate. These class of endogenous short-rate models are also referred to as “equilibrium models” [Hull, 2018].

2.1.2 Exogenous One-Factor Models

Ho and Lee [1986] proposed the first short-rate model to address the inconsistencies of endogenous models. Their model was deemed to have a drawback due to the absence of mean-reversion which is considered as an important property of the short rate dynamics. The Hull & White (also called the extended Vasicek) model introduces one of the most widely used short-rate model in the financial markets today, the Hull-White one-factor model (see for example Park [2004]). The model rectifies the inconsistency between the implied term structure of the Vasicek model and the market term structure by adding a deterministic function to the Vasicek model which ensures that the model provides an exact fit to the market yield curve. Later, Hull & White modified their previous extension of the Vasicek model to account for time-varying drift and volatility coefficients of the short-rate model. The Black-Karasinski model is also one of the most widely used models which was introduced as an extension of the Vasicek model to address both limitations of possible negative rates and inconsistency between the model implied and the market yield curves. The Black-Karasinski model, as other lognormal short-rate models, leads to an explosion of the bank account value.

Brigo and Mercurio [2007] provides a general framework to deterministically shift endogenous models to exactly fit the observed term structure while still maintaining their desirable properties. By their framework, the deterministically shifted Vasicek model is equivalent to the time homogeneous Hull-White one-factor model which can be referred to as the G1++ for reasons that will be obvious later. The shifted CIR model is called the CIR++ and so on. Exogenous models are also referred to as “no-arbitrage” models which is unrelated to no-arbitrage pricing. The concept of no arbitrage principle can be used to value any derivative or payoff irrespective of model choice, however due to the mismatches between the equilibrium models and the market term structure, there is less confidence in the the model implied price [Hull, 2018]¹.

¹The are other interest rate models such as the Heath-Jarrow Morton framework and the market models which are outside the scope of this work.

2.1.3 Exogenous Multi-Factor Models

While exogenous one-factor models provide market-consistent calibrations, they assume a perfect correlation between spot rates of different maturities. This assumption results in a poor description of the future evolution of interest rates and inaccuracy in pricing some derivatives since it has been proven that interest rates of different maturities do exhibit some form of decorrelation [Brigo and Mercurio, 2007]. One-factor models may be useful in pricing derivatives which do not depend on the correlation of different interest rates but rather on a single interest-rate e.g. caps and floors. As we saw from the previous chapter, the swaption price (1.16) depends on the correlation between forward rates of varying maturities which makes one-factor models inappropriate in their pricing.

Additionally, empirical analysis through principal component analysis has shown that the first two principal components explains 85% to 90% of the variations in the yield curve while three principal components explains 93% to 94% of total variation [Litterman and Scheinkman, 1991, Jamshidian and Zhu, 1996]. The first factor is deemed to represent the parallel shift of the curve, the second factor represents the slope and the third factor is the curvature of the curve. This implies that a two or higher-dimensional process is needed to capture realistic correlation patterns between interest rates and provide a realistic future evolution of the whole yield curve (see [Brigo and Mercurio, 2007, p.137-139] for a comprehensive discussion about the motivations of two to three factor short-rate models). In view of this, we are motivated to consider a two and three-factor short-rate exogenous model as our model choice. It is important to note that the multi-factor models do have their drawbacks such as numerical inefficiency and overfitting (following input noise too closely) especially when the model parameters are dependent on time Brigo and Mercurio [2007]. Such situations tends to make the model interpretation difficult. Their advantages (e.g replicating satisfactory market prices etc.) however outweigh their drawbacks especially in realistic market situations.

Brigo and Mercurio [2007] further extended the Vasicek model by adding another OU process to provide two-dimensional sources of randomness and a deterministic function to ensure an exact fit to the observed yield curve. They showed that by some coordinate

transformation, the G2++ is equivalent to the two-factor Hull-White model. They also explain that a similar technique to their extension could be applied to account for more sources of randomness, i.e. three or more factors in modeling the short-rate process.

This chapter follows Di Francesco [2012] to provide a general framework of the n -factor additive Gaussian model under which the short rate is sum of n correlated Gaussian processes (which evolve as OU processes) and a deterministic function used to provide an exact fit to the market yield curve. The choice of this model is motivated by its mean-reversion and suitability for the current low interest rate environment (to some extent) through the assumption of a normally distributed short rate process. Its assumption of a normally distributed short rate process also provides closed-form solutions of zero-coupon bond and bond options.

2.2 The Gn++ Short-Rate Model

2.2.1 The Risk-Neutral Short-Rate Dynamics

Under the general factor-additive model, the dynamics of the short-rate process under the risk-neutral measure \mathbb{Q} is given by

$$r(t) = \sum_{i=1}^n x_i(t) + f(t) , r(0) = r_0 \quad (2.1)$$

such that each factor $\{x_i(t) : t > 0\}$ evolves according to an Ornstein–Uhlenbeck process and satisfies the stochastic differential equation

$$dx_i(t) = -a_i x_i(t) dt + \sigma_i dW_i(t), \quad x_i(0) = 0 , i = 1, \dots, n \quad (2.2)$$

where a_i and σ_i are positive constants ² which represent the speed of mean reversion to the mean level of 0 and the volatility of the process respectively. $W_i, i = 1, \dots, n$ is a multivariate standard Brownian motion under \mathbb{Q} . We assume that the filtration $\mathbb{F} = \{(\mathcal{F}_t)_{0 \leq t \leq T^*}\}$ is generated by the multi-dimensional Brownian motion $W_i, i = 1, \dots, n$.

²The drift and volatility can be time-dependent as in the original paper and Hull-White model.

For every $t > 0$,

$$dW_i(t)dW_j(t) = \rho_{ij}dt \text{ for } i, j = 1, \dots, n$$

where $-1 \leq \rho_{ij} \leq 1$, is the correlation between the Brownian motion W_i and W_j and as usual $\rho_{ii} = 1$, for $i = 1, \dots, n$. The correlation matrix $(\rho_{ij})_{i,j=1,\dots,n}$ is assumed to be symmetric and positive semi-definite. The function f is deterministic and well defined in the interval $[0, T^*]$. By applying Itô's lemma on (2.2), conditional on \mathcal{F}_s we have that

$$x_i(t) = x_i(s)e^{-a_i(t-s)} + \int_s^t \sigma_i e^{-a_i(t-u)} dW_i(u). \quad (2.3)$$

The last term in (2.3) is an integral of a deterministic function with respect to the Brownian motion which makes it a Gaussian random variable with null mean. Hence conditional on \mathcal{F}_s , the process $\{x_i(t), i = 1, \dots, n\}$ is normally distributed with mean $x_i(s)e^{-a_i(t-s)}$ and variance

$$\begin{aligned} \text{var}[x_i(t)|\mathcal{F}_s] &= \mathbb{E} \left[\left(\int_s^t \sigma_i e^{-a_i(t-u)} dW_i(u) \right)^2 \right] \\ &= \left[\left(\int_s^t \sigma_i^2 e^{-2a_i(t-u)} d(u) \right)^2 \right] && \text{By Itô's Isometry} \\ &= \frac{\sigma_i^2}{2a_i} (1 - e^{-2a_i(t-s)}). \end{aligned}$$

Therefore (2.1) can be expressed as

$$r(t) = \sum_{i=1}^n \left(x_i(s)e^{-a_i(t-s)} + \int_s^t \sigma_i e^{-a_i(t-u)} dW_i(u) \right) + f(t) \quad (2.4)$$

for every $s < t$. It follows that, conditional on \mathcal{F}_s , the short-rate process is normally distributed with mean

$$\mathbb{E}^{\mathbb{Q}}[r(t)|\mathcal{F}_s] = \sum_{i=1}^n x_i(s)e^{-a_i(t-s)} + f(t) \quad (2.5)$$

and variance

$$\begin{aligned}
\text{var}[r(t)|\mathcal{F}_s] &= \text{var} \left[\sum_{i=1}^n \left(\int_s^t \sigma_i e^{-a_i(t-u)} dW_i(u) \right) \right] \\
&= \sum_{i,j=1}^n \text{cov} \left(\int_s^t \sigma_i e^{-a_i(t-u)} dW_i(u), \int_s^t \sigma_j e^{-a_j(t-u)} dW_j(u) \right) \\
&= \sum_{i,j=1}^n \mathbb{E} \left(\int_s^t \sigma_i e^{-a_i(t-u)} dW_i(u) \int_s^t \sigma_j e^{-a_j(t-u)} dW_j(u) \right).
\end{aligned}$$

By Itô's Isometry, this becomes

$$\text{var}[r(t)|\mathcal{F}_s] = \sum_{i,j=1}^n \left(\int_s^t \sigma_i \sigma_j \rho_{ij} e^{-(a_i+a_j)(t-u)} du \right)$$

which simplifies to

$$\text{var}[r(t)|\mathcal{F}_s] = \sum_{i,j=1}^n \frac{\sigma_i \sigma_j}{a_i + a_j} \rho_{ij} (1 - e^{-(a_i+a_j)(t-s)}). \quad (2.6)$$

The means that with a positive probability, the short rate can be negative, which is usually considered as a drawback of the Gaussian additive interest rate model.

2.2.2 Analytical Zero Coupon Bond Price

Through a suitable choice of the function f , the short-rate model gives an exact fitting to the observed term structure if the model zero-coupon bond price $P(0, T)$ is equal to the market bond price $P^M(0, T)$. The value of the zero-coupon bond at time $t = 0$ is expressed by the usual relationship

$$P(0, T) = \mathbb{E}^{\mathbb{Q}} \left[e^{-\int_0^T r(t) dt} \right].$$

In order to compute the value of the zero coupon bond under the Gn++ model, we need to integrate $r(t)$ over the term of the bond. By first considering the integral of the

process, $\sum_{i=1}^n x_i(t)$, $i = 1, \dots, n$, conditional on \mathcal{F}_0 , we have

$$\int_0^T \sum_{i=1}^n x_i(t) dt = \int_0^T \sum_{i=1}^n \int_0^t \sigma_i e^{-a_i(t-u)} dW_i(u) dt \quad (2.7)$$

Applying *Fubini's theorem* on stochastic integrals, it can be shown that

$$\int_0^T \sum_{i=1}^n x_i(t) dt = \sum_{i=1}^n \int_0^T e^{au} \int_u^T \sigma_i e^{-a_i t} dt dW_i(u) \quad (2.8)$$

$$= \sum_{i=1}^n \int_0^T \frac{\sigma_i (1 - e^{a_i(T-u)})}{a_i} dW_i(u). \quad (2.10)$$

This implies that $\int_0^T \sum_{i=1}^n x_i(t) dt$ is a deterministic Itô integral and it is normally distributed with mean

$$\mathbb{E}^{\mathbb{Q}} \left[\int_0^T \sum_{i=1}^n x_i(t) dt \right] = 0$$

and variance

$$\begin{aligned} \text{var} \left[\int_0^T \sum_{i=1}^n x_i(t) dt \right] &= \sum_{i,j=1}^n \int_0^T \rho_{ij} \frac{\sigma_i (1 - e^{a_i(T-u)})}{a_i} \frac{\sigma_j (1 - e^{a_j(T-u)})}{a_j} du \\ &= \sum_{i,j=1}^n \rho_{ij} \frac{\sigma_i \sigma_j}{a_i a_j} \left(T - \frac{1 - e^{-a_i T}}{a_i} - \frac{1 - e^{-a_j T}}{a_j} + \frac{1 - e^{-(a_i + a_j)T}}{a_i + a_j} \right) \\ &:= V(0, T). \end{aligned} \quad (2.11)$$

The model zero-coupon bond price can be expressed as

$$\begin{aligned} P(0, T) &= \mathbb{E}^{\mathbb{Q}} \left[e^{-\int_0^T \sum_{i=1}^n x_i(t) + f(t) dt} \right] \\ &= e^{-\int_0^T f(t) dt} \mathbb{E}^{\mathbb{Q}} \left[e^{-\int_0^T \sum_{i=1}^n x_i(t) dt} \right]. \end{aligned}$$

Using the fact that for $Z \sim N(\mu_z, \sigma_z^2)$, $E[e^Z] = e^{\mu_z + \frac{1}{2}\sigma_z^2}$. Then

$$P(0, T) = e^{-\int_0^T f(t) dt} e^{\frac{1}{2}V(0, T)}. \quad (2.12)$$

The model provides an exact fit to market discount factor curve if for $T > 0$

$$P^M(0, T) = e^{-\int_0^T f(t)dt} e^{\frac{1}{2}V(0, T)}. \quad (2.13)$$

Denoting $f^M(0, T)$ as the market instantaneous forward rate then (2.13) becomes

$$e^{-\int_0^T f^M(0, t)dt} = e^{-\int_0^T f(t)dt} e^{\frac{1}{2}V(0, T)}. \quad (2.14)$$

Since the basis agree, we can differentiate the exponents in Equation (2.14) with respect to T and obtain an explicit solution for the deterministic function f as

$$f(T) = f^M(0, T) + \frac{1}{2} \sum_{i, j=1}^n \rho_{ij} \frac{\sigma_i \sigma_j}{a_i a_j} (1 - e^{-a_i T})(1 - e^{-a_j T}). \quad (2.15)$$

In order to compute the analytical bond price $P(t, T)$ at time t for every $0 < t < T$, we can apply similar techniques in (2.10) to show that, conditional on \mathcal{F}_t , the integral $\int_t^T \sum_{i=1}^n x_i(s)ds$ is normally distributed such that

$$\mathbb{E}^{\mathbb{Q}} \left[\int_t^T \sum_{i=1}^n x_i(s)ds \middle| \mathcal{F}_t \right] = \sum_{i=1}^n x_i(t) \frac{(1 - e^{-a_i(T-t)})}{a_i}, \quad (2.16)$$

$$\text{var} \left[\int_t^T \sum_{i=1}^n x_i(s)ds \middle| \mathcal{F}_t \right] = \sum_{i, j=1}^n \rho_{ij} \frac{\sigma_i \sigma_j}{a_i a_j} \left(T - t - \frac{1 - e^{-a_i(T-t)}}{a_i} - \frac{1 - e^{-a_j(T-t)}}{a_j} + \frac{1 - e^{-(a_i+a_j)(T-t)}}{a_i + a_j} \right) \quad (2.17)$$

$$:= V(t, T). \quad (2.18)$$

Hence we can compute the model bond price $P(t, T)$ at any time $0 < t < T$ as

$$P(t, T) = \mathbb{E}^{\mathbb{Q}} \left[e^{-\int_t^T r(s)ds} \right] = \mathbb{E}^{\mathbb{Q}} \left[e^{-\int_t^T \sum_{i=1}^n x_i(s) + f(s)ds} \right] \quad (2.19)$$

$$= e^{-\int_t^T f(s)ds} \mathbb{E}^{\mathbb{Q}} \left[e^{-\int_t^T \sum_{i=1}^n x_i(s)} \right] \quad (2.20)$$

$$= e^{-\int_0^T f(s)ds} e^{\int_0^t f(s)ds} e^{-\sum_{i=1}^n x_i(t) \frac{1 - e^{-a_i(T-t)}}{a_i} + \frac{1}{2}V(t, T)}. \quad (2.21)$$

Using equation (2.14) we can express the model bond price in (2.21) as

$$\begin{aligned} P(t, T) &= \frac{P^M(0, T)}{P^M(0, t)} e^{\frac{1}{2}[V(t, T) - V(0, T) + V(0, t)]} e^{-\sum_{i=1}^n x_i(t) \frac{1 - e^{-a_i(T-t)}}{a_i}} \\ &= A(t, T) e^{-\sum_{i=1}^n B_i(t, T) x_i(t)} \end{aligned} \quad (2.22)$$

where

$$\begin{aligned} A(t, T) &= \frac{P^M(0, T)}{P^M(0, t)} e^{\frac{1}{2}(V(t, T) - V(0, T) + V(0, t))}, \\ B_i(t, T) &= \frac{1 - e^{-a_i(T-t)}}{a_i}. \end{aligned} \quad (2.23)$$

2.2.3 The Short-Rate Dynamics Under The Forward Measure

In order to obtain a closed-form expression that approximates the swaption to facilitate easier and time efficient calibration to market prices, we need define r under the forward measure dynamics \mathbb{Q}^T . Referring to the detailed proofs in Brigo and Mercurio [2007], Casalini and Bonino [2020] and the references therein, for any fixed maturity T , by the Girsanov's Theorem, the dynamics of the process $\{x_i(t), i = 1, \dots, n\}$ under \mathbb{Q}^T is given by

$$dx_i(t) = -a_i x_i(t) - \sigma_i \left(\sum_{j=1}^n \sigma_j \rho_{ij} B_j(t, T) \right) dt + \sigma_i dW_i^T(t) \quad (2.24)$$

where W_i^T is standard Brownian motion under \mathbb{Q}^T with $dW_i^T(t) dW_j^T(t) = \rho_{ij}$. Applying Itô's lemma on Equation (2.24), conditional on \mathcal{F}_s ,

$$x_i(t) = x_i(s) e^{-a_i(t-s)} - M_i^T(s, t) + \sigma_i \int_s^t e^{-a_i(t-u)} dW_i^T(u) \quad (2.25)$$

where

$$M_i^T(s, t) = \sigma_i \sum_{j=1}^n \frac{\sigma_j}{a_j} \rho_{ij} \left(\frac{1 - e^{-a_i(t-s)}}{a_i} - \frac{e^{-a_j(T-t)} - e^{-a_j(T-s) - a_i(t-s)}}{a_i + a_j} \right) \quad (2.26)$$

is the additional deterministic drift term. Hence, the short rate $r(t)$ is normally distributed under \mathbb{Q}^T with mean and variance given respectively by,

$$\begin{aligned}\mathbb{E}^T[r(t)|\mathcal{F}_s] &= \sum_{i=1}^n (x_i(s)e^{-a_i(t-s)} - M_i^T(s, t)) + f(t), \\ \text{Var}^T[r(t)|\mathcal{F}_s] &= \sum_{i=1}^n \frac{\sigma_i \sigma_j}{a_i + a_j} \rho_{ij} (1 - e^{-(a_i + a_j)(t-s)}).\end{aligned}\tag{2.27}$$

2.2.4 Swaption Price Under The Gn++ Model

Recall from the previous chapter that, for a European payer swaption with maturity T_α , strike K , nominal value N , which gives the holder the right to enter at time T_α , a swap with payment dates $T_{\alpha+1}, \dots, T_\beta$ where she pays the fixed rate and receives the floating rate, the price of the swaption at time $t = 0$ is given by (1.17). Since the forward swap rate at time T_α is given as $S_{\alpha\beta}(T_\alpha) = \frac{P(T_\alpha, T_\alpha) - P(T_\alpha, T_\beta)}{\sum_{k=\alpha+1}^\beta \tau_k P(T_\alpha, T_k)}$, and $P(T_\alpha, T_\alpha) = 1$, then the swaption price becomes

$$PS[0, T_\alpha, T_\beta, K, N] = NP(0, T_\alpha) \mathbb{E}^{T_\alpha} \left[\left(1 - \sum_{k=\alpha+1}^\beta c_k P(T_\alpha, T_k) \right)^+ \right]\tag{2.28}$$

where $c_k = K\tau_k$ and $c_\beta = 1 + K\tau_\beta$. By equation (2.23),

$$\begin{aligned}PS[0, T_\alpha, T_\beta, K, N] &= NP(0, T_\alpha) \int_{\mathbb{R}^n} \left(1 - \sum_{k=\alpha+1}^\beta c_k A(T_\alpha, T_k) e^{-\sum_{i=1}^n B_i(T_\alpha, T_k) x_i(T_\alpha)} \right)^+ \\ &\quad g(x_1, \dots, x_n) dx_1 \dots dx_n\end{aligned}\tag{2.29}$$

where g denotes the joint density function of the multivariate Gaussian random vector $X = [x_1(T_\alpha), \dots, x_n(T_\alpha)]$ with dynamics postulated under \mathbb{Q}^{T_α} . The random vector has mean

$$\mathbb{E}[X] = \boldsymbol{\mu} = [-M_1^T(0, T_\alpha), \dots, -M_n^T(0, T_\alpha)]$$

and covariance matrix $\mathbf{C}(T_\alpha)$ such that

$$C_{ij}(T_\alpha) = \frac{\sigma_i \sigma_j}{a_i + a_j} \rho_{ij} (1 - e^{-(a_i + a_j)T_\alpha}).$$

Thus

$$g(x_1, \dots, x_n) = \frac{1}{\sqrt{(2\pi)^n} |\mathbf{C}(T_\alpha)|} \exp\left(-\frac{1}{2}(X - \boldsymbol{\mu})^\top (\mathbf{C}(T_\alpha))^{-1} (X - \boldsymbol{\mu})\right)$$

In practice, the numerical solution of the integral in equation (2.29) is computationally inefficient for a large n . [Brigo and Mercurio, 2007, p. 173-174] derived a simplification of (2.29) to a one-dimensional integral for case when $n = 2$, i.e the G2++ model which resulted in semi-closed form of (2.29). In order to numerically implement the semi-closed form formula for the G2++ by Brigo and Mercurio [2007], the bounds will have to be truncated to apply for example a Gaussian quadrature or a Monte Carlo integration in solving the integral. However in calibrating the model to market price described subsequently, which is root finding problem across hundreds of iterations to estimate the parameters, these methods prove to be computationally intensive given the number instruments, iterations and simulation paths required to converge to an accurate solution. A similar case applies to the G3++ model. Hence in calibrating the Gn++ to market data, we will use an approximation of the swaption price by Schrager and Pelsser [2006] and then validate the quality of calibration via Monte-Carlo simulation.

Schrager and Pelsser [2006] proposed a method that approximates the European swaption price for affine term structure models which includes the Gn++ model. As shown in their paper, their method leads to a closed-form formula for the price of an European swaption in the framework of both one and multi-factor Gaussian short rate models. For an At-The-Money swaption, the price can be approximated by

$$PS[0, T_\alpha, T_\beta, K, N] \simeq N \frac{\text{VOL}}{\sqrt{2\pi}} \sum_{k=\alpha+1}^{\beta} \tau_k P(0, T_k) \equiv N \frac{\text{VOL}}{\sqrt{2\pi}} P_{T_{\alpha+1}}^{T_\beta} \quad (2.30)$$

where VOL is the approximated volatility of the underlying swap and is given by

$$\text{VOL} = \sqrt{\sum_{i,j=1}^n \sigma_i \sigma_j \rho_{ij} A_i A_j \frac{e^{(a_i+a_j)T} - 1}{a_i + a_j}}$$

and for every $i = 1, \dots, n$,

$$A_i = \frac{1}{a_i} \left[e^{-a_i T} \frac{P(0, T)}{P_{T_{\alpha+1}}^{T_\beta}} - e^{-a_j T_\beta} \frac{P(0, T_\beta)}{P_{T_{\alpha+1}}^{T_\beta}} - K \sum_{k=\alpha+1}^{\beta} e^{-a_i t_k} \tau_k \frac{P(0, T_k)}{P_{T_{\alpha+1}}^{T_\beta}} \right].$$

Although (2.30) is an approximation of the true price, it has provided satisfactory calibration results in similar works, for example Russo and Torri [2019] in calibrating two-factor Hull-White and Di Francesco [2012] for the G2++ and G3++ model. One of the drawbacks of (2.30) is that the approximation error tends to be high for longer maturity and longer tenor swaptions as seen in Schrage and Pelsser [2006] and Di Francesco [2012].

Chapter 3

Gn++ Model Calibration to Market Data

Calibration is the process of determining the parameters of the interest rate model. It generally consists of choosing liquid instruments similar to the products to be priced or valued and determining the parameters so that the difference between the market prices of the instruments and those predicted by the model are minimized. The method of calibration usually depends on the application of the interest rate model and the availability of deep liquid markets. The Gn++ short-rate model can be calibrated to a time series of historical interest rates or interest rate volatility as in Park [2004] and Aas et al. [2018] or to current prices of interest rate derivatives. For the purpose of market-consistent valuations, the latter is obviously the relevant choice. To make our valuations as consistent as possible, it is important to parameterize our model to highly liquid interest rate derivatives if they are available. Swaptions, caps and floors are some of the liquid instruments on the market. Caps and floors do not rely on the correlation between forward rates and so one-factor models provide highly satisfactory fit to their market volatility surface. As previously mentioned, swaptions rely on the correlation between forward rates and so they are more suitable to be calibrated to by multi-factor model. We calibrate our models to ATM swaption volatilities (prices) since they are there more actively traded (liquid) and so their market quotes are more reliable. It is market

practice to quote swaptions in terms of their implied volatilities and not necessarily their prices. The quoted volatilities can however be translated into prices by using the Black formula (1.18).

3.1 The Calibration Problems

The calibration algorithm essentially tries to find the set of parameters $\theta^* = (a_i^*, \sigma_i^*, \rho_{ij}^*, \text{ for } i, j = 1, \dots, n)$ that minimizes the sum of absolute relative errors between market and model prices. This optimization could be implemented in two different ways:

1. Minimizing the sum of absolute relative errors between the market and Gn++ model swaption prices as in Di Francesco [2012].
2. Minimizing the sum of absolute relative errors between the market and model implied volatilities as in Brigo and Mercurio [2007] and Ferranti [2015].

Assuming we have N set of instruments, with the first method, our objective function will then be of the form

$$\theta^* = \arg \min_{\theta} \sum_{i=1}^N \frac{|\text{Price}_i^{Mkt} - \text{Price}_i^{Gn++}|}{\text{Price}_i^{Mkt}} \quad (3.1)$$

where the Price_i^{Mkt} and Price_i^{Gn++} are the market price and theoretical price of the i th swaption respectively. On the other hand, for the second method, we would have,

$$\theta^* = \arg \min_{\theta} \sum_{i=1}^N \frac{|\sigma_i^{Mkt} - \sigma_i^{Gn++}|}{\sigma_i^{Mkt}} \quad (3.2)$$

where σ_i^{Mkt} and σ_i^{Gn++} are the market/quoted and model implied volatility respectively. For the first objective function the market price is computed by the Black formula (1.18). Hence we have all the necessary quantities to implement the first objective function right away.

However for the second objective function, the theoretical implied volatility has to be calculated by inverting the Gn++ swaption price. For the ATM swaptions, this is quite

straightforward. However the results get a bit complicated if we consider non-ATM swaptions. But since we only calibrate our model to only ATM swaptions the we do not address such complexities.

In fact, for given set of parameters $\theta = (a_i, \sigma_i, \rho_{ij}, i, j = 1, \dots, n)$, the algorithm calculates the model analytical price Price^{Gn++} and then tries to find the implied volatility σ_i^{Gn++} that makes the market price equal theoretical price. So the algorithm tries to solve for the model implied volatility σ^{Gn++} , such that when plugged into the expression for d_1 , the Black price yields the model price. That is

$$NS_{\alpha,\beta}(0) [2\Phi(d_1) - 1] \sum_{i=\alpha+1}^{\beta} \tau_i P(0, T_i) = \text{Price}^{Gn++}. \quad (3.3)$$

Hence we can solve for the model implied volatility as

$$\sigma^{Gn++} = \frac{2}{\sqrt{T_\alpha}} \Phi^{-1} \left[\frac{\text{Price}^{Gn++}}{2NS_{\alpha,\beta}(0) \sum_{i=\alpha+1}^{\beta} \tau_i P(0, T_i)} + \frac{1}{2} \right]. \quad (3.4)$$

Imposed Constraints

A major problem about the about finding the theoretical implied volatility is when the quantity

$$\left[\frac{\text{Price}^{Gn++}}{2NS_{\alpha,\beta}(0) \sum_{i=\alpha+1}^{\beta} \tau_i P(0, T_i)} + \frac{1}{2} \right] > 1 \quad (3.5)$$

during the optimization algorithm, hence the inverse normal CDF can not be computed. During these stages, the algorithm is still navigating through the vector space of θ to arrive at an optimal solution and so some parameter combinations are problematic. This is not surprising given the high number of parameters that are being optimized (5 parameters for the G2++ model and 9 for the G3++ model). When the situation in (3.5) happens, the algorithm stops and a solution is not attained. One way to solve this problem is by penalizing the the objective function for those combination of parameters that produces this error. Another alternative is by assigning an approximation of the model implied volatility as described in Ferranti [2015] using either the approximation by Li [2006]

or Brenner and Subrahmanyam [1988]. Brenner and Subrahmanyam [1988] proposed a method to approximate the implied volatility of ATM equity call options by considering the Taylor expansion of the cumulative normal distribution function Φ around $d_1 = 0$. Applying their method in the context of ATM payer swaptions, we can approximate the model implied swaption volatility in (3.3) as

$$\sigma^{Gn++} \approx \frac{\text{Price}^{Gn++} \sqrt{2\pi}}{\sum_{i=\alpha+1}^{\beta} \tau_i P(0, T_i) NS_{\alpha, \beta}(0) \sqrt{T_\alpha}}. \quad (3.6)$$

Li [2006] however argued the approximation proposed by [Brenner and Subrahmanyam, 1988] lacked accuracy, often providing option pricing errors well exceeding the bid-ask spreads. They proposed a method to improve accuracy of equity option implied volatilities by considering rational approximations. Indeed, Ferranti [2015] showed that by applying the more accurate approximation in Li [2006] on (3.3), the approximated theoretical swaption implied volatility

$$\sigma^{Gn++} \approx \frac{1}{\sqrt{T_\alpha}} \left(\frac{2.506297c - 0.686461c^2}{1 - 0.277069c - 0.237552c^2} \right) \quad (3.7)$$

where $c = \frac{\text{Price}^{Gn++}}{\sum_{i=\alpha+1}^{\beta} \tau_i P(0, T_i) NS_{\alpha, \beta}(0)}$ provided better calibration results than the one in (3.6), in the context of a G2++ model.

Despite this, we attempted to solve this problem by simply penalizing the objective function (“brick wall” penalty to be specific). This is because for our considered calibration data (to be described subsequently), penalizing the objective function provided a lower mean absolute deviation from the market volatility surface than the second approach even while using the rational approximation (3.7). This was confirmed for a number of experiments for both the G2++ and G3++ model. Although the accuracy in replicating the market implied volatility surface was very similar for a lot of swaptions in both approaches.

In addition to the calibration problem in (3.5), for some combination of parameters in the G3++ model specifically, we are faced with the situation where the approximated swap volatility in the analytical swaption price formula (2.30) is undefined, i.e the esti-

mated square volatility is < 0 . Also, after conducting several calibration experiments, we noticed that for the G3++ model, the estimated correlation coefficients did not provide a positive semi-definite matrix without any constraint on the parameters. These peculiar issues associated with the G3++ model are not surprising given the larger number of parameters that are being optimized. Again, we attempt to solve these two issues by simply applying “brick wall” penalty¹ for these combination of parameters. We acknowledge that these additional constraints may also slow the optimization process and limit the freedom of the algorithm in exploring the parameter space by creating “forbidden” regions in the objective function. They however reduce the chances of being trapped in a local minimum instead of a global one thereby reducing a premature convergence [Price et al., 2005].

3.2 Optimization Algorithm

In order to solve the optimization problems discussed in previous section, we need to implement an optimization algorithm. Deterministic optimization include algorithms that rely heavily on mathematical theory without any element of randomness. They are mostly gradient-based algorithms which rely on the computation of the of the partial derivatives of the objective functions with respect to the parameters to be optimized, e.g. (3.1) and (3.2) in the current study. Stochastic optimizations on the other hand, introduce some randomness in the search procedure for a solution to the optimization problem. The choice of an optimization algorithm is in itself an optimization problem as it relies on the problem at hand and the trade-off between efficiency and computational time among others. Deterministic algorithms are generally faster than stochastic algorithms in terms of convergence to a solution. However these “solutions” are more likely to be local optimums than global. This is because deterministic algorithms are designed to move greedily to states that immediately reduce the value of the objective function and so they have the tendency of getting stuck on local optimums. Although stochastic algorithms have a much slower convergence towards a solution, their ability to overcome a local optimum

¹Assigning a huge objective function value.

in the objective function increases the probability of finding the global optimum. Additionally, to solve global (or multi-modal) optimization problems, most deterministic algorithms require starting points that are good guesses of the input parameters to be optimized in order to kick-start the optimization process. These could be derived from previous experiences or a mathematical intuition about the problem. If the user-defined initial starting points are in the wrong neighbourhood, the optimization could converge prematurely to a local optimum or it could completely fail to even converge to a solution at all. On the other hand, if the initial guess is good enough and a certain level of accuracy is sought (e.g. tolerance level), deterministic algorithms could converge to such a desired solution with a few gradient computations thereby reducing computational time. Stochastic algorithms will require comparatively longer time to reach the same level of accuracy [Cavazutti, 2013, Binder and Aichinger, 2013]. In the context of interest rate calibration, good starting points could be prior parameters from a recent calibration. Stochastic algorithms on the other hand usually require the range of the parameter values to be specified, from which it generates a population of parameters and gradually evolves this population towards a global solution. For more details on stochastic and deterministic optimization algorithms, we refer to Cavazutti [2013], Price et al. [2005] and the references cited therein. Since one of the main drawbacks of deterministic algorithms is their tendency of getting stuck on local optimums, it would not be ideal to use them in solving our optimization problems. This is due to the fact that the objective function in (3.1) and (3.2) is non-convex thus implying the existence of many local minimums. Also, given the dimension of our parameter space (7-dimensional vector for G2++ and 9-dimensional for the G3++), we are faced with the initial starting point problem when we consider a deterministic algorithm.

There are several families of stochastic optimizations. Among them are Simulated Annealing and Evolutionary algorithms. Simulated Annealing (SA) solves the optimization problems by converging towards points that reduces the value of the objective function while simultaneously, occasionally moving to regions that contains points that increases the value of the objective function by a user-defined probability termed “acceptance prob-

ability". According to literature (for example Price et al. [2005] and Cavazutti [2013]) SA are more suitable for optimization problems with a discrete parameter space, although it has been used by authors such Brigo and Mercurio [2007], Russo and Torri [2019] to calibrate the G2++ and two factor Hull-White model. Despite being flexible, SA requires an initial starting point. However it is less likely to be trapped in a region that contains a local optimum. For more details on SA, we refer to Price et al. [2005] and Cavazutti [2013].

Evolutionary algorithms are stochastic optimization algorithms whereby the sample population used in the search for a solution evolves over time through mutations, re-combinations and survival of high performing individuals. There are three main variations of evolutionary algorithms which are Evolutionary Search (ES), Genetic Algorithms (GA) and Differential Evolution (DE). For what concerns this work, we limit our discussion to DE as GA and ES have been proven to be computationally intensive and more suitable for other types of optimizations problems.

Differential Evolution (DE) is a population based stochastic optimizer that searches for the minimum of the objective function by evaluating the function at randomly chosen points within the bounds of the parameters to be optimized. The algorithm begins by generating an initial population of vectors from the predefined bounds of parameters of the D-dimensional vector to be optimized. It then evaluates the objective function on a population of trial vectors which is derived from combinations of vectors from the initial and an intermediary population with high performing trial vectors replacing the initial vectors in the next generation. This process continues until there is convergence or a pre-specified stopping criteria has been met.

It is important to note that both stochastic and deterministic optimization do not fully guarantee convergence to a global solution. A good technique is to apply a stochastic and deterministic algorithms in cascade Cavazutti [2013]. A stochastic optimization is first used to explore the parameter space in order to converge to a region that is highly likely to contain the global minimum, then the solution is refined by using it as a starting point for a local deterministic search. We first use a stochastic optimization to calibrate

the Gn++, specifically the differential evolution optimization algorithm and then apply a local deterministic search to refine the solution when it is convenient. This is motivated by a similar approach implemented in Brigo and Mercurio [2007] for the G2++ model. This is not to say that the DE is the best stochastic optimization as there does not exist a perfect algorithm. However given the nature of our problem (non-monotonic, ill-posed and high dimensional), DE proves to be the most suitable stochastic algorithm for our problem since it has been proven to be reliable, robust and also generated satisfactory calibration results in Di Francesco [2012] in calibrating the G2++ and G2++ model with constant and time-dependent parameters.

3.2.1 Differential Evolution Algorithm

There are several variations of the DE algorithm that differ based on only how an initial population is mutated to form the intermediary population. For our specific task of calibrating the Gn++ model, we use the algorithm known as DE/target-to-best/1/bin or DE/local-to-best/1/bin described below using terms by Price et al. [2005]. We replace a few terms to avoid to ambiguity with other notations within this study. This algorithm is implemented as the default strategy in the R package DEoptim by Mullen et al. [2009].

1. Initialization: To kick start the DE algorithm, the upper and lower bounds of every parameter of the D-dimensional vector $\theta = (a_i, \sigma_i, \rho_{i,j}, i, j = 1, \dots, n)$ need to be specified; from which an initial population of parameter vectors are generated. Ideally, the population size Np should be $\geq 10 \times D$ [Price et al., 2005]. We specifically set $Np = 400$. Throughout the optimization process, the population evolves through perturbations, mutation and survival of high performing individuals. Denoting θ_b and θ_u as the vectors that contain lower and upper bound of the parameters respectively, we have that $\theta_b = (a_i = 0, \sigma_i = 0, \rho_{i,j} = -1, \forall i, j = 1, \dots, n)$ and $\theta_u = (a_i = 1, \sigma_i = 1, \rho_{i,j} = 1, \forall i, j = 1, \dots, n)$.

To proceed, we shall denote $g = 0, \dots, g_{\max}$ as the generation to which a vector belongs where g_{\max} is the maximum number of generations or iterations. Also,

$m = 1, \dots, Np$ will indicate the index of a vector/member/individual in a population. Finally $k = 1, \dots, D$ will represent the parameter index of a vector. The algorithm begins by generating members of the initial population, as

$$y_{k,m}(0) = \theta_{b,k} + \tilde{z}_{k,m}(\theta_{u,k} - \theta_{b,k}), \text{ for } m = 1, 2, \dots, Np, \quad k = 1, 2, \dots, D.$$

where $\tilde{z}_{k,m} \sim U[0, 1)$ and is randomly generated for each parameter $k = 1, \dots, D$ and vector $m = 1, 2, \dots, Np$.

Once the initial population has been simulated, it becomes the parent population in the first generation $g = 0$, from which an intermediary population is created through differential mutations. In subsequent generations, the parent population is replaced by *surviving* members and mutants of the previous generation.

2. **Mutation:** At the mutation stage, members of the intermediary population are simulated by adding a vector from the parent population with the same index m , to a scaled difference between the parent vector and the best performing member of the parent population in that generation g with an arbitrary index best ; plus the scaled difference of another two *randomly* chosen vectors from the parent population with indices r_1 and r_2 . This strategy is known as the DE/target-to-best/1/bin. The m -th member of the intermediary population in the g -th generation is generated as

$$\mathbf{v}_m(g) = \mathbf{y}_m(g) + F [\mathbf{y}_{\text{best}}(g) - \mathbf{y}_m(g)] + F [\mathbf{y}_{r_1}(g) - \mathbf{y}_{r_2}(g)], \quad r_1, r_2, m = 1, \dots, Np$$

and $r_1 \neq r_2 \neq m$

where $\mathbf{y}_{\text{best}}(g)$ is the vector with least objective function value of the g -th generation and F is the step size which is effectively defined in $(0, 1)$. We use the default value of F in DEOptim which is 0.8. To ensure that mutated parameters are confined in their defined bounds, if $v_{k,m}(g) < \theta_{b,k}$ it is replaced by $\theta_{b,k} + \tilde{z}_{k,m}(\theta_{u,k} - \theta_{b,k})$ and if $v_{k,m}(g) > \theta_{u,k}$, replaced by $\theta_{u,k} + \tilde{z}_{k,m}(\theta_{b,k} - \theta_{u,k})$.

3. **Trial:** At this stage, a trial population is generated from a combination of the parent and intermediary population. Here vectors of the intermediary population compete with the those from the parent population as members of the trial population. The k -th parameter of the m -th trial vector in the g -th generation is defined as

$$u_{k,m}(g) = \begin{cases} v_{k,m}(g) & \text{if } \tilde{z}_{k,m} \leq C_r \text{ or } k = \hat{k} \\ y_{k,m}(g) & \text{otherwise.} \end{cases}$$

where $\hat{k} \leq D$ is a randomly generated index used to ensure that the set of trial vectors differs at least by one vector from the parent vector, while $C_r \in [0, 1]$ is a user-defined crossover probability used to control the fraction of parameters values of the trial vectors that originate from vectors in the intermediary population. Again for the crossover probability we use the default value of 0.5 in `DEOptim`.

4. **Selection:** At the selection stage, a trial vector $\mathbf{u}_m(g)$ replaces a target vector of the same index in the parent population $\mathbf{y}_m(g)$ if its objective function less than or equal to that of the target vector, else the target vector retains its place in the next generation $g + 1$. Thus

$$\mathbf{y}_m(g + 1) = \begin{cases} \mathbf{u}_m(g) & \text{if } f(\mathbf{u}_m(g)) \leq f(\mathbf{y}_m(g)) \\ \mathbf{y}_m(g) & \text{otherwise.} \end{cases}$$

where f is the objective function. The algorithm repeats the mutation, trial and selection steps until there is convergence or it stops if a suitably defined termination criterion is met. For example, the maximum number of iterations/generations has been reached or when the objective function value has been reduced beyond the tolerance level. Our stopping criteria for the G2++ calibration is to terminate the algorithm after 300 generations and 600 generations for the G3++ model. These criteria were chosen after several experiments with different stopping criteria.

3.3 Calibration Results

In this section, we present the calibration results of model to market prices available on Friday 28th June, 2019.

Input Market Data

The Gn++ interest rate model takes the market yield curve together with market swaption prices as an input in its calibration process. We used the zero-coupon curve available on the Bloomberg Terminal which is constructed using cash rates, interest rate futures and swaps. The market zero curve on Bloomberg as of 28th June 2019, is provided in Figure 3.1². It is easy to notice that the spot rates provided by Bloomberg are available

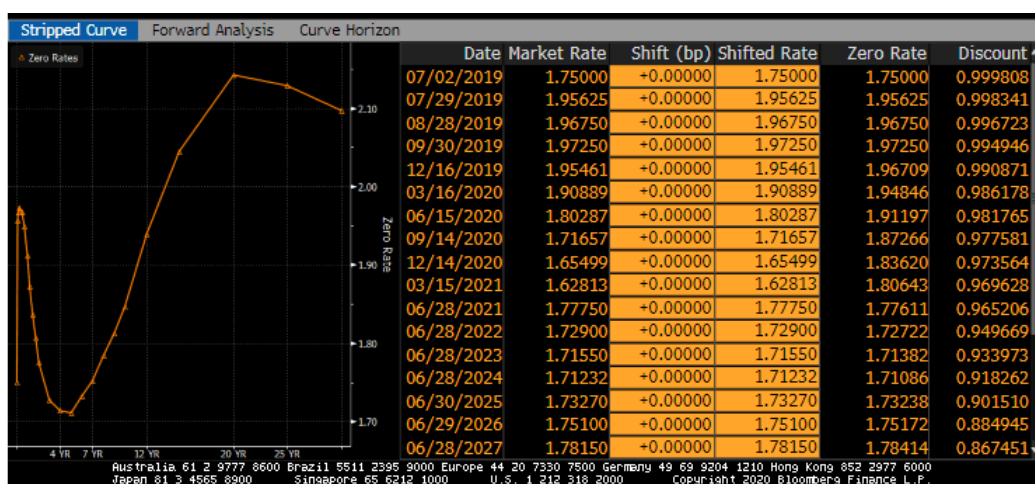


Figure 3.1: Market yield curve on June 28, 2019

Source: Bloomberg.com

for only a finite set of maturities. However it turns out that we need the market bond prices on other maturities not available on Bloomberg. Indeed to compute the market and model swaption prices in (1.18) and (2.30) as well as the implied volatility, we need as input, the market bond prices on the settlement dates between the swaption's maturity and expiry $\mathcal{T} = \{T_\alpha, \dots, T_\beta\}$ with an associated year fractions $\tau_{\alpha+1}, \dots, \tau_\beta$, giving rise to the need of interpolation of those market spot rates. We use a cubic spline to interpolate the missing spot rates due to their accuracy in fitting observable market prices. Further, given that the interpolation function is continuous and differentiable, we are able derive

²We acknowledge Bloomberg for the permission to use pictures from their terminal.

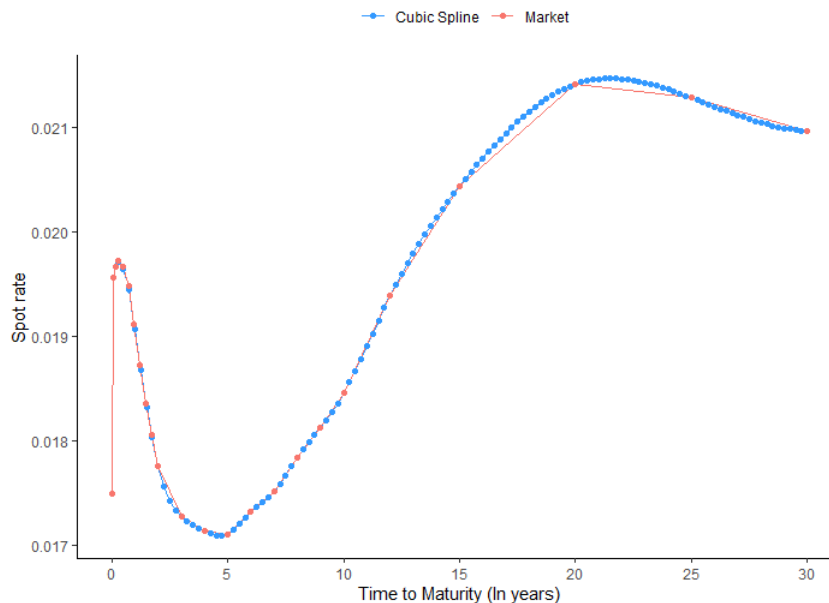


Figure 3.2: Market interpolated yield curve

the forward rate to simulate the short rate paths in subsequent chapters. The market interpolated zero-coupon curve for the considered day is provided in the Figure 3.2. The interpolated curve is smooth, continuous and consistent with the observable market spot rates.

Next, we obtained market swaption prices listed as market volatilities also available on the Bloomberg Terminal. The market swaption surface also known as the market volatility cube as of 28th June, 2019 is provided in Figure 3.3. These swaptions are all based on the 3-month Canadian Inter-Bank Offered Rate abbreviated as CAD-IBOR as the floating rate. On the left, in the row names are the swaption maturities ranging between 1 month to 30 years and in the column headings are the swaption tenors also ranging between 1 and 30 years³.

A requirement of market consistent valuations is to calibrate models to instrument that have a similar feature as the liabilities to be valued. Since short tenor and maturity swaptions are irrelevant to valuing long dated insurance liabilities, we exclude swaptions with tenors/maturities being less than a year. We specifically limit the model inputs to swaptions with a maximum maturity of 20 years and a maximum tenor of 10 years because swaptions beyond these maturity and tenor are less liquid and so their quotes

³Maturities greater than 25 are not captured here.



Figure 3.3: Market volatility surface on June/28/2019

Source: Bloomberg.com

are not as reliable. Also, to save computational time, we chose a subset of swaptions that met this criteria but which still exhaustive enough (70 swaptions in total) for our implementation. This set is provided in the volatility matrix in Table 3.1.

Table 3.1: Market volatilities on June 28

Maturity/Tenor	1	2	3	4	5	7	10
1	0.3858	0.3940	0.4129	0.4158	0.4122	0.3858	0.3343
2	0.4287	0.4306	0.4252	0.4195	0.4070	0.3845	0.3333
4	0.4185	0.4323	0.4124	0.3983	0.3851	0.3583	0.3155
5	0.4000	0.3901	0.3789	0.3769	0.3674	0.3402	0.3023
7	0.3892	0.3635	0.3487	0.3397	0.3242	0.3054	0.2792
8	0.3768	0.3466	0.3306	0.3227	0.3099	0.2911	0.2697
10	0.3373	0.3053	0.2954	0.2887	0.2821	0.2631	0.2511
12	0.3351	0.3033	0.2941	0.2879	0.2817	0.2629	0.2526
15	0.3362	0.3043	0.2950	0.2886	0.2823	0.2660	0.2558
20	0.3501	0.3168	0.3072	0.3005	0.2939	0.2753	0.2635

By solving (3.1) and (3.2), we obtain the calibrated parameters of the G2++ and G3++ model provided in Tables 3.2 and 3.3 respectively.

Table 3.2: G2++ Model Parameters

Calibration	a_1	a_2	σ_1	σ_2	ρ_{12}
Prices	0.0416	0.8922	0.00916	0.0129	-0.7151
Volatilities	0.0420	0.9859	0.00916	0.0149	-0.7217

Table 3.3: G3++ Model Parameters

Calibration	a_1	a_2	a_3	σ_1	σ_2	σ_3	ρ_{12}	ρ_{13}	ρ_{23}
Prices	0.0397	0.8220	0.1158	0.00864	0.01309	0.00236	-0.5871	0.2420	-0.8409
Volatilities	0.0513	0.8339	0.5535	0.00998	0.0191	0.00913	-0.516	-0.2178	-0.4811

Henceforth we shall refer to the parameters resulting from minimizing the market and Gn++ prices as *price parameters* and those from minimizing market and Gn++ implied volatilities as *volatility parameters*. At a glance, we notice that the two set parameters are within close ranges for the G2++ model while the same cannot be said the G3++ model. One possible explanation could be because the G3++ parameter vectors live in a 9-dimensional space with four additional degrees of freedom (than the G2++ model) in replicating the market implied volatility surface. Another possible explanation could be attributed to the nature of the market input. Typically when maturity is held constant,

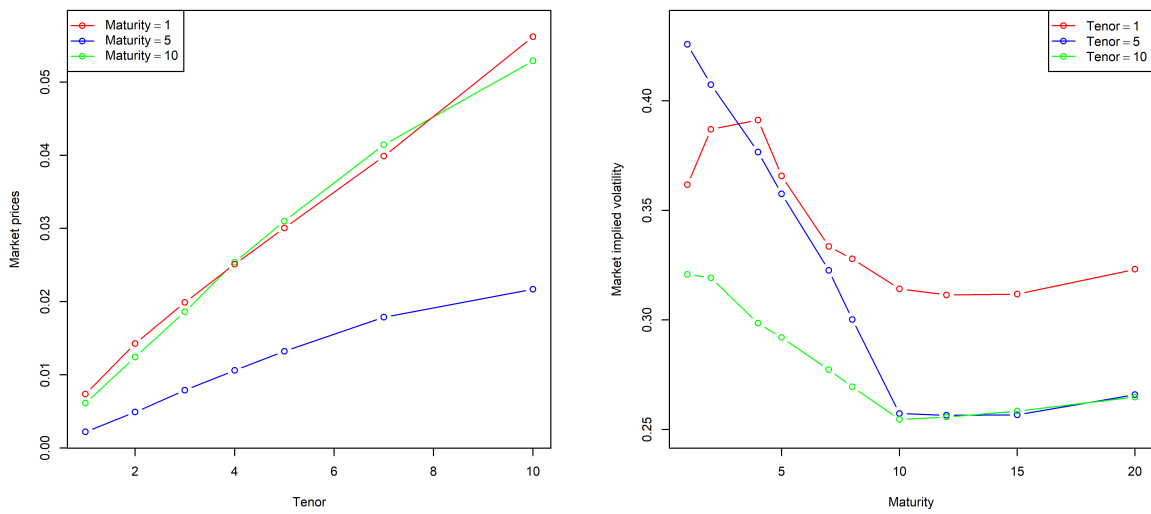


Figure 3.4: General phenomenon of market swaption prices and implied volatility

swaption prices increases with an increase tenor. The dynamics of swaption implied

volatilities are quite different. For very short tenor swaptions (typically less than 5 years) when the tenor is held constant, implied volatility tend to momentarily increase with an increase in maturity until it “maxes” out and then starts declining until it stabilizes in the long term. For longer tenor swaption (typically 5 or more years), when tenors are held constant, implied volatility declines with an increase in maturity until it reaches a certain threshold where its starts to stabilize for the longer term maturities. This phenomenon implies that the two objective functions in (3.2) and (3.1) will assign different weights to the same swaption which is reflected in the calibrated parameter values of the G3++ model. This pattern in swaption prices and implied volatility is more adequately represented in Figure 3.4.

To validate the calibration results, we analyse the consistency of the models with replicating the observable market prices via Monte-Carlo simulations in the next chapter.

Chapter 4

Model Validation of the Gn++ model

The validation step assesses the quality of the interest rate model calibration by comparing the model simulated output (e.g model implied volatilities) to market observable prices. This is to ensure that calibrated parameters used to simulate cash flow scenarios for the contract valuations also replicate observable market inputs (to a satisfactory degree) via Monte-Carlo simulation. We begin by first simulating the model swaption price and then inverting it to calculate the model implied volatility in order to compare it with the benchmark; market implied volatilities.

4.1 Simulation of Swaption Prices

We simulate the swaption prices using the swaption price formula in (2.28),¹² To implement the simulation, for each instrument, we need the price of a bond maturing at the swaption maturity $P(0, T_\alpha)$ which is the same as the market bond price, the strike price

¹A similar implementation can be done under the risk-neutral measure where the bank account is the numeraire since the prices from both methods are mathematically equivalent. Adjustments are made when simulating the OU processes by adjusting the drift of the processes when simulating the bond price and also when simulating the discount factor. Details of simulations under \mathbb{Q} are provided in a subsequent section.

²Simulations under the \mathbb{Q}^T is particularly more convenient and accurate when it is difficult to simulate the discount factors exactly thereby avoiding discretization errors due to approximations of the short-rate's integral.

K (as provided on Bloomberg) and the simulated future bond prices at the maturity of the swaption $P(T_\alpha, T_k)$ for $k = \alpha + 1, \dots, \beta$. This reduces the simulation scheme to only that of the bond prices at $t = T_\alpha$ since the rest of the inputs are readily available. The bond prices are determined analytically by (2.22) and (2.23) with the modified OU-processes postulated under the \mathbb{Q}^T . Since we are valuing a large number of swaptions with several maturities T_α , we change the formulation in (2.28) so that the numeraire is the zero-coupon bond price $P(0, T^*)$. This way, we are able to consider a single forward measure relative to a time horizon T^* often called the “terminal forward measure”. This circumvents the need to simulate the process $x_i(t)$, $i = 1, \dots, n$ under the forward measure for every maturity T_α . Hence the formulation changes to

$$PS[0, T_\alpha, T_\beta, K, N] = NP(0, T^*)E^{T^*} \left[\frac{\left(1 - \sum_{k=\alpha+1}^{\beta} c_i P(T_\alpha, T_k)\right)^+}{P(T_\alpha, T^*)} \right]. \quad (4.1)$$

The term $P(T_\alpha, T^*)$ compounds the swaption payoff at maturity to the time horizon T^* . The proof behind this technique is provided in Brigo and Mercurio [2007]. We recall from Chapter 2 that the dynamics of the process $\{x_i(t) : t > 0, i = 1, \dots, n\}$ under the forward measure satisfy (2.24). We can simulate the processes by simply discretizing (2.24) with respect to time; i.e finitizing dt . If we denote $\Delta t = t_{k+1} - t_k$, we obtain the update formula

$$x_i(t_{k+1}) \approx x_i(t_k) - a_i x_i(t_k) \Delta t - M_i^{T^*}(t_k, t_{k+1}) + \sigma_i \sqrt{\Delta t} Z_i(k+1) \quad (4.2)$$

where $[Z_1(k+1), \dots, Z_n(k+1)]^\top \sim N(\mathbf{0}, (\rho_{ij})\Delta t)$ and $\mathbf{0}$ denotes the zero vector. If we consider the Choleski decomposition of the covariance matrix $(\rho_{ij})\Delta t$, such that $BB^\top = (\rho_{ij})\Delta t$. We can rewrite the update formula in (4.8) as

$$x_i(t_{k+1}) \approx x_i(t_k) - a_i x_i(t_k) \Delta t - M_i^{T^*}(t_k, t_{k+1}) + \sigma_i \sqrt{\Delta t} B^i \tilde{Z}_i(k+1) \quad (4.3)$$

where B^i represents the i th row of B and $[\tilde{Z}_1(k+1), \dots, \tilde{Z}_n(k+1)]^\top$ are iid $N(0, 1)$.

The update formula above has a shortcoming which is that its accuracy can be guaranteed

if and only if Δ_t is suitably small [Gillespie, 1996]. An exact updating formula exists for the process $\{x_i(t) : t > 0, i = 1, \dots, n\}$ by considering the joint distribution of the random vector $X(t_{k+1}) = [x_1(t_{k+1}), \dots, x_n(t_{k+1})]^\top$. We can deduce from subsection 2.2.4 in Chapter 2 that under the forward measure \mathbb{Q}^{T^*} , conditional on \mathcal{F}_{t_k} , the vector $X(t_{k+1}) = [x_1(t_{k+1}), \dots, x_n(t_{k+1})]^\top$ is jointly normally distributed with mean and covariance matrix $\mathbf{C}(\Delta t)$. Thus,

$$\begin{aligned} E[X(t_{k+1})|\mathcal{F}_{t_k}] &= [x_1(t_k)e^{-a_1\Delta t} - M_1^{T^*}(t_k, t_{k+1}), \dots, x_n(t_k)e^{-a_n\Delta t} - M_n^{T^*}(t_k, t_{k+1})] \\ C_{ij}(\Delta t) &= \frac{\sigma_i\sigma_j}{a_i + a_j}\rho_{ij}(1 - e^{-(a_i+a_j)\Delta t}). \end{aligned} \quad (4.4)$$

Assuming the covariance matrix $\mathbf{C}(\Delta t)$ is positive semi-definite, if we consider the Cholesky decomposition such that $LL^\top = \mathbf{C}(\Delta t)$, then we can have an exact updating formula for the process $\{x_i(t) : t > 0\}$ such that given \mathcal{F}_{t_k} ,

$$\begin{bmatrix} x_1(t_{k+1}) \\ \vdots \\ x_n(t_{k+1}) \end{bmatrix} = \begin{bmatrix} x_1(t_k)e^{-a_1\Delta t} - M_1^{T^*}(t_k, t_{k+1}) \\ \vdots \\ x_n(t_k)e^{-a_n\Delta t} - M_n^{T^*}(t_k, t_{k+1}) \end{bmatrix} + L \begin{bmatrix} \tilde{Z}_1(k+1) \\ \vdots \\ \tilde{Z}_n(k+1) \end{bmatrix} \quad (4.5)$$

where $\tilde{Z}_1(k+1), \dots, \tilde{Z}_n(k+1)$ are iid $N(0, 1)$. The simulated process of $\{x_i(t) : t > 0, i = 1, \dots, n\}$ allows us to simulate bond prices at any point in time $0 < t < T^*$ and subsequently compute the Monte-Carlo swaption price by (4.1). Assuming we have simulated a considerably large number of M paths across all trajectories, the Monte-Carlo swaption price is computed as

$$PS^{(\text{MC})}[0, T_\alpha, T_\beta, K, N] = NP(0, T^*) \frac{1}{M} \sum_{m=1}^M \left[\frac{\left(1 - \sum_{k=\alpha+1}^{\beta} c_k A(T_\alpha, T_k) e^{-\sum_{i=1}^n B_i(T_\alpha, T_k) x_i^{(m)}(T_\alpha)}\right)^+}{A(T_\alpha, T^*) e^{-\sum_{i=1}^n B_i(T_\alpha, T^*) x_i^{(m)}(T_\alpha)}} \right]. \quad (4.6)$$

Through the law of large numbers, (4.6) approaches the true price (2.28) as $M \rightarrow \infty$. Computations of the model implied volatility easily follows from the relationship in (3.4) by replacing the model analytical prices with Monte-Carlo swaption prices. Using the calibrated parameters in Tables 3.2 and 3.3, we implemented a simulation of 50,000

antithetic paths for each process $\{x_i(t) : i = 1, \dots, n\}$ with a time step $\Delta t = 0.25$ and time horizon $T^* = 30$.

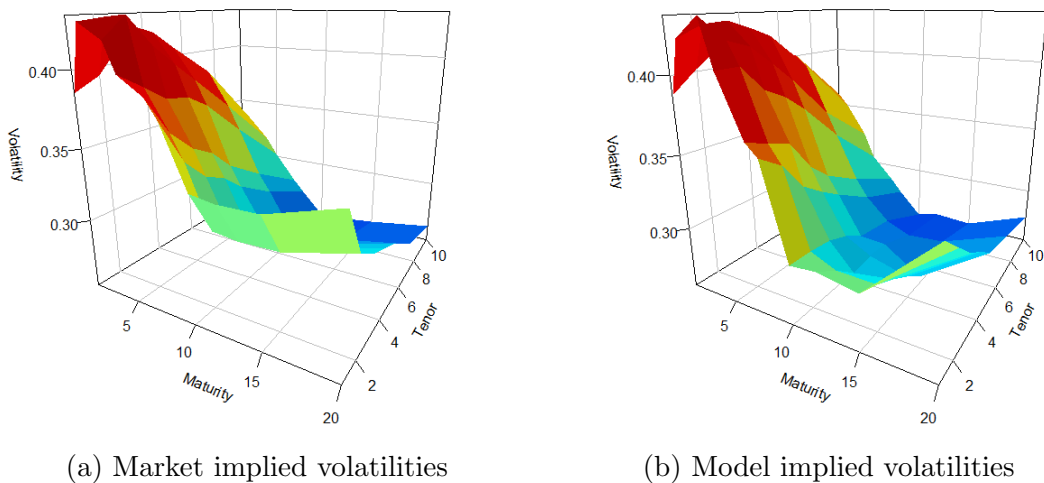


Figure 4.1: G2++ calibration to market prices on June 28: volatility surface

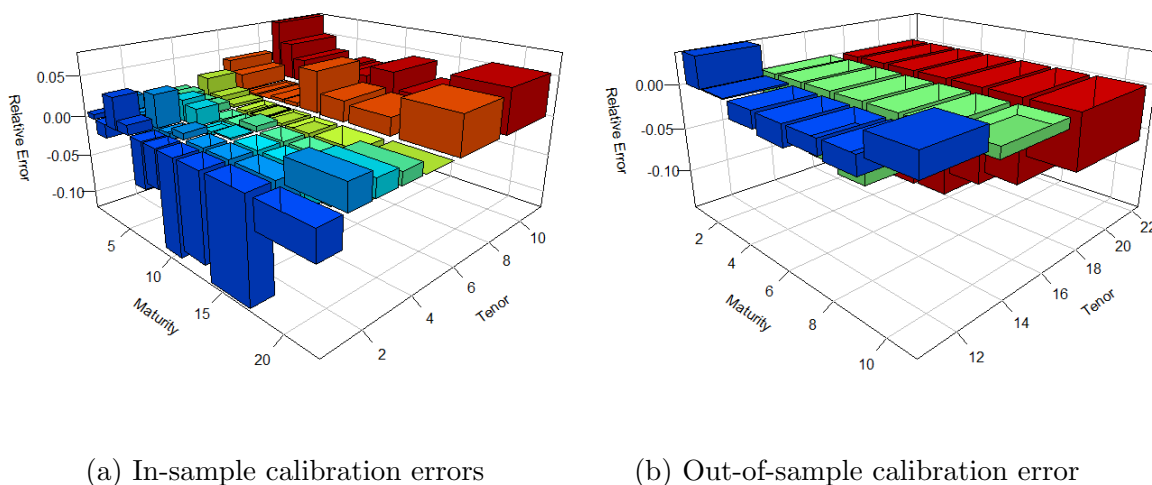


Figure 4.2: G2++ calibration to market prices on June 28: calibration errors

The market and model implied volatility surface as well as the relative calibration errors of the G2++ price parameters are provided in Figures 4.1, 4.2 and Tables 4.1, 4.2 respectively. We can observe other the short tenor volatility term structure, the G2++ model (with price parameters) is able to replicate the market observed volatility surface satisfactorily. We must admit that we do not expect the theoretical implied volatility to provide a perfect fit to the market observe surface since we calibrated our model to 70 swaptions with different features (strike, tenors, maturity etc). In fact, a perfect fit to the

Table 4.1: G2++ calibration to market prices on June 28: implied volatilities

Maturity/Tenor	1	2	3	4	5	7	10
1	0.3878	0.4010	0.4130	0.4207	0.4104	0.4002	0.3606
2	0.4215	0.4287	0.4300	0.4248	0.4182	0.3930	0.3501
4	0.4343	0.4196	0.4146	0.4018	0.3883	0.3574	0.3251
5	0.4049	0.4053	0.3886	0.3806	0.3686	0.3399	0.3051
7	0.3671	0.3610	0.3558	0.3351	0.3221	0.3067	0.2866
8	0.3592	0.3492	0.3294	0.3188	0.3096	0.2926	0.2762
10	0.2981	0.2977	0.2959	0.2906	0.2812	0.2771	0.2585
12	0.3000	0.2904	0.2784	0.2809	0.2800	0.2696	0.2634
15	0.2955	0.2897	0.2824	0.2735	0.2631	0.2717	0.2611
20	0.3386	0.3257	0.3133	0.3050	0.2940	0.2883	0.2779

Table 4.2: G2++ calibration to market prices on June 28: calibration errors

Maturity/Tenor	1	2	3	4	5	7	10
1	0.0052	0.0178	0.0003	0.0117	-0.0043	0.0372	0.0786
2	-0.0169	-0.0045	0.0112	0.0127	0.0275	0.0221	0.0504
4	0.0378	-0.0293	0.0054	0.0089	0.0084	-0.0024	0.0305
5	0.0122	0.0391	0.0256	0.0099	0.0032	-0.0007	0.0092
7	-0.0568	-0.0069	0.0203	-0.0136	-0.0064	0.0044	0.0266
8	-0.0468	0.0075	-0.0038	-0.0120	-0.0011	0.0051	0.0241
10	-0.1163	-0.0248	0.0017	0.0066	-0.0032	0.0531	0.0294
12	-0.1049	-0.0424	-0.0535	-0.0243	-0.0059	0.0255	0.0427
15	-0.1211	-0.0479	-0.0427	-0.0525	-0.0680	0.0215	0.0209
20	-0.0328	0.0280	0.0199	0.0149	0.0004	0.0471	0.0545

market volatility term structure is not necessary and could be signal of potential danger since the liquidity of the market quoted swaptions differ and so not all market quotes are reliable [Brigo and Mercurio, 2007]. In Table 4.2, we can see that other than the swaptions with longer maturities of 10, 12 and 15 \times 1 and the longest tenor of 10 \times 1 swaptions the absolute relative error is less than 8% with 22 error values being close to 0. The poor fit to the short tenor \times long maturities swaptions could be explained by the magnitude of swaption prices as one moves around the volatility matrix. Typically, when maturity is held constant, the swaption price increases with an increase in tenor and since we are minimizing difference in prices the algorithm will naturally tend to focus on swaptions with higher prices, thus those with longer tenors. This explains one of the reasons why some practitioners do not favor this calibration method. Another possible explanation could be associated to the approximation error in (2.30) during the calibration stage. As

seen in the calibration of Di Francesco [2012] and reiterated by Russo and Torri [2019], the approximation by Schrager and Pelsser [2006] tends to provide larger errors for longer maturity and longer tenor swaptions. In addition to the samples we used in our calibration, we tested the quality of the calibration on swaptions not included in the calibration sample to see if the calibrated model is stable with unseen instruments. On the right hand of Figure 4.2 we can see that the out-of-sample calibration errors is maintained within the range of the in-sample calibration errors. The out-of-sample calibration errors increases with an increase in tenor which could be explained by the approximation error by the swaption price in (2.30). Nevertheless, the G2++ model (with price parameters) provides a good fit the to market volatility surface is satisfactory with a mean absolute error (MAE) of 2.66%.

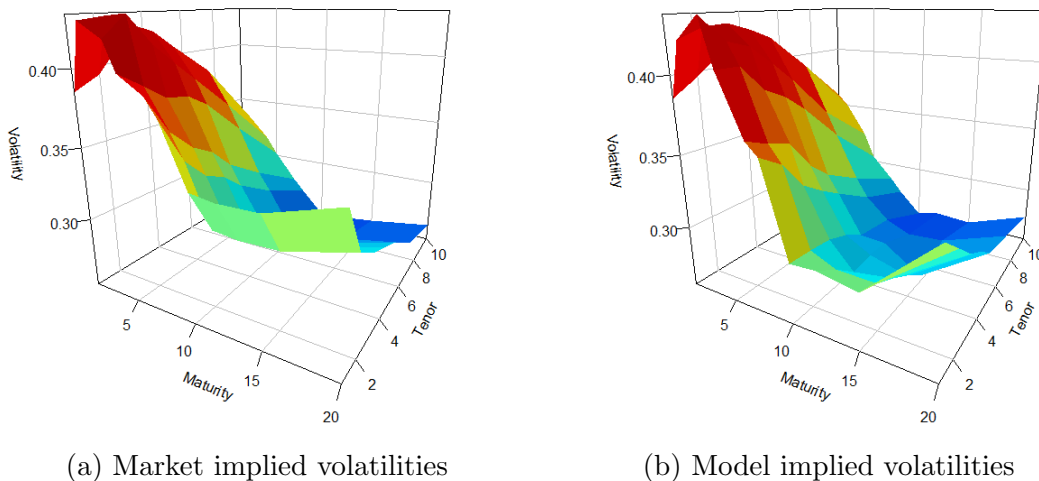
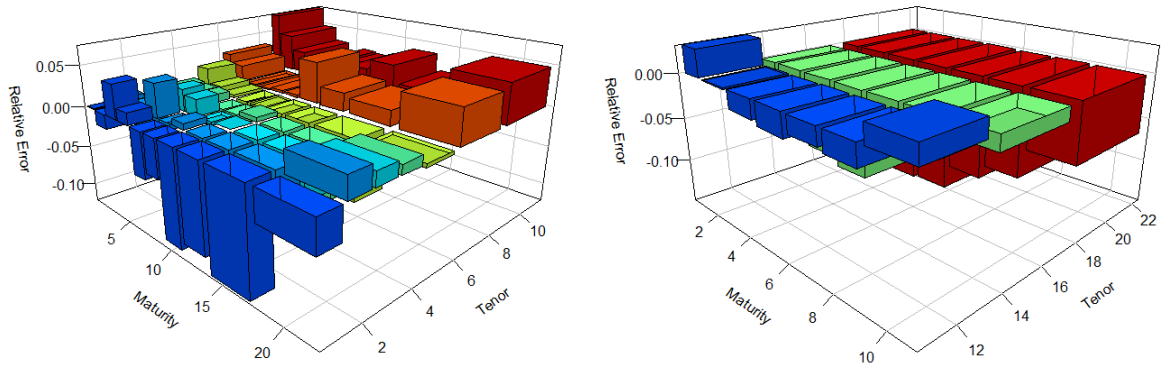


Figure 4.3: G2++ calibration to market implied volatilities on June 28: volatility surface



(a) In-sample calibration errors

(b) Out-of-sample calibration error

Figure 4.4: G2++ calibration to market implied Volatilities on June 28: calibration errors

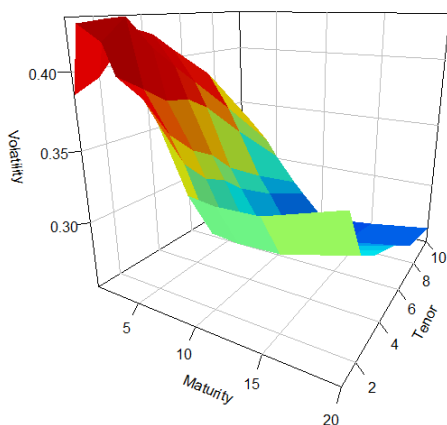
Figures 4.3, 4.4 together with Tables 4.3 and 4.4 show calibration results for the G2++ volatility parameters. Again with the volatility parameters, the model generally produces a good fit for the market volatility surface with the most pronounced inconsistency around the shortest tenor structure when maturity increases. We notice that, the problem with the long maturity swaptions \times short tenor is also prevalent with this calibration type although the relative error slightly declined. The out-of-sample errors are also not too far from the range of in-sample ones; with an increase in error when tenor increases. Realizing the same trend is observed in Table 4.2, this could be mainly due to the approximation error in (2.30). Regardless of this, 23 of the in-sample errors are close to 0. In general the G2++ model (with volatility parameters) provides a satisfactory fit to market volatility surface with an MAE of 2.60%.

Table 4.3: G2++ calibration to market implied volatilities on June 28: implied volatilities

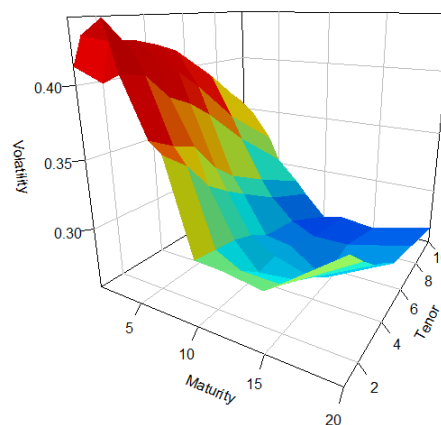
Maturity/Tenor	1	2	3	4	5	7	10
1	0.3860	0.3963	0.4094	0.4179	0.4082	0.3983	0.3589
2	0.4210	0.4275	0.4293	0.4244	0.4177	0.3924	0.3493
4	0.4357	0.4202	0.4150	0.4021	0.3884	0.3572	0.3246
5	0.4059	0.4057	0.3888	0.3807	0.3685	0.3396	0.3045
7	0.3675	0.3610	0.3557	0.3348	0.3218	0.3062	0.2859
8	0.3594	0.3491	0.3291	0.3185	0.3091	0.2920	0.2754
10	0.2981	0.2974	0.2955	0.2901	0.2807	0.2764	0.2576
12	0.2997	0.2900	0.2778	0.2803	0.2793	0.2688	0.2624
15	0.2951	0.2891	0.2817	0.2727	0.2623	0.2707	0.2600
20	0.3377	0.3246	0.3122	0.3038	0.2928	0.2869	0.2764

Table 4.4: G2++ calibration to market implied Volatilities on June 26: calibration errors

Maturity/Tenor	1	2	3	4	5	7	10
1	0.0005	0.0059	-0.0085	0.0051	-0.0097	0.0324	0.0737
2	-0.0179	-0.0073	0.0096	0.0116	0.0264	0.0206	0.0481
4	0.0410	-0.0280	0.0064	0.0095	0.0085	-0.0032	0.0287
5	0.0148	0.0401	0.0262	0.0100	0.0030	-0.0018	0.0071
7	-0.0558	-0.0070	0.0199	-0.0143	-0.0075	0.0025	0.0239
8	-0.0462	0.0071	-0.0044	-0.0130	-0.0025	0.0030	0.0211
10	-0.1162	-0.0257	0.0005	0.0050	-0.0051	0.0504	0.0259
12	-0.1057	-0.0440	-0.0553	-0.0264	-0.0084	0.0224	0.0387
15	-0.1222	-0.0499	-0.0450	-0.0550	-0.0709	0.0178	0.0163
20	-0.0355	0.0245	0.0163	0.0110	-0.0038	0.0421	0.0488

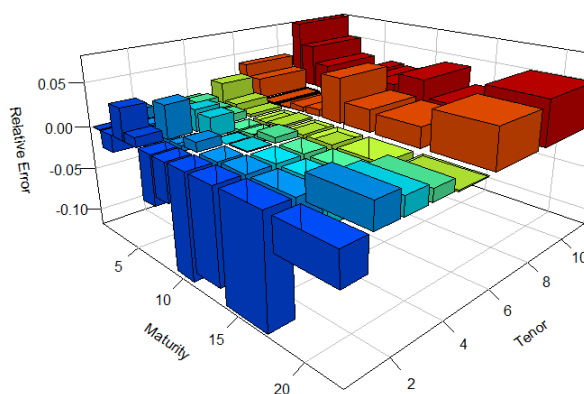


(a) Market implied volatilities

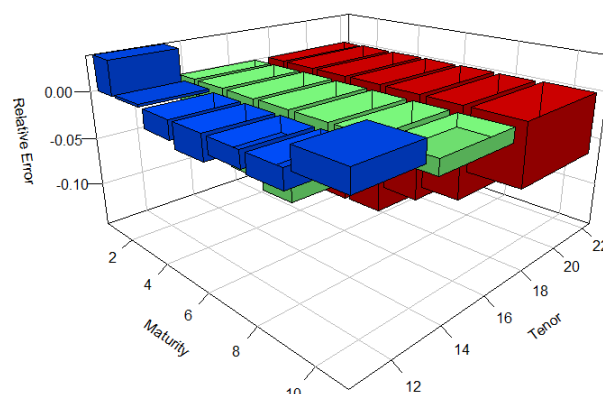


(b) Model implied volatilities

Figure 4.5: G3++ calibration to market prices on June 28: volatility surface



(a) In-sample calibration errors



(b) Out-of-sample calibration error

Figure 4.6: G3++ calibration to market prices on June 28: calibration errors

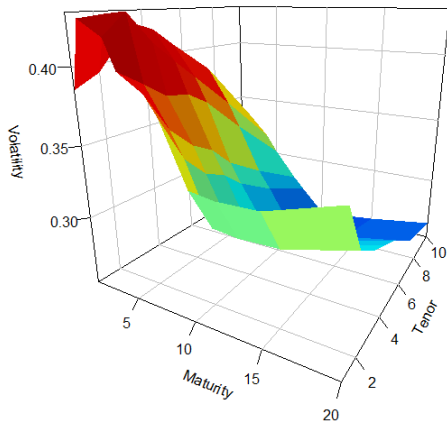
Figures 4.5, 4.6 and Tables 4.5, 4.6 show calibration results for the G3++ price parameters. By visual inspection, one can observe that increasing the number of factors from 2 to 3 provides a similar fit to the market surface as in the two-factor case. The G3++ (with price parameters) also struggles to replicate the longer maturity portion of the volatility term structure. Out-of-sample errors are not far from those in-sample; with out-of-sample errors increasing for an increase in tenor. Overall the replication is satisfactory with an MAE of 2.62% which is less than that of the G2++ model with similar calibration method.

Table 4.5: G3++ calibration to market prices on June 28: implied volatilities

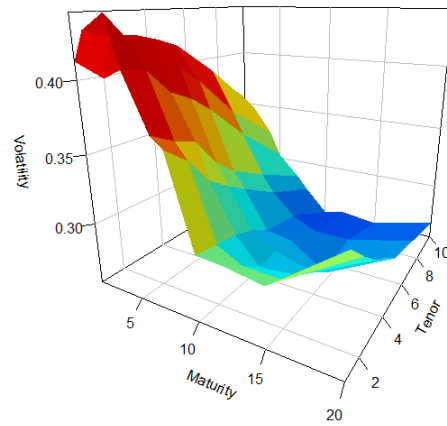
Maturity/Tenor	1	2	3	4	5	7	10
1	0.3857	0.3988	0.4116	0.4201	0.4104	0.4007	0.3611
2	0.4203	0.4280	0.4298	0.4253	0.4189	0.3939	0.3507
4	0.4337	0.4195	0.4148	0.4022	0.3888	0.3578	0.3252
5	0.4043	0.4049	0.3883	0.3805	0.3685	0.3397	0.3046
7	0.3673	0.3614	0.3564	0.3358	0.3228	0.3072	0.2868
8	0.3601	0.3502	0.3304	0.3199	0.3105	0.2933	0.2765
10	0.2979	0.2975	0.2958	0.2905	0.2811	0.2768	0.2580
12	0.3002	0.2907	0.2786	0.2811	0.2802	0.2696	0.2631
15	0.2962	0.2904	0.2830	0.2740	0.2635	0.2720	0.2611
20	0.3381	0.3251	0.3128	0.3044	0.2934	0.2876	0.2770

Table 4.6: G3++ calibration to market prices on June 28: calibration errors

Maturity/Tenor	1	2	3	4	5	7	10
1	-0.0004	0.0122	-0.0032	0.0103	-0.0043	0.0386	0.0801
2	-0.0195	-0.0061	0.0109	0.0137	0.0293	0.0245	0.0524
4	0.0362	-0.0297	0.0058	0.0099	0.0097	-0.0013	0.0307
5	0.0108	0.0379	0.0249	0.0094	0.0029	-0.0013	0.0077
7	-0.0563	-0.0058	0.0221	-0.0116	-0.0043	0.0060	0.0273
8	-0.0443	0.0105	-0.0005	-0.0087	0.0021	0.0076	0.0253
10	-0.1169	-0.0254	0.0013	0.0062	-0.0036	0.0521	0.0274
12	-0.1041	-0.0416	-0.0528	-0.0236	-0.0055	0.0254	0.0416
15	-0.1189	-0.0457	-0.0406	-0.0506	-0.0665	0.0226	0.0208
20	-0.0343	0.0263	0.0182	0.0131	-0.0015	0.0446	0.0514

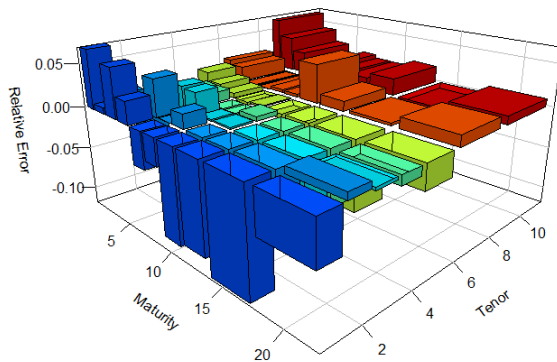


(a) Market implied volatilities

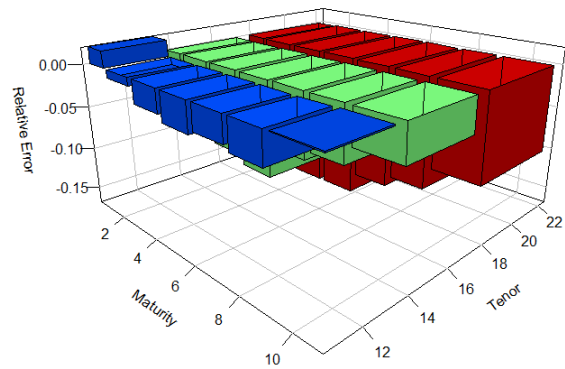


(b) Model implied volatilities

Figure 4.7: G3++ calibration to market implied volatilities on June 28: volatility surface



(a) In-sample calibration errors



(b) Out-of-sample calibration error

Figure 4.8: G3++ calibration to market implied Volatilities on June 28: calibration errors

The fit of the G3++ model by the volatility parameters is also satisfactory with the long maturity \times shortest tenor problem still prevalent. For this model in particular, the fit to the longest tenor swaption of 10 years mostly better than the previous models. Out-of-sample calibration errors are not too far from the in-sample range; with out-of-sample errors increasing with an increase in tenor. The MAE for the G3++ model (with volatility parameters) is 2.49%.

From the model validations, we can make an interesting observation. The overall fit to the longer maturities 10, 12, 15 \times 1 is poor for all models with the calibration error being greater 10%. Another interesting observation we can make is that minimizing the sum of

Table 4.7: Mean of absolute relative calibration errors

	G2++	G3++
<u>Calibration method</u>		
Price	2.66%	2.62%
Volatility	2.60%	2.49%

absolute relative differences between market and model implied volatilities tend to yield lower MAEs than minimizing the sum of absolute relative differences between market and model swaption prices. This results holds for the selected datasets and calibration steps employed in this study. For the sake of brevity, going forward, we shall only concentrate on the “volatility” parameters.

Table 4.8: G3++ calibration to market implied volatilities on June 28: implied volatilities

Maturity/Tenor	1	2	3	4	5	7	10
1	0.4119	0.3983	0.4040	0.4117	0.4028	0.3946	0.3556
2	0.4317	0.4267	0.4260	0.4215	0.4157	0.3913	0.3477
4	0.4423	0.4220	0.4159	0.4031	0.3896	0.3580	0.3239
5	0.4104	0.4069	0.3894	0.3814	0.3693	0.3400	0.3033
7	0.3726	0.3637	0.3578	0.3366	0.3232	0.3066	0.2844
8	0.3650	0.3521	0.3313	0.3202	0.3104	0.2921	0.2736
10	0.3012	0.2986	0.2961	0.2903	0.2804	0.2751	0.2545
12	0.3007	0.2895	0.2768	0.2789	0.2776	0.2660	0.2578
15	0.2961	0.2885	0.2803	0.2707	0.2597	0.2668	0.2539
20	0.3337	0.3191	0.3062	0.2973	0.2858	0.2786	0.2661

Table 4.9: G3++ calibration to market implied volatilities on June 28: calibration errors

Maturity/Tenor	1	2	3	4	5	7	10
1	0.0678	0.0109	-0.0216	-0.0099	-0.0227	0.0229	0.0638
2	0.0070	-0.0090	0.0020	0.0048	0.0213	0.0177	0.0432
4	0.0568	-0.0239	0.0086	0.0121	0.0116	-0.0007	0.0265
5	0.0261	0.0430	0.0277	0.0120	0.0052	-0.0007	0.0033
7	-0.0425	0.0006	0.0260	-0.0092	-0.0031	0.0040	0.0188
8	-0.0314	0.0160	0.0021	-0.0077	0.0016	0.0036	0.0144
10	-0.1071	-0.0219	0.0023	0.0055	-0.0060	0.0455	0.0135
12	-0.1025	-0.0455	-0.0587	-0.0311	-0.0146	0.0120	0.0204
15	-0.1191	-0.0521	-0.0500	-0.0621	-0.0801	0.0029	-0.0076
20	-0.0469	0.0074	-0.0034	-0.0107	-0.0275	0.0121	0.0099

To conclude the section, we are left with the question of which model is more market-consistent? As previously mentioned the market-consistency test aims measure *how well*

a model is able to replicates market observed prices and not *necessarily reproduce* all observable inputs. Based on the considered data set on the calibration date, both the 3-factor and 2-factor additive models reproduce the market volatility cube of the selected swaptions well. The answer then lies with the subjectivity of an acceptable tolerance level and type of product to be valued. For example if the product very similar to a 10, 12 or 15×1 swaption, the suitability of the models might be questioned. For the purposes of this work and requirement of the IFRS17 of models to replicate enough market inputs, both the G2++ model and G3++ shall be considered to be market-consistent.

4.2 Simulation of The Discount Factor

In this section, we provide a joint simulation scheme for the stochastic discount factor and short rate. In addition to being the fundamental quantity describing the yield curve for short-rate models, the short rate is an important quantity in generating risk-neutral scenarios as it represents the drift of most asset classes e.g. equity index, real-estate etc. The stochastic discount factor is also an important element used to discount cash flow scenarios in risk neutral valuations. Recall that

$$\begin{aligned} D(0, t) &= \exp\left(-\int_0^t r(s)ds\right) \\ &= \exp\left(-\int_0^t \sum_{i=1}^n x_i(s)ds + f(s)ds\right). \end{aligned}$$

If we denote $Y_{t_k} = \int_0^{t_k} \sum_{i=1}^n x_i(s)ds$ and recall the relationship $P(0, T) = \exp(-\int_0^T f^M(0, s)ds)$, by (2.18) and (2.15), the integral of the short rate is normally distributed with mean

$$\begin{aligned} \mathbb{E}\left[\int_0^{t_{k+1}} r(s)ds \middle| \mathcal{F}_{t_k}\right] &= Y_{t_k} + \sum_{i=1}^n x_i(t_k) \frac{1 - e^{-a_i(t_{k+1}-t_k)}}{a_i} - \ln P(0, t_{k+1}) + \\ &\quad \frac{1}{2} \sum_{i,j=1}^n \rho_{ij} \frac{\sigma_i \sigma_j}{a_i a_j} \left[t_{k+1} - \frac{1 - e^{-a_i t_{k+1}}}{a_i} - \frac{1 - e^{-a_j t_{k+1}}}{a_j} + \frac{1 - e^{-(a_i+a_j)t_{k+1}}}{(a_i + a_j)} \right] \\ &= Y_{t_k} + \sum_{i=1}^n x_i(t_k) \frac{1 - e^{-a_i(t_{k+1}-t_k)}}{a_i} - \ln P(0, t_{k+1}) + \frac{1}{2} V(0, t_{k+1}) \end{aligned}$$

and variance

$$\text{var} \left[\int_0^{t_{k+1}} r(s) ds \middle| \mathcal{F}_{t_k} \right] = \text{var} \left[\int_{t_k}^{t_{k+1}} \sum_{i=1}^n x_i(s) ds \right] := V(t_k, t_{k+1}) \quad (4.7)$$

We implement the simulation of the integral of the short rate in two parts. First we consider only the process $\{Y_t : t > 0, Y_0 = 0\}$ and then incorporate the integral of the deterministic function later.

The integral of the short rate depends on the process $\{\sum_{i=1}^n x_i(t) : t > 0, i = 1, \dots, n\}$, so we implement a joint simulation with the process $\{x_i(t) : t > 0, i = 1, \dots, n\}$ under measure \mathbb{Q} . We provide an expression for the covariance between the short rate and its integral. Following Chapter 3 of Glasserman [2013],

$$\begin{aligned} \text{cov} \left(\sum_{i=1}^n x_i(t_{k+1}), Y_{t_{k+1}} \middle| \mathcal{F}_{t_k} \right) &= \text{cov} \left(\sum_{i=1}^n x_i(t_{k+1}), \int_{t_k}^{t_{k+1}} \sum_{i=1}^n x_i(s) ds \middle| \mathcal{F}_{t_k} \right) \\ &= \int_{t_k}^{t_{k+1}} \text{cov} \left(\sum_{i=1}^n x_i(t_k) e^{-a_i(t_{k+1}-t_k)} + \sigma_i \int_{t_k}^{t_{k+1}} e^{-a_i(t_{k+1}-u)} dW_i(u), \right. \\ &\quad \left. \sum_{i=1}^n x_i(t_k) e^{-a_i(s-t_k)} + \sigma_i \int_{t_k}^s e^{-a_i(s-u)} dW_i(u) \right) ds \end{aligned}$$

assuming $t_k < s < t_{k+1}$

$$= \int_{t_k}^{t_{k+1}} \sum_{i,j=1}^n \mathbb{E} \left(\int_{t_k}^s \sigma_i e^{-a_i(t_{k+1}-u)} dW_i(u) \int_{t_k}^s \sigma_j e^{-a_j(s-u)} dW_j(u) \right)$$

and by Itô's Isometry, this becomes

$$= \int_{t_k}^{t_{k+1}} \sum_{i,j=1}^n \left(\int_{t_k}^s \sigma_i \sigma_j \rho_{ij} e^{-a_i(t_{k+1}-u)} e^{-a_j(s-u)} du \right)$$

which simplifies to

$$= \sum_{i,j=1}^n \frac{\rho_{ij} \sigma_i \sigma_j}{(a_i + a_j)} \left[\frac{1}{a_i} - \frac{e^{-a_i(t_{k+1}-t_k)}}{a_i} - \frac{e^{-a_j(t_{k+1}-t_k)}}{a_j} + \frac{e^{-(a_i+a_j)(t_{k+1}-t_k)}}{(a_i + a_j)} \right]$$

so that denoting $t_{k+1} - t_k = \Delta t$, for $p = 1, \dots, n$

$$\begin{aligned} \text{cov} \left(x_p(t_{k+1}), Y_{t_{k+1}} \middle| \mathcal{F}_{t_k} \right) &= \sum_{j=1}^n \frac{\rho_{pj} \sigma_p \sigma_j}{(a_p + a_j)} \left[\frac{1}{a_p} - \frac{e^{-a_p \Delta t}}{a_i} - \frac{e^{-a_j(\Delta t)}}{a_j} + \frac{e^{-(a_p + a_j)\Delta t}}{(a_p + a_j)} \right] \\ &:= \tilde{\gamma}_{(p)}(\Delta t). \end{aligned}$$

Under the \mathbb{Q} , conditional on \mathcal{F}_{t_k} , the vector $\hat{X}(t_{k+1}) = [x_1(t_{k+1}), \dots, x_n(t_{k+1}), Y_{t_{k+1}}]^\top$ is jointly normally distributed with covariance matrix $\hat{\mathbf{C}}(\Delta t)$. Thus

$$\mathbb{E}[\hat{X}(t_{k+1}) | \mathcal{F}_{t_k}] = \left[x_1(t_k) e^{-a_1 \Delta t}, \dots, x_n(t_k) e^{-a_n \Delta t}, Y_{t_k} + \sum_{i=1}^n x_i(t_k) \frac{1 - e^{-a_i \Delta t}}{a_i} \right]$$

and given that $\text{cov}[x_i(t_{k+1}), x_j(t_{k+1}) | \mathcal{F}_{t_k}]$ is,

$$\hat{C}_{ij}(\Delta t) = \frac{\sigma_i \sigma_j}{a_i + a_j} \rho_{ij} (1 - e^{-(a_i + a_j)\Delta t}),$$

the covariance matrix of $\hat{X}(t_{k+1})$ is

$$\hat{\mathbf{C}}(\Delta t) = \begin{bmatrix} C_{11}(\Delta t) & \cdots & C_{1n}(\Delta t) & \tilde{\gamma}_1(\Delta t) \\ \vdots & \ddots & \vdots & \vdots \\ C_{n1}(\Delta t) & \cdots & C_{nn}(\Delta t) & \tilde{\gamma}_n(\Delta t) \\ \tilde{\gamma}_1(\Delta t) & \cdots & \tilde{\gamma}_n(\Delta t) & V(t_k, t_{k+1}) \end{bmatrix}.$$

Assuming the covariance matrix $\hat{\mathbf{C}}(\Delta t)$ is positive semi-definite, if we consider the Cholesky decomposition such that $LL^\top = \hat{\mathbf{C}}(\Delta t)$, then we can have an exact updating formula for the process $\{x_i(t) : t > 0\}$ and $\{Y(t) : t > 0\}$ such that given \mathcal{F}_{t_k} ,

$$\begin{bmatrix} x_1(t_{k+1}) \\ \vdots \\ x_n(t_{k+1}) \\ Y_{t_{k+1}} \end{bmatrix} = \begin{bmatrix} x_1(t_k) e^{-a_1 \Delta t} \\ \vdots \\ x_n(t_k) e^{-a_n \Delta t} \\ Y_{t_k} + \sum_{i=1}^n x_i(t_k) \frac{1 - e^{-a_i \Delta t}}{a_i} \end{bmatrix} + L \begin{bmatrix} \tilde{Z}_1(k+1) \\ \vdots \\ \tilde{Z}_n(k+1) \\ \tilde{Z}_{n+1}(k+1) \end{bmatrix}$$

and an exact updating formula for the short rate $r(t)$ ³ and its integral $\int_0^t r(s)ds$ such that given \mathcal{F}_{t_k} ,

$$\begin{bmatrix} r(t_{k+1}) \\ \int_0^{t_{k+1}} r(s)ds \end{bmatrix} = \begin{bmatrix} \sum_{i=1}^n x_i(t_{k+1}) + f(t_{k+1}) \\ Y_{t_{k+1}} - \ln P(0, t_{k+1}) + \frac{1}{2}V(0, t_{k+1}) \end{bmatrix}$$

where $\tilde{Z}_i(k+1), \dots, \tilde{Z}_n(k+1)$ are iid $N(0, 1)$ with $x_i(0) = 0, i = 1, \dots, n, Y(0) = 0$ and $r(0) = f(0)$.

We implemented a simulation of 50,000 antithetic paths with a time step $\Delta t = 0.25$ for both the short rate and the discount factor. Figure 4.9 provides 5,000 randomly sampled paths of the future evolution of the short rate over time. Although the presence of negative

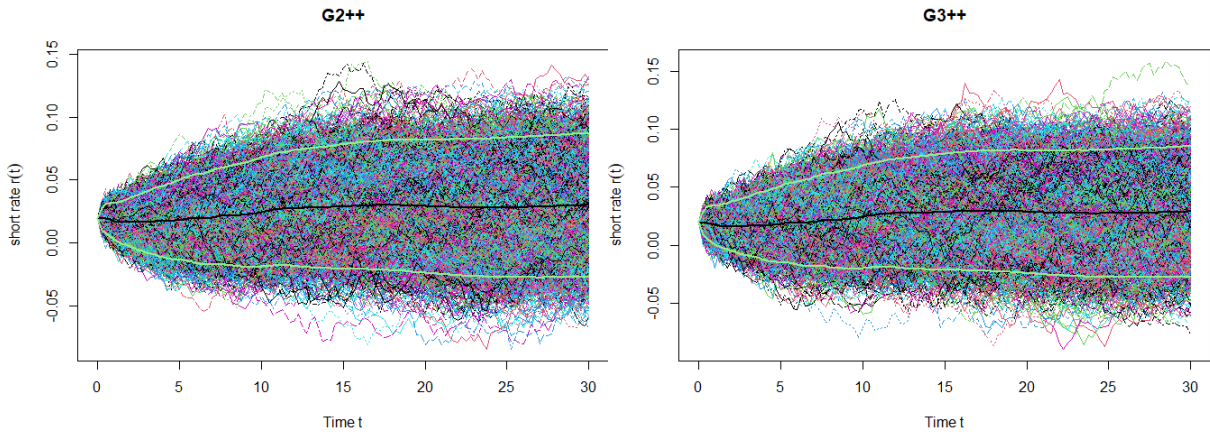


Figure 4.9: Evolution of the short rate over time

short rate is a desirable for the current low interest environment, many jurisdictions or entities usually place a floor on the lower bound such that $r(t)$ does not fall beyond the prescribed value. For example, the Canadian institute of actuaries recommends to place a lower bound of -0.0075 on $r(t)$ [Canadian Institute of Actuaries, 2013]. We provide the empirical probability of $\mathbb{Q}(r(t) < -0.0075)$ for $0 < t \leq 30$ in Figure 4.10. It is evident from that Figure 4.10 that empirical $\mathbb{Q}(r(t) < -0.0075)$ increases over time with the G3++ model having a higher proportion of negative short rate values across time. The distributions of the 5-year and 30-year discount factor is provided in Figure 4.11.

³values of the market forward rates in deterministic $f(t)$ is calculated by differentiating the spline function used to interpolate the market yield curve

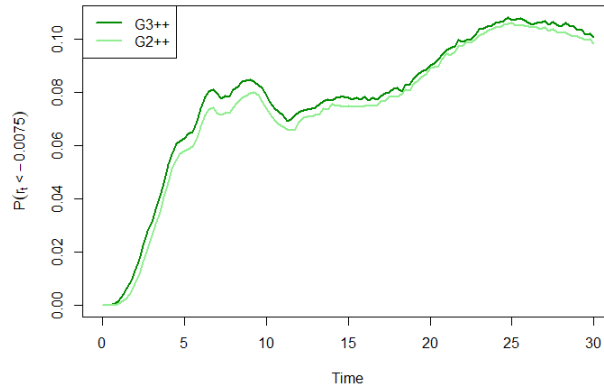


Figure 4.10: Proportion of $r(t) < -0.0075$

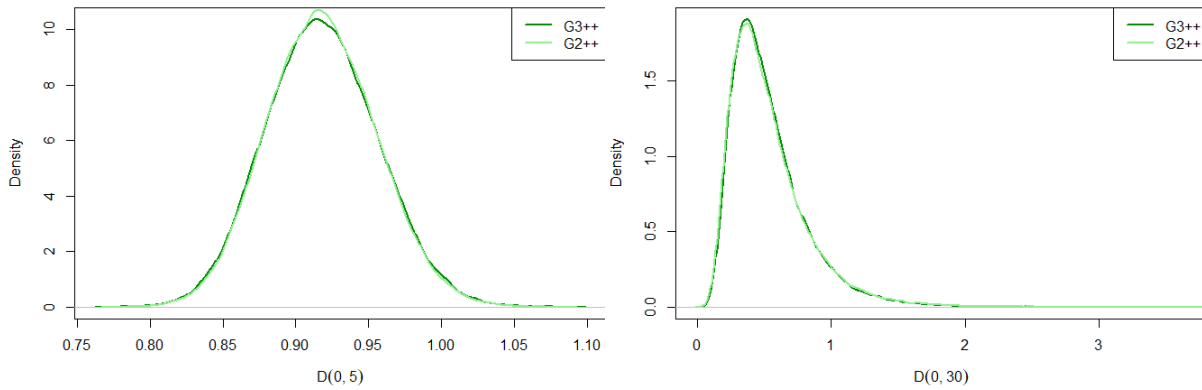


Figure 4.11: Distribution of discount factor

It obvious both models and maturities have discount factors which are greater than one sometimes which is due to the existence of negative interest rate. The distribution of the 30-year discount factor has a longer tail for both models due to the increase in probability of negative short rates (and its integral) as t increases. Having provided the necessary simulation scheme for the quantities useful in market-consistent valuations, we provide a specific application to the valuation of segregated fund.

4.3 Application To A Segregated Fund Policy

Segregated funds (called variable annuities in the US, unit-linked insurance in the United Kingdom and parts of Asia) are fund-linked products that combine both investment and

insurance features. The policyholder pays an initial premium which is invested in the underlying fund (made of equity, bonds, or a mix of both) that follows the financial market growth. At maturity, the policyholder receives a lump sum that is dependent on the market performance. To protect the policyholder against the downside risk of the market, the insurer provides additional benefits to the contracts referred to as benefit riders. There are several types of segregated fund riders available on the market which include: the Guaranteed Minimum Maturity Benefit (GMMB), Guaranteed Minimum Death Benefit (GMDB), Guaranteed Minimum Withdrawal Benefit (GMWB) and Guaranteed Minimum Income Benefit (GMIB). In this thesis we focus on GMMBs and direct the interested reader to a host of literature dedicated on the rest, for example Hardy [2003].

Insurers issuing GMMBs guarantee a full or partial return of premium contingent on survival at the maturity of the contract. Thus at maturity, the policyholder receives the maximum between the underlying account value and the guarantee amount. The guarantee cost (excess of the guarantee amount over the account value) is financed via a fee charged to the account value. During the period of the contract, the insured may surrender the policy which comes at a charge called a surrender penalty or lapse penalty. An insurer selling a GMMB is faced with other risks in addition to surrender such as mortality.

4.3.1 GMMB Contract Cashflows

The main cashflows involved in valuing a GMMB, are the guarantee payout (if triggered) by the insurer at maturity, the guarantee fees collected by the insurer at periodic intervals and the surrender charge when it occurs.

We consider a set of equally spaced time intervals $\mathcal{T} = \{t | 0 = t_0, t_1, \dots, t_N = T\}$ where T is the maturity of the contract. $\Delta t = t_{k+1} - t_k$ represents the time step size and for every $k = 0, 1, 2, \dots, N$, $t_k = k\Delta t$ so that $t_0 = 0$. We assume premiums are invested in a pure bond fund that follows a “rolling-horizon” trading strategy where funds are continuously reinvested in zero-coupon bonds with a target fixed maturity τ . The underlying fund assumptions and notations is greatly influenced by work done

in Augustyniak et al. [2019] and references mentioned therein, with adjustments made where necessary.

At time $t = t_k$, the underlying fund value is

$$F_{t_k} = F_{t_{k-1}} \frac{P(t_k, t_k + \tau - \Delta t)}{P(t_{k-1}, t_{k-1} + \tau + \Delta t)} = \prod_{n=1}^k \frac{P(t_n, t_n + \tau - \Delta t)}{P(t_{n-1}, t_{n-1} + \tau - \Delta t)}, \quad k = 1, \dots, N, \quad F_0 = 1.$$

At time $t = 0$, the policyholder pays the initial premium A_0 . At time $t = t_k$, the policy account evolves as

$$A_{t_k} = A_{t_{k-1}} (1 - \varepsilon) \frac{F_{t_k}}{F_{t_{k-1}}}$$

where ε is the periodic guarantee charge. The proportion of policy holders active at time $t = t_k$ is

$${}_{t_k}a_x = {}_{t_{k-1}}a_x \left(\frac{{}_{t_k}p_x}{{}_{t_{k-1}}p_x} \right) (1 - \mathcal{L}(m_{t_{k-1}})), \quad {}_0a_x = 1$$

where $\frac{{}_{t_k}p_x}{{}_{t_{k-1}}p_x}$ is the conditional probability of an aged- x policyholder alive at t_{k-1} to survive to time t_k . K is the guaranteed amount and $m_{t_{k-1}} = \frac{A_{t_{k-1}}}{K}$ is the measure of the moneyness of the guarantee at time $t = t_{k-1}$.

$\mathcal{L} : (0, \infty) \rightarrow [0, 1]$ is a function on the moneyness which indicates the proportion of policyholders who surrender their policy at time $t = t_k$. In summary the cash inflow to the insurer at time $t = t_k$ is

$$\text{the guarantee fee} = {}_{t_{k-1}}a_x \varepsilon A_{t_{k-1}} \frac{F_{t_k}}{F_{t_{k-1}}}, \quad k = 1, \dots, N$$

and

$$\text{the surrender penalty} = {}_{t_{k-1}}a_x \left(\frac{{}_{t_k}p_x}{{}_{t_{k-1}}p_x} \right) \mathcal{L}(m_{t_{k-1}}) A_{t_k} \mathcal{P}(t_k)$$

where \mathcal{P} is a deterministic function which indicates proportion of the account value retained by the insurer in the event of a surrender.

The maturity payout at $t = T$ is $G_T = \max(K, A_T) = A_T + (K - A_T)^+$ so that cash

outflow by the insurer is an embedded put option. Considering surrender behaviour and mortality, this is expressed as

$${}_T a_x \max(K - A_T, 0).$$

The net cashflow at anytime $t = t_k$ is then given by

$$CF_{t_k} = \mathbb{I}_{\{t_k=T\}} {}_T a_x \max(K - A_T, 0) - {}_{t_{k-1}} a_x \varepsilon A_{t_{k-1}} \frac{F_{t_k}}{F_{t_{k-1}}} - {}_{t_{k-1}} a_x \left(\frac{{}_{t_k} p_x}{{}_{t_{k-1}} p_x} \right) \mathcal{L}(m_{t_{k-1}}) A_{t_k} \mathcal{P}(t_k)$$

$$k = 1, \dots, N.$$

The market-consistent value of the GMMB guarantee at time $t = 0$, on the initial recognition $t = 0$ of the contract is

$$\Pi_0^{\text{guar}} = E^{\mathbb{Q}} [D(0, T) {}_T a_x \max(K - A_T, 0)]. \quad (4.8)$$

The expected value of the future cash inflow to insurer on initial recognition is

$$\Pi_0^{\text{in}} = E^{\mathbb{Q}} \left[\sum_{j=1}^N D(0, t_k) \left({}_{t_{k-1}} a_x \varepsilon A_{t_{k-1}} \frac{F_{t_k}}{F_{t_{k-1}}} + {}_{t_{k-1}} a_x \left(\frac{{}_{t_k} p_x}{{}_{t_{k-1}} p_x} \right) \mathcal{L}(m_{t_{k-1}}) A_{t_k} \mathcal{P}(t_k) \right) \right]. \quad (4.9)$$

So that the value of the GMMB liability is

$$\Pi = \Pi_0^{\text{guar}} - \Pi_0^{\text{in}}. \quad (4.10)$$

Due to the complexities associated with the GMMB policy (surrender, mortality, fees etc) and segregated funds in general, it is impossible to find closed-form expression for the liability value in (4.10) which necessitates stochastic simulations techniques as recommended by the IFRS 17 standard.

The GMMB contract details are as follows. Policyholders are assumed to have a dynamic surrender behaviour. The annual surrender proportion for year $t + 1$ is defined as

computed as

$$\mathcal{L}^{\text{ann}}(m_t) = \begin{cases} 0.02 & \text{if } m_t \leq 0.4434 \\ 0.02 + 0.0616(m_t - 0.4434) & \text{if } 0.4434 < m_t < 1.74 \\ 0.1 & \text{otherwise.} \end{cases}$$

These rates are directly from taken those provided in Augustyniak et al. [2019] which is claimed to be representative of rates charged on the Canadian market. Quarterly rates are derived directly by $\mathcal{L}(m_t) = (1 - \mathcal{L}^{\text{ann}}(m_t))^{\frac{1}{4}}$. Surrender charges are assumed to decrease by 1% every year from 7% in the first year to 0% after the seventh year. This is given by

$$\mathcal{P}(t) = \max\left(0, 0.07 - 0.01 \left\lfloor \frac{(t-1)}{4} \right\rfloor\right).$$

Mortality assumptions are modeled as in Augustyniak et al. [2019]⁴ using the Canadian experience.

We consider quarterly intervals $\Delta t = 1/4$ at which the fund is “rebalanced” and fees are charged.

We consider an initial premium of $A_0 = 100$, maturity period of $T = 20$ with guarantee amount of $K = 100$. The fee rate for the contract is inspired by those in Augustyniak et al. [2019]⁵. The quarterly guarantee fee charge is $\varepsilon = 0.00519$. The market-consistent valuations for the two short rate models are provided in Table 4.10. From Table 4.10, we

Table 4.10: Market-consistent GMMB Valuations on June 28, 2019

<u>$T = 20, K = 100$</u>	Π_0^{guar}	Π_0^{in}	Π
G2++	5.001	22.013	-17.003
G3++	4.958	22.013	-17.055

can observe that although both model lead to the same expected cash in flow, the G3++

⁴We thank the authors for making the source code on mortality assumptions and improvements accessible.

⁵Using the RBC fund. See Augustyniak et al. [2019] for more details

model provides a lower guarantee value which is 22.52% of the expected cash inflow while the G2++ model provides a guarantee value that represents 22.7% of the cash in flow.

Chapter 5

Robustness Study

Interest rate models are highly sensitive to the data to calibrate them. However these observable market inputs (e.g. implied volatilities, spot rates etc.) are designed to change following each trade to reflect their realized prices. Hence it is not surprising for calibrated model parameters to greatly differ by day. We investigate the robustness of the two short rate models by re-calibrating them to three sets of market data with a two-day lag, where there does not seem to be a huge shift in the market conditions e.g. yield curve and implied volatility surface. This is to ensure that the calibrated model is not only consistent with the market on the valuation date but it is also robust to the market data used as an input in the calibration process. We consider market data across three different days with a two day lag, Monday June 24, 2019, Wednesday June 26, 2019 and Friday June 28, 2019. The market yield curves on the three days are provided in Figure 5.1.

Figure 5.1 shows there has not been a major shift in the market yield curve within the week. The yield curves in Figure 5.1 overlap at a certain points especially towards short end while being spread out over a few bps towards the longer end. Spot rates on Wednesday is the highest for most maturities particularly from the mid curve to the long end. The rates on the short end of curve are the lowest on Monday while Friday has lowest rates for long end. The market implied volatility surfaces in Figure 5.2 show there has not been a significant shift in the market ATM swaption volatility surface between

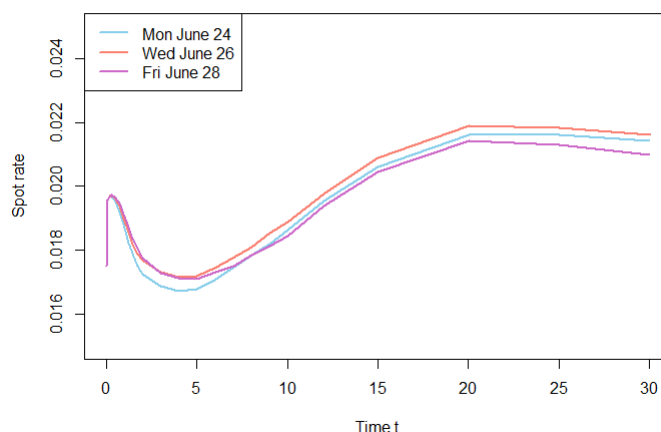
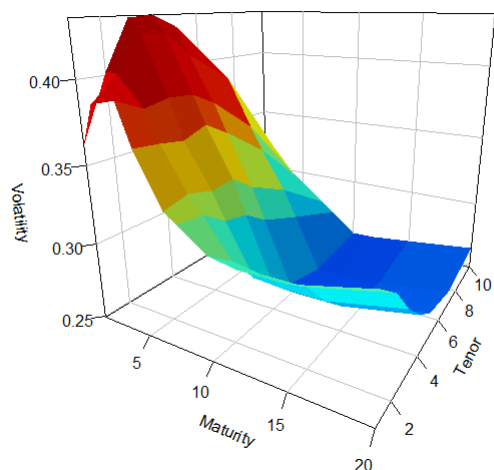


Figure 5.1: Market yield curves

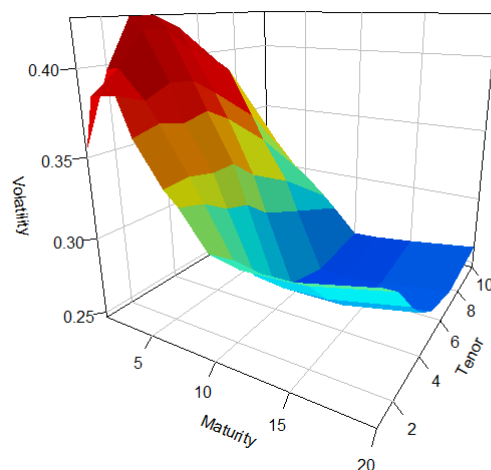
Monday and Wednesday. The most pronounced change on Friday compared to the other two days is that shortest tenor volatility term structure has a higher hump than the other two days. Additionally by observing the implied volatility matrices in Tables 3.1, A.1 and A.6, the market implied volatilities are generally higher on Friday, with Wednesday having the lowest quotes and Monday being in-between. After analysing the market situation across the three days we can conclude there has not been a major change in either the yield curve or the implied volatility surface. In the next section we present the calibrated results of the G2++ and G3++ models on these three days and examine how they “respond” to the market input, their “forecast” of the future term structure and how stable these “forecasts” are.

5.1 Calibration To Three Days With A Two Day Lag

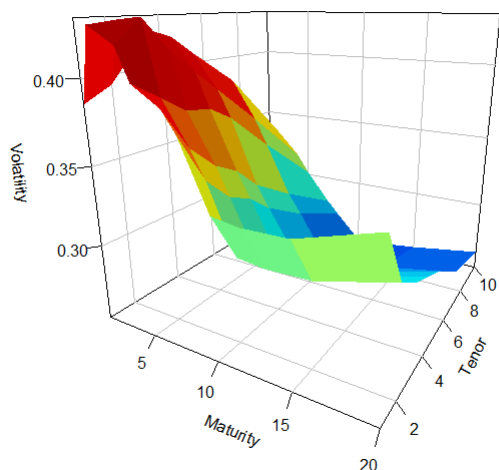
We calibrated the G2++ and G3++ models by minimizing model and market implied volatilities and validated the results using procedures described in Chapters 3 and 4. The validation results for Monday and Wednesday are provided in Appendix A. The calibrated parameters including those from the previous chapter on Friday June 28, 2019 are provided in Tables 5.1 and 5.2.



(a) Mon June 24



(b) Wed June 26



(c) Fri June 28

Figure 5.2: Market volatility surface on all three days

Table 5.1: G2++ Model Parameters

Ref. dates	a_1	a_2	σ_1	σ_2	ρ_{12}
Mon 06/24/19	0.0427	0.6515	0.00923	0.00610	-0.9846
Wed 06/26/19	0.0499	0.5525	0.0100	0.00654	-0.9865
Fri 06/28/19	0.0420	0.9859	0.00916	0.0149	-0.7217

We can observe from Table 5.1 of the calibrated G2++ models that, the parameters of the first factor $x_1(t)$ is mostly stable across the three days with its mean reversion

hovering around 0.04 and volatility being around 0.009. The second factor is mostly deviant on Friday compared to the other two days given the state of the market on this day. One interesting observation with the G2++ is that, for the calibration on Friday where the correlation, ρ_{12} is farthest from -1 ; the MAE of 2.60% from the market volatility surface is the lowest compared to 3.17% and 3.23% for correlations of 0.9846 and 0.9865 respectively. This explains why it is recommended to assign a non-trivial value to ρ_{12} in order to capture the correlation between forward rates more effectively and provide a better fit to the market volatility surface Brigo and Mercurio [2007].

Table 5.2: G3++ Model Parameters

Ref. dates	a_1	a_2	a_3	σ_1	σ_2	σ_3	ρ_{12}	ρ_{13}	ρ_{23}
Mon 06/24/19	0.04964	0.7027	0.7315	0.00971	0.00941	0.00743	-0.2741	-0.9000	-0.00729
Wed 06/26/19	0.04352	0.7936	0.5486	0.00940	0.0135	0.0119	-0.2072	-0.2798	-0.8790
Fri 06/28/19	0.0513	0.8339	0.5535	0.00998	0.0191	0.00913	-0.516	-0.2178	-0.4811

We can observe from Table 5.2 that the G3++ model has more variance in its parameters. This is not surprising given the additional degrees of freedom compared to the G2++ (the parameters have freedom to vary) hence the variability of its estimated parameters. We should state that we have no expectation on the parameter values as this is a naive (assuming no prior knowledge of parameter values) calibration. In fact, the optimization problems described previously are ill-posed, such they do not depend continuously on data but are rather highly sensitive to the input market data. The implication of this is that small changes in the market data may lead to arbitrarily large changes in the parameters of the interest rate model [Albrecher et al., 2013, Binder and Aichinger, 2013]. A technique employed by practitioners to obtain stable parameters is to apply so-called regularization methods where an additional penalty term is added to the objective functions in either (3.1) and (3.2) to penalize deviations from a set of desired/prior parameter values while still maintaining market-consistency. For more details on such regularization techniques and other parameter stabilization techniques in the context of interest rate calibrations, see for example Albrecher et al. [2013] and Joshi and Kwon [2010] and the references mentioned therein.

These parameters observations do not necessarily give us proper insight about the future evolution of the term structure implied by the calibrated model since the short rate model depends on the interactions between all the factors. Our specific interest rely on not just value of these parameters but rather how robust the calibrated models are with respect to different input data and parameter specifications across the reference dates.

We begin by analyzing the distribution of $r(t)$ for some selected future times across the three days. To make the comparison between the different simulations results consistent, we used the same set of generated random $N(0, 1)$ numbers so that the variance in the differences will be less influenced by the variation in the randomly generated normal iid's described previously. We can observe from Figures 5.3 and 5.4 that the distribution

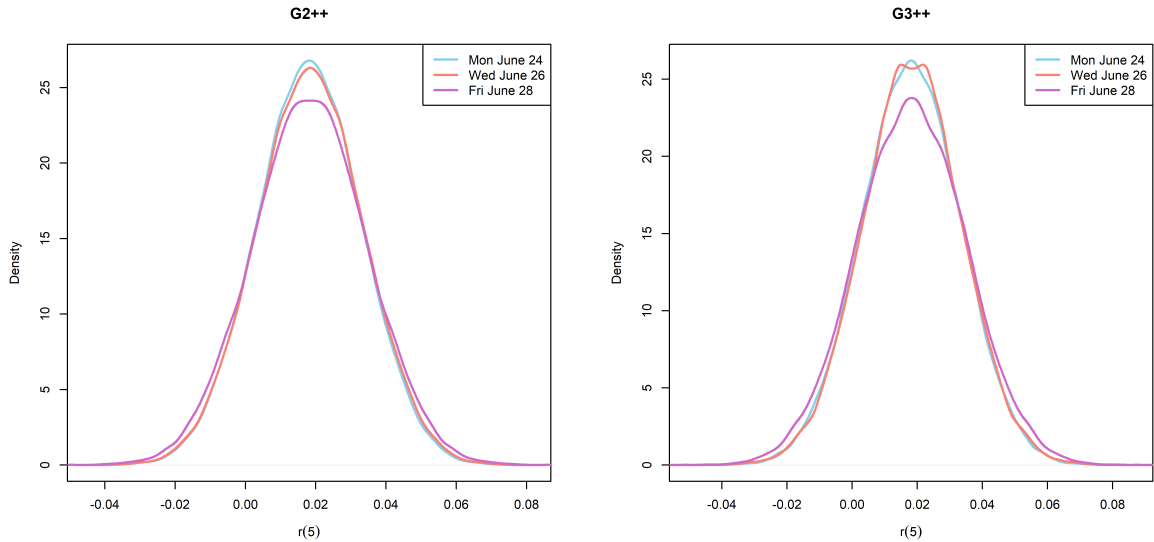


Figure 5.3: Distribution of five year short rate

of the 5 year short rates on Monday Friday has the largest variance (for both calibrated models) compared to the other two days. In the long term however, there is a stability in variance of the thirty year short rate on the three days. This is consistent with the market situation (based on the implied volatility surface) where there is a much higher implied volatility for short maturities and tenors swaptions on Friday and a similar implied volatility long maturities and tenors on the three dates.

To gain additional insight into how similar (or different) the short rate distribution is as implied by the calibrated models across the three dates, we compute the pairwise devia-

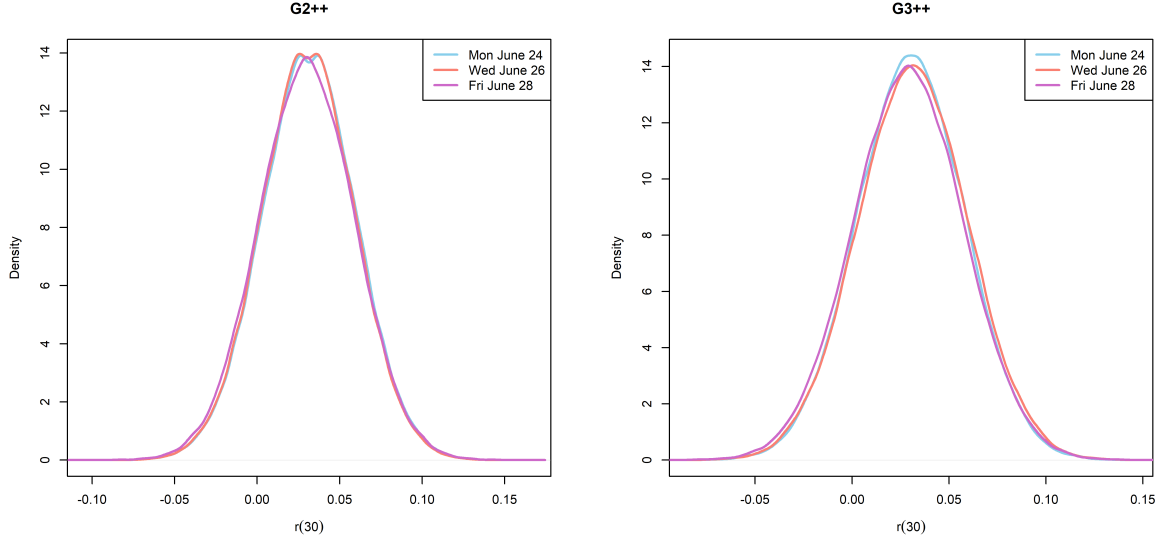


Figure 5.4: Distribution of thirty year short rate

tion of $r(t)$ and r . Here, the deviations are measured in terms of the root mean square deviation/error (RMSD/E). As mentioned previously, for each model (either G2++ or G3++) we simulated M paths of the short rate process r for all times t , using the same randomly generated normal iid's for all three reference dates. We define the deviations of $r(t)$ between two reference dates g and h as

$$MSD(r(t)^g, r(t)^h) = \mathbb{E} (\|r(t)^g - r(t)^h\|_{\mathcal{L}^2}^2)$$

where \mathcal{L}^2 is the Euclidean norm. The RMSD or simply the deviation between $r(t)^g$ and $r(t)^h$ is,

$$\begin{aligned} d(r(t)^g, r(t)^h) &= \sqrt{\mathbb{E} (\|r(t)^g - r(t)^h\|_{\mathcal{L}^2}^2)} \\ &\approx \sqrt{\frac{1}{M} \sum_{i=1}^M (r(t)_i^g - r(t)_i^h)^2} \end{aligned} \quad (5.1)$$

where $r(t)_i^g$ refers to the i th path of $r(t)$ on day g and M is the number of simulation paths.

For the short process r , we compute the deviation of r between days g and h as

$$d(r^g, r^h) \approx \sqrt{\sum_{j=1}^N \frac{1}{M} \sum_{i=1}^M (r(t)_i^g - r(t)_i^h)^2} \quad (5.2)$$

where M is the number of simulation paths and N is number of time steps. Using (5.1), we obtain the deviations of $r(t)$ with respect to the three days in Figure 5.5. We can

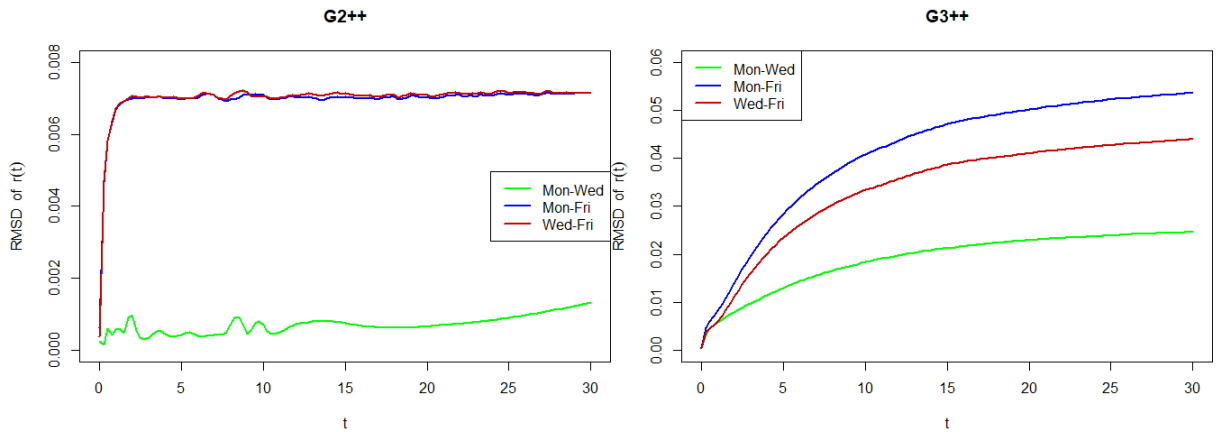


Figure 5.5: Deviations of $r(t)$ across the three days

observe that the deviations of $r(t)$ is more significant in the G3++ model than in the G2++. For the G2++ model, deviations between Monday and Wednesday is almost negligible by lying close to 0 for most times t . Additionally for the G2++ model, the deviations of $r(t)$ between Friday and the other two days rise for short term rates and they stabilize around 0.007 in the longer term. This sharp contrast seems to be effected by the G2++ parameter values (parameter values on Monday and Wednesday are more closer in magnitude than on Friday) since the shift in the market input is not huge, as shown.

Using (5.2), we compute the deviations of r across the three days which are provided in Tables 5.4 and 5.5. In Table 5.4 we observe that, in addition to deviations of $r(t)$, the deviations of the short rate process r between Friday and the other two days more pronounced. This further shows the sensitivity of G2++ to parameter values. Although the G3++ Figure 5.5 also shows the deviations between Monday and Wednesday to be the lowest, the deviations are much higher as a result of parameter values since ρ_{23} differs

greatly between the two calibration dates. The deviations on Friday are higher here as well although at a more significant magnitude. Given that we used the same set of random variables and market data which shows no indication of a major market shift, both the G2++ and G3++ model are not robust to different parameter specification, with the G3++ model being the more sensitive one.

Table 5.3: Deviations of r

Table 5.4: G2++

	Mon	Wed	Fri
Mon	0	0.00822	0.07683
Wed	0.00822	0	0.07736
Fri	0.07683	0.07736	0

Table 5.5: G3++

	Mon	Wed	Fri
Mon	0	0.2183	0.47834
Wed	0.2183	0	0.39165
Fri	0.47834	0.39165	0

A plot of the deterministic function f of both models that ensures consistency with the market yield curve in Figure 5.6. We can observe that f assumes the same shape for

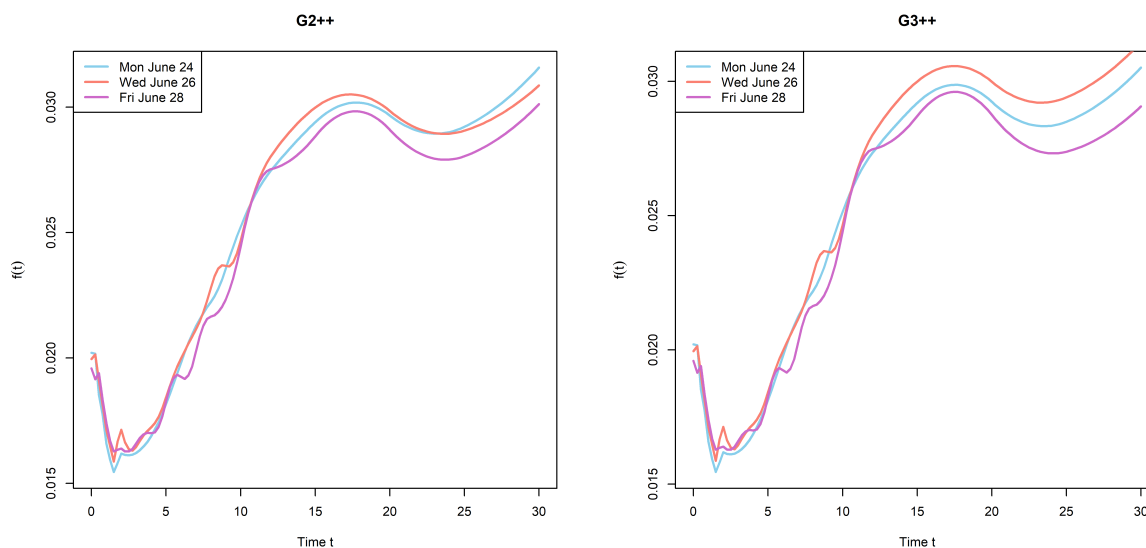


Figure 5.6: $f(t)$ across the three days

both models on all three days. The main dissimilarity occurs in the long term where $f(t)$ differs by a few basis points between the two models. The shape of $f(t)$ across the three days also reflects the movement in market yield curves since $f(t)$ is highly influenced by the market instantaneous forward rates.

Robustness With Respect To Valuations of The GMMB

These different parameter specification and and their implications are not of practical consequence to derivatives traders, since they calibrate their models everyday [Park, 2004]. For the valuation actuary however, this might be of practical consequence since the calibration is done on single day to satisfy regulatory requirements. Hence it is important for the interest rate model to not only satisfy the market-consistency criterion but also to be robust enough to provide stable financial statements.

In this section, we analyse the valuation results of the segregated fund described in Chapter 4 with the calibrated models on the three reference dates. Since the model calibration to market data is done on single day to satisfy regulatory requirements, it is important for the model to provide stable valuation results thereby providing reliable valuation results for stakeholders and users of financial statements. For each calibrated model (G2++

Table 5.6: GMMB Valuations: G2++ model

	Mon 06/24	Wed 06/26	Fri 06/28
$T = 20, K = 100$			
$\overline{\Pi}_0^{\text{guar}}$	4.847	4.690	5.001
Π_0^{in}	22.014	21.998	22.013
Π	-17.168	-17.308	-17.003
$\frac{\overline{\Pi}_0^{\text{guar}}}{\Pi_0^{\text{in}}}$	0.220	0.213	0.227

Table 5.7: GMMB Valuations: G3++ model

	Mon 06/24	Wed 06/26	Fri 06/28
$T = 20, K = 100$			
$\overline{\Pi}_0^{\text{guar}}$	4.775	4.723	4.958
Π_0^{in}	22.014	21.998	22.013
Π	-17.230	-17.275	-17.055
$\frac{\overline{\Pi}_0^{\text{guar}}}{\Pi_0^{\text{in}}}$	0.217	0.215	0.225

or G3++), we use the same set of pseudo-random numbers in simulating the underlying fund on the three days. The GMMB valuation results on all three days are provided in Table 5.6 for the G2++ model and Table 5.7 for the G3++ model. It is evident that the

valuation results for both models is consistent with the market observed term structure and volatility surface on the calibration date. Valuations of the expected cash inflow, the embedded guarantee and liability of the segregated fund are highest on Friday reflecting the most volatile swaption volatility surface and lower bond yields particularly toward long end of the yield curve. The opposite is true for Wednesday, with Monday being in-between. Given that there has not been a significant shift in the market, for any robust model, the market-consistent valuation results implied by its calibration to the market should be stable. For example if the $\frac{\Pi_0^{\text{guar}}}{\Pi_0^{\text{in}}} = 22\%$ on Monday June 24 2019 and $\frac{\Pi_0^{\text{guar}}}{\Pi_0^{\text{in}}} = 50\%$ on Wednesday June 26 2019, then this is a sign of potential danger in the model or the entire calibration process and needs to be properly addressed. This particular robustness check is a vital step in ensuring confidence in the entire calibration process and subsequently in the valuation results implied by calibrated model so as to prevent distortions in perceived financial risks..

Having observed how sensitive the models are in terms of parameter specifications, we investigate the deviations of the underlying fund F over the duration of the contract on the three calibration dates. In Figure 5.7, the deviations between the underlying fund

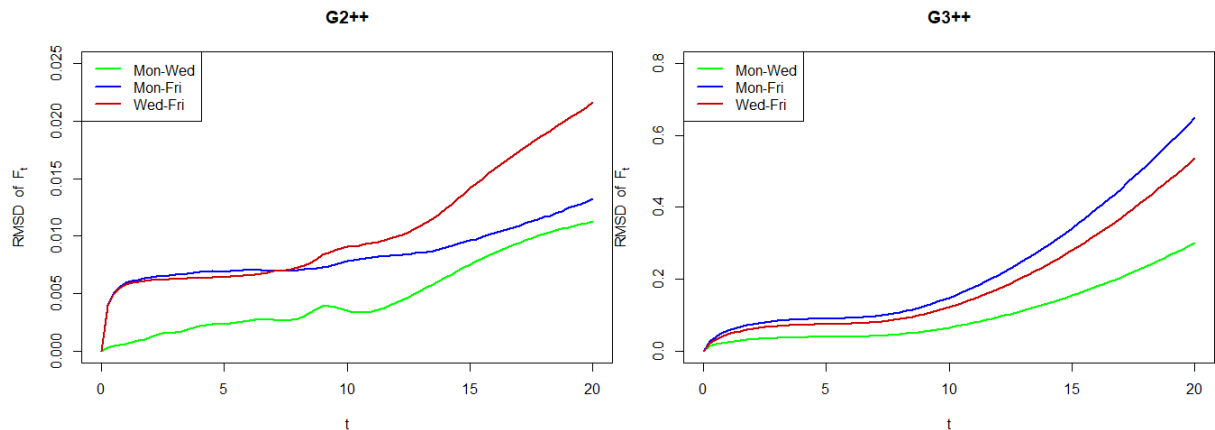


Figure 5.7: Deviations of F_t across the three days

values over time are much higher than the short rate deviations. We also notice that the deviations do not stabilize even in the long term; but rather increase in the long term. Further the G3++ model provides much larger pairwise deviations of the underlying fund over time. Tables 5.9 and 5.10 also show the pairwise deviations of the underlying fund

across all times step and paths. The deviations on the underlying fund F reiterates how

Table 5.8: Deviations of F

Table 5.9: G2++

	Mon	Wed	Fri
Mon	0	0.05211	0.07706
Wed	0.05211	0	0.10486
Fri	0.07706	0.10486	0

Table 5.10: G3++

	Mon	Wed	Fri
Mon	0	1.1744	2.57751
Wed	1.1744	0	2.1186
Fri	2.57751	2.1186	0

sensitive the G2++ and particularly, the G3++ are to parameter specifications; given that there was no significant shift in the market data input.

To the close the chapter, we conclude that as most interest rate models, both the G2++ and G3++ are sensitive to the market data used to calibrate them. While the G2++ model provided more stable parameters over the three chosen dates the G3++ model showed a much larger variance in parameter values due to its additional degrees of freedom. A method to obtain stable parameters over multiple calibration dates is to apply for example, regularization techniques. Although both models provide stable valuation results that reflect the market situation on the calibration date, they are not robust to different parameter specifications particularly for the G3++ model since it is less parsimonious. Given that the interest rate model calibration is done by insurers on a single day of the year to satisfy regulatory requirements, insurers should be extra cautious when calibrating both the G2++ and G3++ model to avoid distortions in the perceived risks.

Conclusion

This thesis presented the general steps in calibrating the G2++ and G3++ short-rate models to swaptions. We explained through established literature that two to three sources of randomness are needed in providing a realistic evolution of the future term structure due to the decorrelation between spot rates with different maturities. We also highlighted some issues that arised during the calibration process such as the imposed constraints placed on models and those peculiar to the G3++ model which were simply resolved by applying a “brick wall” penalty. The “brick wall” penalty was applied to combinations of parameters that either stopped the optimization algorithm or led to non-positive semi-definite correlation matrices. We also discussed the drawbacks of deterministic optimization algorithms in solving this is non-convex optimization problem such as their tendency of getting stuck in local optimums. Although a global solution is not guaranteed with stochastic optimization algorithms, we explained that they have higher chances of escaping local optimums due to the randomness in their search, although this comes with an increased computational effort. We implemented the calibration of both short rate models in two folds; we minimized the sum of absolute relative differences between market and model swaption prices in one respect and then minimized the sum of absolute relative differences between market and model implied swaption volatilities in another. In the calibration algorithm, we used an approximation of the swaption price by Schrage and Pelsser [2006] as opposed to quadratures or Monte-Carlo integration for a faster numerical efficiency. Although this approximation led to higher relative errors of around 10% – 12.3% from the market implied volatilities for swaptions with maturities 10, 12 or 15 and 1 year tenor, the overall fit of the calibrated models in replicating the

market volatility surface was satisfactory, with the mean absolute relative errors being below 3%, for both models and calibration methods. In assessing the calibrated models' fit in replicating the market volatility surface, we found that by minimizing the sum of model and market implied volatilities, both the G2++ and G3++ models provided better replication of market volatility surface as opposed to minimizing the sum of market and model swaption prices. Overall the G3++ model provided the best replication of the market volatility surface with a mean absolute error of 2.49%. After the verification of quality of the calibrated models, we provided a simulation scheme of the short rate, future bond prices and the discount factor which are essential in derivative pricing and market-consistent valuations. The simulated short rate process showed that the G3++ provided a higher empirical probability of negative interest rates than the G2++ model. Through a numerical illustration of a market-consistent valuation of a return of premium GMMB, the ratio of the expected cash out flow to expected cash in flow to the insurer hovered around 22% for both calibrated models. To test the robustness of the calibrated short rate models, we calibrated both the G2++ and G3++ models to market data of three different days with a two-day lag. The market input data showed that there was not a significant shift in the market on the considered dates. Through visual inspection of the calibrated parameters, we observed that as most interest models, both the G2++ and G3++ were sensitive to the market input data with the G3++ model showing a much larger variance in calibrated parameter values since it has 4 more degrees of freedom. Calibrated parameters of the G2++ were more stable between Monday June 24, 2019 and Wednesday June 26, 2019 given the similarity of the data used on the two calibration dates. On Friday June 28, 2019 however, where the shift in the market volatility surface was more pronounced, the calibrated parameter values of the G2++ were more deviant. We recommended that where there is a need for stable parameters, a useful technique could be an application of regularization methods to penalize parameter deviations. To gain more insight about the robustness of both models, we computed the pairwise root mean square deviations (RMSD) of the short rate and the underlying fund of the GMMB across the three reference dates. Results show that both models are not robust to dif-

ferent parameter specifications given that there has not being a significant change in the market, and the fact the we used the same random normal iid's in simulating the short rate and underlying fund. From the RMSD values, we noticed that the calibrated G3++ model showed more sensitivity to different parameter specifications.

Since the market-consistent valuations is done on a single day, we also examined the valuation results implied the calibrated model on the three calibration date. This particular robustness check is a vital step in ensuring confidence in the entire calibration process and subsequently in the valuation results implied by calibrated model so as to prevent distortion in perceived risk. Results show both the G2++ and G3++ provided stable valuation results which were only reflective of the market situation on the valuation date. The proportion of the expected cash out flow to the expected cash in flow to the insurer stabilized around 22% on the three dates for the G3++ model and 21 – 22% for the G2++ model.

We concluded the although G2++ and G3++ models have some desirable properties such analytical tractability, providing satisfactory replication of the market volatility surface and stability in valuation results, they are not robust to different parameter specifications hence one has to be cautious when calibrating them particularly where the calibration is done on a single day of the year to satisfy regulatory requirements.

Bibliography

- Kjersti Aas, Linda R Neef, Lloyd Williams, and Dag Raabe. Interest rate model comparisons for participating products under Solvency II. *Scandinavian Actuarial Journal*, 2018(3):203–224, 2018.
- Hansjoerg Albrecher, Andreas Binder, Volkmar Lautscham, and Philipp Mayer. *Introduction to quantitative methods for financial markets*. Springer Science & Business Media, 2013.
- Maciej Augustyniak, Frédéric Godin, and Emmanuel Hamel. A mixed bond and equity fund model for the valuation of segregated fund policies. *Available at SSRN 3479445*, 2019.
- Andreas Binder and Michael Aichinger. *A workout in computational finance*. John Wiley & Sons, 2013.
- Tomas Björk. *Arbitrage theory in continuous time*. Oxford university press, 2009.
- Menachem Brenner and Marti G Subrahmanyam. A simple formula to compute the implied standard deviation. *Financial Analysts Journal*, 44(5):80–83, 1988.
- Damiano Brigo and Fabio Mercurio. *Interest rate models-theory and practice: with smile, inflation and credit*. Springer Science & Business Media, 2007.
- Canadian Institute of Actuaries. Calibration of stochastic risk-free interest rate models for use in CALM valuation. <https://www.cia-ica.ca/docs/default-source/2013/213107e.pdf>, 2013.

- Canadian Institute of Actuaries. Comparison of IFRS 17 to Current CIA Standards of Practice. <https://www.cia-ica.ca/docs/default-source/2018/218117e.pdf>, 2018.
- Riccardo Casalini and Mario Bonino. Extending the G2++ Model: Fitting the Term Structure of Implied Volatility. *Available at SSRN 3598285*, 2020.
- Marco Cavazutti. *Optimization Methods: From Theory to Design*. Springer, 2013.
- Laura Coroneo, Ken Nyholm, and Rositsa Vidova-Koleva. How arbitrage-free is the Nelson-Siegel model? *Journal of Empirical Finance*, 18(3):393–407, 2011.
- Marco Di Francesco. A general Gaussian interest rate model consistent with the current term structure. *ISRN Probability and Statistics*, 2012.
- Matteo Ferranti. Calibration and simulation of the Gaussian two-additive-factor interest rate model. Master’s thesis, Universita’ Degli Studi di Padova, 2015.
- Daniel T Gillespie. Exact numerical simulation of the ornstein-uhlenbeck process and its integral. *Physical review E*, 54(2):2084, 1996.
- Paul Glasserman. *Monte-Carlo methods in financial engineering*, volume 53. Springer Science & Business Media, 2013.
- Mary Hardy. *Investment guarantees: modeling and risk management for equity-linked life insurance*, volume 215. John Wiley & Sons, 2003.
- Thomas SY Ho and Sang-Bin Lee. Term structure movements and pricing interest rate contingent claims. *the Journal of Finance*, 41(5):1011–1029, 1986.
- John C Hull. *Options, futures and other derivatives*. New York, NY : Pearson, 2018.
- IASB. *Basis for conclusion on IFRS17 insurance contracts*. IFRS, 2017.
- Farshid Jamshidian and Yu Zhu. Scenario simulation: Theory and methodology. *Finance and stochastics*, 1(1):43–67, 1996.

- Mark S Joshi and Oh Kang Kwon. Monte-Carlo market Greeks in the displaced diffusion LIBOR market model. *Available at SSRN 1535058*, 2010.
- Minqiang Li. You don't have to bother newton for implied volatility. *Available at SSRN 952727*, 2006.
- Robert Litterman and Jose Scheinkman. Common factors affecting bond returns. *Journal of fixed income*, 1(1):54–61, 1991.
- Moody's Analytics. Scenario modeling for IFRS 17: Economic Scenarios and Yield Curves, 2020.
- Katharine M Mullen, David Ardia, David L Gil, Donald Windover, and James Cline. DEoptim: An R package for global optimization by differential evolution. 2009.
- F Park. Implementing interest rate models: A practical guide. *Capital Markets and Portfolio Research (CMPR)*, 2004.
- Hal Pedersen, Mary Pat Campbell, Stephan L Christiansen, Samuel H Cox, Daniel Finn, Ken Griffin, Nigel Hooker, Matthew Lightwood, Stephen M Sonlin, and Chris Suchar. Economic scenario generators: a practical guide. *The Society of Actuaries (July 2016)*, 2016.
- Kenneth Price, V., Rainer Storn, M., and Jounie Lampinen, A. *Differential evolution: A practical approach to global optimization*. springer, 2005.
- Vincenzo Russo and Gabriele Torri. Calibration of one-factor and two-factor Hull-White models using swaptions. *Computational Management Science*, 16(1-2):275–295, 2019.
- David F Schrage and Antoon A.J. Pelsser. Pricing swaptions and coupon bond options in affine term structure models. *Mathematical Finance*, 16(4):673–694, 2006.
- J Michael Steele. *Stochastic calculus and financial applications*, volume 45. Springer Science & Business Media, 2012.

Appendix A

A.1 Validation Results On Monday June 24

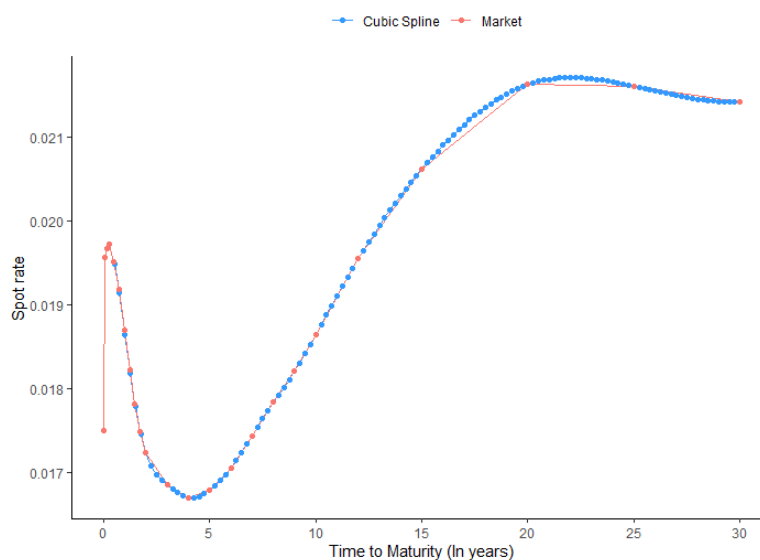


Figure A.1: Market interpolated spot curve on Monday June 24

Table A.1: Market volatilities on June 24

Maturity/Tenor	1	2	3	4	5	7	10
1	0.3617	0.4023	0.4324	0.4338	0.4257	0.3946	0.3208
2	0.3870	0.4017	0.4233	0.4223	0.4074	0.3877	0.3192
4	0.3912	0.3833	0.3868	0.3853	0.3766	0.3523	0.2985
5	0.3657	0.3641	0.3611	0.3670	0.3575	0.3353	0.2920
7	0.3335	0.3373	0.3325	0.3343	0.3226	0.3073	0.2773
8	0.3279	0.3260	0.3149	0.3116	0.3002	0.2876	0.2695
10	0.3142	0.3021	0.2819	0.2671	0.2573	0.2495	0.2546
12	0.3114	0.2994	0.2802	0.2660	0.2565	0.2489	0.2557
15	0.3118	0.2998	0.2806	0.2663	0.2567	0.2513	0.2584
20	0.3231	0.3106	0.2907	0.2758	0.2659	0.2588	0.2648

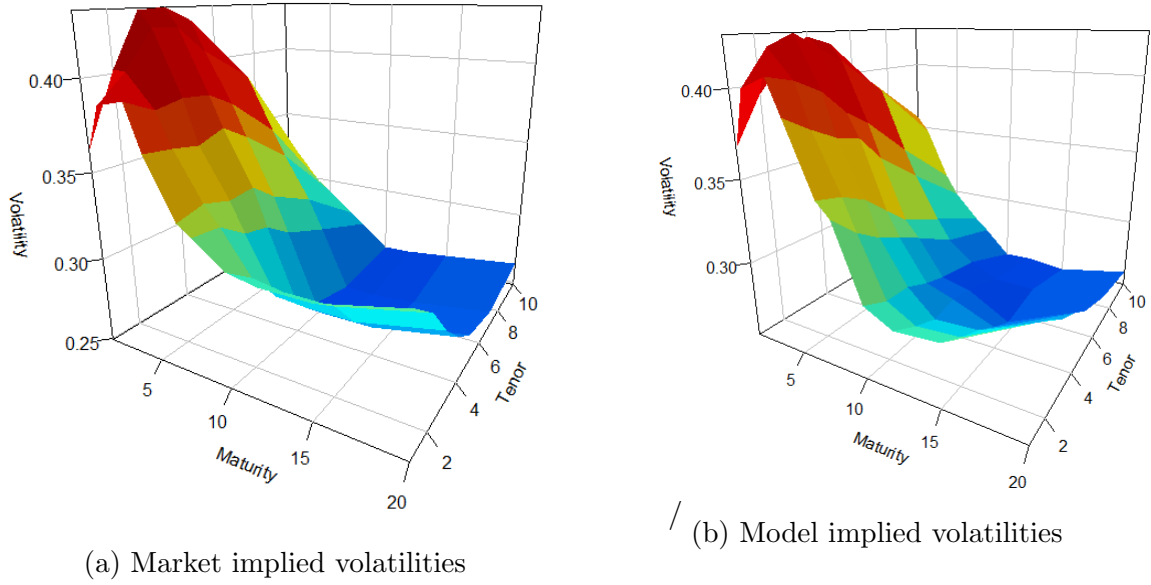


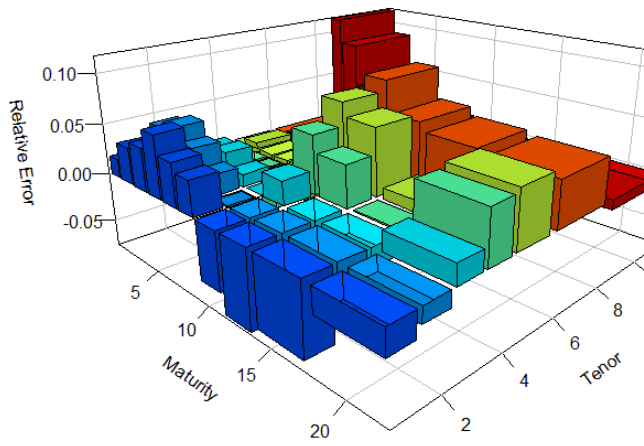
Figure A.2: G2++ implied volatility surface on June 24

Table A.2: G2++ implied volatilities on June 24

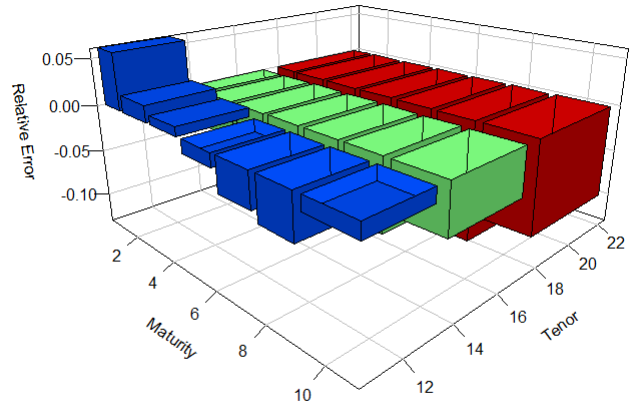
Maturity/Tenor	1	2	3	4	5	7	10
1	0.3682	0.3945	0.4124	0.4246	0.4196	0.3919	0.3581
2	0.4008	0.4207	0.4276	0.4187	0.4099	0.3868	0.3477
4	0.4079	0.4041	0.3960	0.3810	0.3717	0.3459	0.3114
5	0.3881	0.3786	0.3708	0.3665	0.3497	0.3280	0.2976
7	0.3479	0.3443	0.3367	0.3234	0.3113	0.2987	0.2794
8	0.3391	0.3254	0.3151	0.3078	0.3008	0.2849	0.2720
10	0.2961	0.2895	0.2885	0.2823	0.2778	0.2721	0.2543
12	0.2877	0.2800	0.2734	0.2769	0.2734	0.2634	0.2554
15	0.2902	0.2824	0.2754	0.2668	0.2596	0.2637	0.2527
20	0.3153	0.3060	0.2962	0.2897	0.2805	0.2705	0.2622

Table A.3: G2++ calibration errors on June 24

Maturity/Tenor	1	2	3	4	5	7	10
1	0.0180	-0.0194	-0.0462	-0.0213	-0.0143	-0.0067	0.1163
2	0.0357	0.0474	0.0102	-0.0086	0.0061	-0.0023	0.0893
4	0.0426	0.0542	0.0237	-0.0112	-0.0131	-0.0181	0.0431
5	0.0613	0.0398	0.0267	-0.0013	-0.0217	-0.0217	0.0190
7	0.0431	0.0206	0.0127	-0.0327	-0.0351	-0.0281	0.0075
8	0.0342	-0.0017	0.0005	-0.0121	0.0021	-0.0094	0.0092
10	-0.0577	-0.0417	0.0235	0.0568	0.0795	0.0904	-0.0011
12	-0.0762	-0.0649	-0.0243	0.0408	0.0660	0.0581	-0.0014
15	-0.0692	-0.0581	-0.0187	0.0017	0.0111	0.0494	-0.0219
20	-0.0242	-0.0148	0.0191	0.0506	0.0550	0.0451	-0.0098

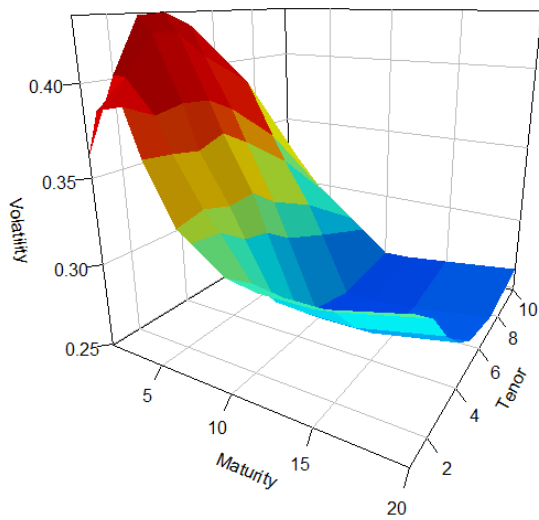


(a) In-sample calibration errors

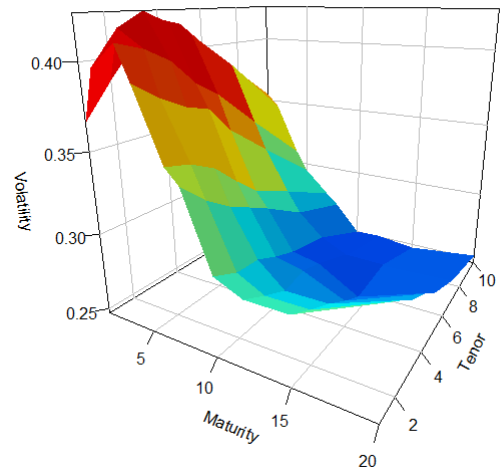


(b) Out-of-sample calibration error

Figure A.3: G2++ calibration errors on June 24

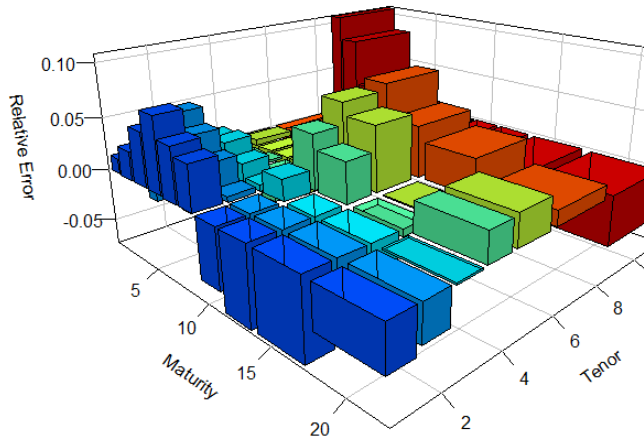


(a) Market implied volatilities

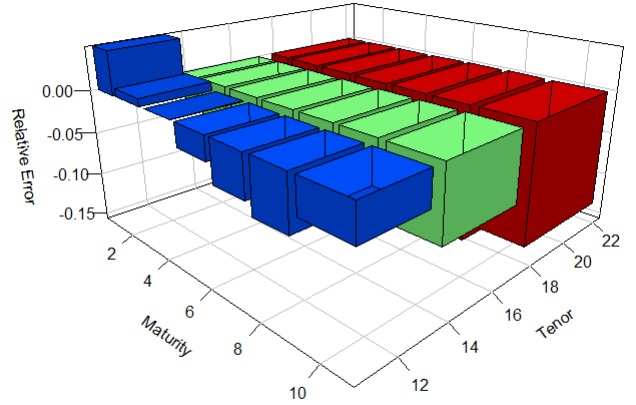


(b) Model implied volatilities

Figure A.4: G3++ implied volatilities on June 24



(a) In-sample calibration errors



(b) Out-of-sample calibration error

Figure A.5: G3++ calibration errors on June 24

Table A.4: G3++ implied volatilities on June 24

Maturity/Tenor	1	2	3	4	5	7	10
1	0.3667	0.3873	0.4061	0.4200	0.4164	0.3898	0.3554
2	0.3974	0.4168	0.4253	0.4176	0.4096	0.3865	0.3461
4	0.4110	0.4063	0.3981	0.3830	0.3733	0.3464	0.3099
5	0.3916	0.3808	0.3725	0.3678	0.3505	0.3275	0.2951
7	0.3505	0.3464	0.3386	0.3249	0.3123	0.2986	0.2776
8	0.3420	0.3275	0.3167	0.3090	0.3015	0.2843	0.2696
10	0.2962	0.2889	0.2874	0.2807	0.2757	0.2690	0.2496
12	0.2885	0.2800	0.2730	0.2760	0.2720	0.2608	0.2510
15	0.2892	0.2809	0.2736	0.2646	0.2569	0.2599	0.2471
20	0.3104	0.3005	0.2902	0.2832	0.2735	0.2624	0.2524

Table A.5: G3++ calibration errors on June 24

Maturity/Tenor	1	2	3	4	5	7	10
1	0.0139	-0.0373	-0.0608	-0.0318	-0.0218	-0.0122	0.1080
2	0.0269	0.0376	0.0047	-0.0110	0.0053	-0.0030	0.0844
4	0.0506	0.0599	0.0293	-0.0060	-0.0087	-0.0167	0.0382
5	0.0707	0.0460	0.0316	0.0023	-0.0197	-0.0234	0.0105
7	0.0510	0.0270	0.0184	-0.0281	-0.0319	-0.0282	0.0011
8	0.0429	0.0047	0.0058	-0.0083	0.0043	-0.0113	0.0003
10	-0.0574	-0.0439	0.0197	0.0511	0.0717	0.0780	-0.0195
12	-0.0736	-0.0647	-0.0257	0.0375	0.0604	0.0477	-0.0184
15	-0.0726	-0.0630	-0.0250	-0.0064	0.0009	0.0341	-0.0436
20	-0.0392	-0.0326	-0.0016	0.0269	0.0287	0.0137	-0.0468

A.2 Validation Results On Wednesday June 26

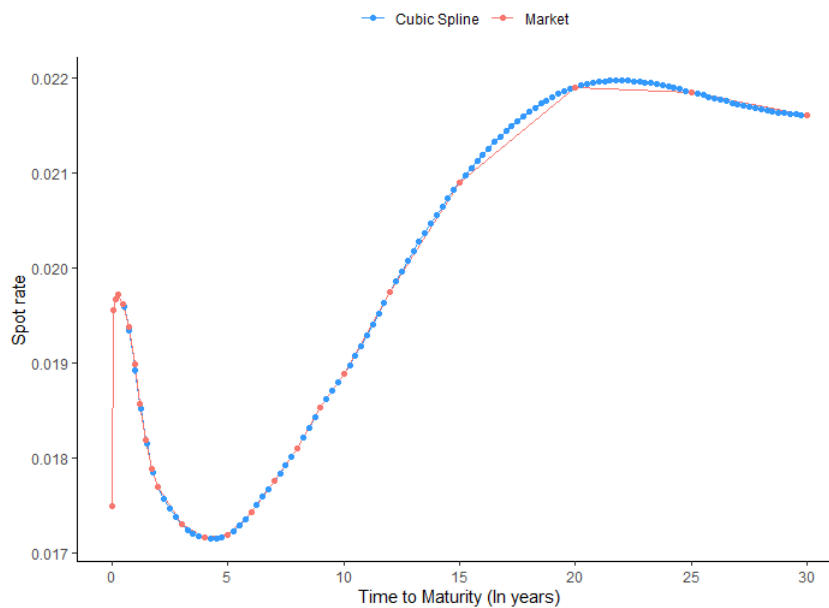
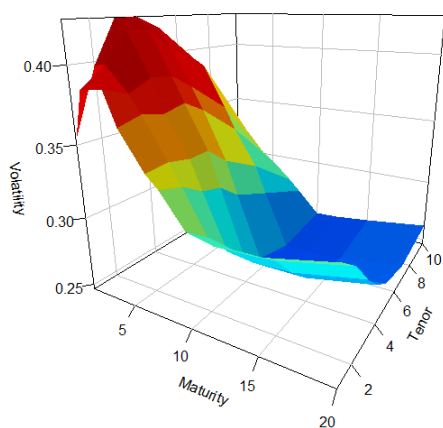


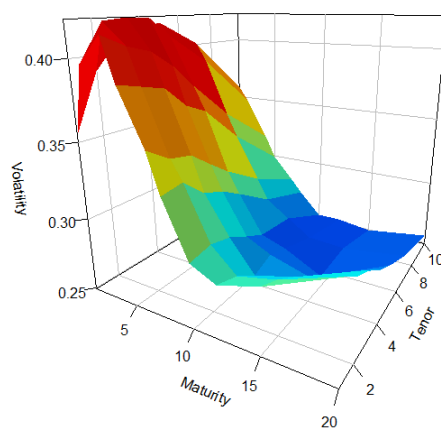
Figure A.6: Market interpolated curve on Monday June 26

Table A.6: Market volatilities on June 26

Maturity/Tenor	1	2	3	4	5	7	10
1	0.3533	0.3973	0.4262	0.4268	0.4188	0.3927	0.3208
2	0.3857	0.3991	0.4191	0.4178	0.4053	0.3871	0.3202
4	0.3877	0.3823	0.3893	0.3882	0.3780	0.3550	0.3009
5	0.3662	0.3703	0.3670	0.3706	0.3617	0.3387	0.2948
7	0.3413	0.3421	0.3388	0.3392	0.3261	0.3104	0.2796
8	0.3330	0.3286	0.3185	0.3143	0.3019	0.2888	0.2701
10	0.3113	0.2994	0.2796	0.2650	0.2553	0.2471	0.2518
12	0.3076	0.2958	0.2774	0.2637	0.2544	0.2465	0.2528
15	0.3087	0.2969	0.2784	0.2644	0.2550	0.2491	0.2557
20	0.3197	0.3075	0.2883	0.2737	0.2640	0.2568	0.2627

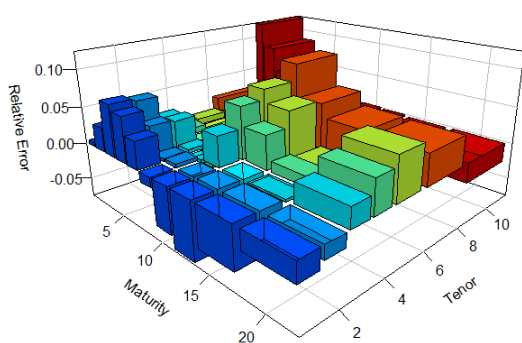


(a) Market implied volatilities

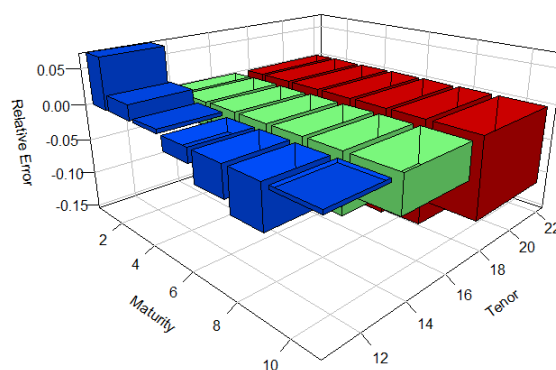


(b) Model implied volatilities

Figure A.7: G2++ volatility surface on June 26



(a) In-sample calibration errors



(b) Out-of-sample calibration error

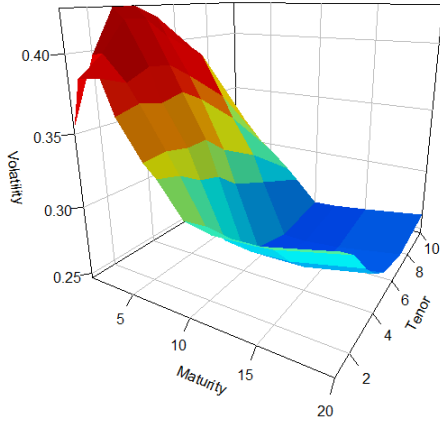
Figure A.8: G2++ calibration errors on June 26

Table A.7: G2++ implied volatilities on June 26

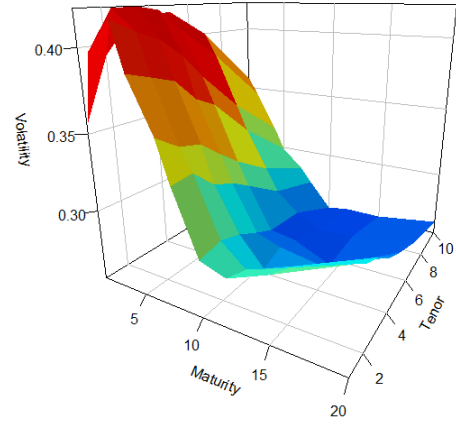
Maturity/Tenor	1	2	3	4	5	7	10
1	0.3547	0.3907	0.4086	0.4139	0.4175	0.4008	0.3600
2	0.3978	0.4206	0.4221	0.4209	0.4087	0.3874	0.3480
4	0.4144	0.4071	0.4023	0.3917	0.3758	0.3488	0.3166
5	0.3882	0.3845	0.3803	0.3663	0.3593	0.3316	0.2991
7	0.3538	0.3434	0.3407	0.3290	0.3182	0.3005	0.2812
8	0.3285	0.3304	0.3169	0.3115	0.3026	0.2849	0.2708
10	0.2925	0.2951	0.2909	0.2831	0.2762	0.2728	0.2528
12	0.2843	0.2796	0.2700	0.2753	0.2709	0.2615	0.2534
15	0.2919	0.2857	0.2775	0.2679	0.2572	0.2598	0.2494
20	0.3118	0.3024	0.2956	0.2854	0.2787	0.2671	0.2559

Table A.8: G2++ calibration errors on June 26

Maturity/Tenor	1	2	3	4	5	7	10
1	0.0041	-0.0166	-0.0414	-0.0303	-0.0032	0.0206	0.1222
2	0.0313	0.0540	0.0073	0.0074	0.0085	0.0009	0.0870
4	0.0689	0.0649	0.0334	0.0089	-0.0058	-0.0176	0.0523
5	0.0600	0.0384	0.0362	-0.0116	-0.0068	-0.0210	0.0146
7	0.0365	0.0039	0.0055	-0.0302	-0.0242	-0.0318	0.0057
8	-0.0134	0.0056	-0.0051	-0.0090	0.0025	-0.0137	0.0025
10	-0.0604	-0.0142	0.0406	0.0683	0.0818	0.1039	0.0039
12	-0.0757	-0.0548	-0.0266	0.0440	0.0648	0.0607	0.0024
15	-0.0545	-0.0378	-0.0032	0.0133	0.0088	0.0428	-0.0246
20	-0.0247	-0.0167	0.0252	0.0429	0.0559	0.0401	-0.0260

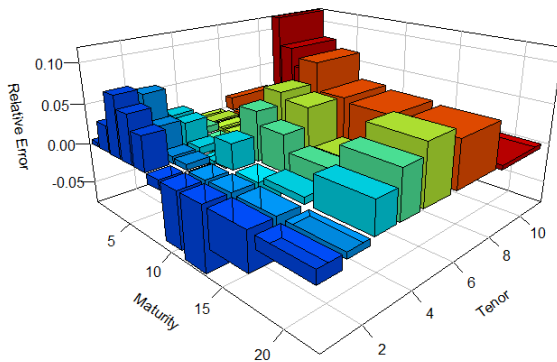


(a) Market implied volatilities

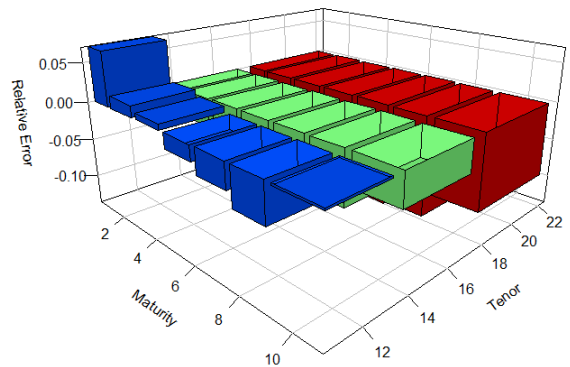


(b) Model implied volatilities

Figure A.9: G3+ volatility surface on June 26



(a) In-sample calibration errors



(b) Out-of-sample calibration error

Figure A.10: G3++ calibration errors on June 26

Table A.9: G3+ implied volatilities on June 26

Maturity/Tenor	1	2	3	4	5	7	10
1	0.3552	0.3935	0.4111	0.4151	0.4175	0.3994	0.3586
2	0.3986	0.4216	0.4219	0.4192	0.4060	0.3839	0.3451
3	0.4168	0.4087	0.4029	0.3915	0.3751	0.3479	0.3166
4	0.3882	0.3839	0.3789	0.3644	0.3571	0.3296	0.2982
5	0.3556	0.3450	0.3419	0.3299	0.3191	0.3017	0.2833
6	0.3292	0.3310	0.3171	0.3115	0.3027	0.2852	0.2722
7	0.2897	0.2924	0.2882	0.2805	0.2738	0.2711	0.2525
8	0.2839	0.2793	0.2697	0.2751	0.2709	0.2622	0.2554
9	0.2947	0.2886	0.2805	0.2710	0.2605	0.2638	0.2547
10	0.3149	0.3054	0.2987	0.2887	0.2822	0.2712	0.2613

Table A.10: G3++ calibration errors on June 26

Maturity/Tenor	1	2	3	4	5	7	10
1	0.0053	-0.0095	-0.0355	-0.0274	-0.0030	0.0171	0.1179
2	0.0335	0.0563	0.0067	0.0034	0.0018	-0.0083	0.0777
4	0.0751	0.0690	0.0349	0.0084	-0.0076	-0.0199	0.0523
5	0.0601	0.0366	0.0324	-0.0167	-0.0128	-0.0268	0.0116
7	0.0420	0.0086	0.0092	-0.0274	-0.0216	-0.0281	0.0133
8	-0.0114	0.0072	-0.0044	-0.0088	0.0026	-0.0124	0.0078
10	-0.0694	-0.0234	0.0308	0.0585	0.0725	0.0969	0.0026
12	-0.0772	-0.0559	-0.0277	0.0434	0.0649	0.0635	0.0103
15	-0.0455	-0.0279	0.0077	0.0251	0.0216	0.0589	-0.0039
20	-0.0150	-0.0067	0.0360	0.0546	0.0689	0.0562	-0.0053